Topics on Composite Higgs

Sebastián Norero Cárdenas

A Thesis Presented for the Degree of
Master in Physics

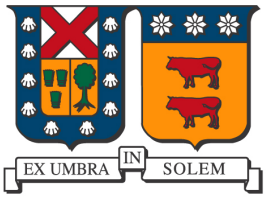

UNIVERSIDAD TECNICA
FEDERICO SANTA MARIA

Department of Physics
Universidad Técnica Federico Santa María
Valparaíso, Chile
27th September 2018

Contents

Acknowledgements

I would like to express my gratitude to my thesis advisor Dr. Alfonso Zerwekh for his guidance and advices throughout my studies for the degree of M.Sc. at Universidad Técnica Federico Santa María and the developing of this thesis. I would like to thank Dr. Claudio Dib and Dr. Marcelo Loewe for reading my thesis and acting as members of the exam committee.

I would also like to thank my friends at UTFSM for their kindness and friendship support. A special mention must be made of Bastián Díaz for a number of helpful discussions and advices throughout my studies.

Lastly, I would like to thank my parents not only for their support while carrying out this thesis, but supporting me my entire life and provide me with the means to enjoy a good education.

Introduction

A currently open question is whether the Higgs boson particle is truly elementary (i.e. pointlike), down to distance scales much shorter than the Electroweak scale, or if, on the contrary, it is a composite bound state of more fundamental degrees of freedom, whose physics should be revealed at energies not far above the weak scale. In either case the discovery of this scalar particle was truly remarkable. If it turns out to be elementary, it would be the first and only known example of this kind in nature. On the other hand, if it turns out that the Higgs boson is a composite state arising from some underlying strong dynamics, we would be in a situation that also presents new characteristics compared to other known composite scalars. We elaborate on this last possibility in the present thesis.

This thesis aims to be a pedagogical and self-contained theoretical review of some of the most relevant aspects of general composite Higgs theories. It begins with section 1 reviewing the basics of the Standard Model. Section 2 reviews some important characteristic of the Higgs boson: its most important decay and production channels, as well as its radiative corrections. Section 3 explains the hierarchy problem, and presents the best-known approaches that address this problem. In section 4 we explain the composite sector of a composite Higgs theory and proceed to present the CCWZ prescription, a fundamental tool when it comes to understand the low-energy and confinement regime of a strong dynamic. Section 5 present the elementary and composite sectors. In section 6 we introduce extra spin-0 and spin-1 resonances. Finally, in section 7 we introduce the phenomenology of a particular composite Higgs model analyzed in Ref. [123] and in which the author of the thesis was part.

1 The Standard Model of Particle Physics

1.1 Quantum Field Theories

Modern particle physics is described in terms of *quantum field theories* (QFTs). A quantum field theory constitutes a mathematical and conceptual framework that combines three of the major themes of moder physics: *classical fields*, *special relativity*, and *quantum mechanics*, in addition to some set of fundamental assumptions. The fundamental entities of these theories are *quantum fields*. A quantum field is some data on spacetime [1]; it is a fundamental property of space. Technically, a typical example of a classical (i.e. non-quantized) field is a section

$$\phi \colon M \to S \tag{1.1}$$

in a vector bundle S over the spacetime manifold M. On the other hand, an example of a quantum field is a linear map from the space of smooth sections of some vector bundle over spacetime to operators. For each particle species, there will be a corresponding quantum field.

1.1.1 Lagrangians

The formulation of a (four-dimensional) quantum field theory begins with its description at the level of a classical field theory, which eventually we proceed to quantize in order to obtain the corresponding quantum field theory. The description of the field can be formulated in terms of a Lagrangian or Hamiltonian formalism. In the Lagrangian formalism, the basic laws of a system consisting of a collection of local fields ϕ_i are encoded in the action S, the time integral of the Lagrangian function[1] L of the system, which in turn can be written as the spatial integral of a Lagrangian density[2] $\mathcal{L}$, namely

$$S := \int L \, dt = \int \mathcal{L}[\phi_i, \partial_\mu \phi_i] \, d^4x \tag{1.2}$$

where d^4x is the integration measure in four-dimensional Minkowski space and i runs from 1 to the number of fields. Now, the dynamics for such a Lagrangian system is determined by the principle of least action, which states that the system evolves from one initial configuration at t_1 to another final configuration at t_2 along the path in its phase space for which S has a minimum and $\delta S = 0$ holds. It follows from this principle that the evolution of the system is governed by the so-called *Euler-Lagrange equations*

$$\frac{\partial \mathcal{L}}{\partial \phi_i} - \partial_\mu \left(\frac{\partial \mathcal{L}}{\partial (\partial_\mu \phi_i)} \right) = 0 \tag{1.3}$$

and for which there will be one such field equation for each field presented in the system. From the point of view of the Hamiltonian formalism, the object of interest is the Hamiltonian function H, the spatial integral of a Hamiltonian density $\mathcal{H}[\phi_i, \pi_i]$ which in turn is a function of the fields ϕ_i

[1] We will use a calligraphic script for densities and an italic script for integrated quantities.
[2] The word "density" is almost always omitted.

and their conjugate momenta density[3]

$$\pi_i := \frac{\partial \mathcal{L}[\phi_j, \dot{\phi}_j]}{\partial \dot{\phi}_i} \tag{1.4}$$

where $\dot{\phi}_i[\phi_j, \pi_j] = \partial_t \phi_i$ and it is implicitly defined by 1.4. The Hamiltonian density is formally defined as the Legendre transform of the Lagrangian density

$$H := \int \mathcal{H}\, d^3x = \int \left(\pi_i \dot{\phi}_i[\phi_j, \pi_j] - \mathcal{L}[\phi_i, \dot{\phi}_i[\phi_j, \pi_j]] \right) d^3x \tag{1.5}$$

The evolution of the system is then governed by the Hamiltonian field equations

$$\dot{\phi}_i = \frac{\partial \mathcal{H}}{\partial \pi_i} \quad \text{and} \quad \dot{\pi}_i = -\frac{\partial \mathcal{H}}{\partial \phi_i} \tag{1.6}$$

The Lagrangian formulation of a field theory is, however, particularly suited to relativistic dynamics. The simplest reason for this is that Lagrangians and all other expressions are explicitly Lorentz invariant. In general, we require the following properties hold for the Lagrangian:

1. It is a function of the fields and their derivatives only, so as to ensure translational invariance.
2. It depends on the fields taken at one spacetime point x^μ only, leading to a local field theory.
3. It is real, so that the total probability is conserved.
4. It is analytic function in the fields. This is not a general requirement, but is common to all field theories that are solved via perturbation theory. In all of these, we expand around a minimum, and this expansion mean that we consider a Lagrangian that is a polynomial in the fields.
5. It is invariant under the Poincaré group, the external symmetry of the theory.
6. It is invariant under certain internal symmetry groups.

We impose two additional requirements:

7. Naturalness[4]: every term in the Lagrangian that is not forbidden by a symmetry should appear.
8. Renormalizability: a renormalizable Lagrangian contains only terms that are of dimension less than or equal to four in the fields and their derivatives.

The requirement of renormalizability ensures that the Lagrangian contains at most two ∂_μ operations, and leads to classical equations of motion that are not higher than second order derivatives. If the full theory of the nature is describe by a QFT, its Lagrangian should indeed be renormalizable. The theories that we will consider in this thesis and, in particular, the SM are, however, only low energy effective field theories, valid up to some energy scale Λ. Therefore, we must include also non-renormalizable terms which have coefficients with inverse mass dimensions $1/\Lambda^n$ with $n = 1, 2, \ldots$.

[3] The fields ϕ_i and conjugates π_i form an infinite dimensional phase space, because fields have an infinite number of degrees of freedom.

[4] Do not confuse this concept with the one presented in (3.2.4).

1.1.2 Symmetries

The central role of symmetry was a primary lesson of the physics of the first half of the 20th century [2]. Symmetries in QFT have a strong predictive, or explanatory, power. The main consequences of the various types if symmetries are summarized in Table (1.1).

Table 1.1: Symmetries and consequences

Type of symmetries	Consequences
Spacetime	Conservation of energy, momentum, and angular momentum
Global (exact)	Conserved charges
Global (spon. broken)	Massless scalars
Global (spon. & expli. broken)	Massive scalars
Local (exact)	Interactions, massless spin-1 mediators
Local (spon. broken)	Interactions, massive spin-1 mediators
Discrete	Selection Rules

In the Standard Model, only local symmetries are imposed. Similarly, in most of the extensions of the Standard Model, only local and discrete symmetries are imposed. While it is possible, in principle, to impose also global continuous symmetries, this is rarely done in current modern buildings.

1.1.3 Gauge Theories

A *gauge theory* is a field theory involving a local internal symmetry group, known as *gauge groups*, under which the Lagrangian of the theory is invariant. Many interesting theories in physics, like the Standard Model of elementary particles, are gauge theories. The main idea underlying a gauge theory is that symmetry generate interaction. For each group generator of the gauge group will necessarily arise a corresponding vector field called a *gauge field*. Gauge fields are included in the Lagrangian to ensure its invariance under the gauge transformations (called *gauge invariance*). When such a theory is quantized, these quanta of the gauge fields are called *gauge bosons*. If the gauge group is non-commutative, then the gauge theory is referred to as *non-abelian gauge theory*.

The specific kind of Lie group in a gauge theory (its dimension, whether it is abelian or not, whether it is simple or splits as a product of several factors, and so on) is reflected in interesting ways in the physics. For example, in the case of the Standard Model (see 1.7), it turns out that:

1. The fact that there are 8 gluons, 3 weak gauge bosons and 1 photon is related to the dimensions of the Lie groups $\mathrm{SU}(3)_\mathrm{C}$ and $\mathrm{SU}(2)_\mathrm{L} \times \mathrm{U}(1)_\mathrm{Y}$.

2. The fact that gluons interact directly with each other while photons do not is related to the fact that $\mathrm{SU}(3)_\mathrm{C}$ is non-abelian while $\mathrm{U}(1)_\mathrm{EM}$ is abelian.

3. The fact that the strong, weak and electromagnetic interactions have different strengths (coupling constants) is related to the product structure of the gauge group 1.7 (GUTs built on simple Lie groups like SU(5) have only a single coupling constant).

1.2 The Standard Model

1.2.1 Introduction

The *Standard Model* (SM) of particle physics is a gauge quantum field theory describing three of the four known fundamental interactions in the nature, namely, the *electromagnetic*, *weak* and *strong* interactions, as well as classifying all known elementary particles. An array of experimental results confirm every feature of the theory to a high degree of precision, at the level of testing higher order perturbation theory.

The local internal symmetry group of the Standard Model is

$$G_{\mathrm{SM}} := \mathrm{SU}(3)_{\mathrm{C}} \times \mathrm{SU}(2)_{\mathrm{L}} \times \mathrm{U}(1)_{\mathrm{Y}} \tag{1.7}$$

which combines the $\mathrm{SU}(2)_{\mathrm{L}} \times \mathrm{U}(1)_{\mathrm{Y}}$ *Glashow-Salam-Weinberg theory* of electroweak interactions, together with the $\mathrm{SU}(3)_{\mathrm{C}}$ theory of *Quantum Chromodynamics* describing strong interactions.

1.2.2 Fields and Notation

Fermions (quarks and leptons) in the SM are simple structureless (as far as we know) spin-1/2 particles. They are modelled by Dirac spinors ψ_n with four components $n = 1, \ldots, 4$, which are functions of the spacetime coordinates $x_\mu = (t, x, y, z)$. Free Dirac fermions obey the Dirac equation

$$(i\partial\!\!\!/ - m)\psi = 0 \tag{1.8}$$

Let i and α be the flavour/generation and color indices respectively, and L, R chiral indices; then the fermionic content of the Standard Model can be labelled as follows:

1. Left-handed lepton doublets:
$$L_{iL} \in (\mathbf{1}, \mathbf{2}, -1/2) \tag{1.9}$$

2. Right-handed lepton singlets:
$$e_{iR} \in (\mathbf{1}, \mathbf{1}, -1), \qquad \nu_{iR} \in (\mathbf{1}, \mathbf{1}, 0) \tag{1.10}$$

3. Left-handed quark doublets:
$$Q^{\alpha}_{iL} \in (\mathbf{3}, \mathbf{2}, 1/6) \tag{1.11}$$

4. Right-handed quark singlets:
$$u^{\alpha}_{iR} \in (\mathbf{3}, \mathbf{1}, 2/3), \qquad d^{\alpha}_{iR} \in (\mathbf{3}, \mathbf{1}, -1/3) \tag{1.12}$$

Massless gauge boson are spin-1 particles with two polarization states (left-handed and right-handed). They are modelled by a four-component vector potential $A_\mu(x)$ with a Lorentz index $\mu = 0, 1, 2, 3$. Although there is only one type of photon mediating electromagnetic interactions, in general there will be $n = \dim(G)$ types of gauge bosons mediating the a corresponding gauge interaction with gauge group G. Massless gauge bosons are physical degrees of freedom and therefore must carry energy and momentum themselves; to describe these physical features, and following

the successful theory of Maxwell on electromagnetism, we introduce in a similar way the a kinetic energy term

$$\mathcal{L} = -\frac{1}{4} F^a_{\mu\nu} F^{a\mu\nu} \tag{1.13}$$

Conditions must be imposed on every $A^a_\mu(x)$ to select only the physical degrees of freedom, as different $A^a_\mu(x)$ can give rise to the same physics. The massless gauge bosons presented in the Standard Model are:

5. Gluons G^A_μ with field strength tensor:

$$G^A_{\mu\nu} = \partial_\mu G^A_\nu - \partial_\nu G^A_\mu - g_s f_{ABC} G^B_\mu G^C_\mu \tag{1.14}$$

   where $A = 1, \ldots, 8$ and f_{ABC} are the $\mathrm{SU}(3)_C$ structure constants.

6. W bosons W^I_μ with field strength tensor:

$$W^I_{\mu\nu} = \partial_\mu W^I_\nu - \partial_\nu W^I_\mu - g \varepsilon_{IJK} W^J_\mu W^K_\nu \tag{1.15}$$

   where $I = 1, 2, 3$ and ε_{IJK} is the is the totally antisymmetric symbol.

7. B boson B_μ with field strength tensor:

$$B_{\mu\nu} = \partial_\mu B_\nu - \partial_\nu B_\mu \tag{1.16}$$

Finally, scalar bosons are spin-0 particles modelled by Klein-Gordon equation

$$(\Box + m^2)\phi = 0 \tag{1.17}$$

As far as we know, the *Higgs Boson* is the only fundamental scalar in the Standard Model:

8. Higgs doublet:

$$H = \begin{pmatrix} \phi^+ \\ \phi^0 \end{pmatrix} = \frac{1}{\sqrt{2}} \begin{pmatrix} \phi_1 + i\phi_2 \\ \phi_3 + i\phi_4 \end{pmatrix} \in (\mathbf{1}, \mathbf{2}, 1/2) \tag{1.18}$$

9. Conjugate Higgs doublet:

$$\tilde{H} = i\sigma^2 H^* \in (\mathbf{1}, \mathbf{2}, -1/2) \tag{1.19}$$

In each of the previous cases, the first two numbers in bold correspond to the dimension of the multiplets under $\mathrm{SU(3)_C} \times \mathrm{SU(2)_L}$ while the third number corresponds to their hypercharge. The electric charge Q, the third component of weak isospin I_3 and the hypercharge Y satisfies the so-called *Gell-Mann-Nishijima formula*

$$Q = I_3 + Y \tag{1.20}$$

Finally, the Standard Model contains 26 free parameters that have to be input by hand. There are the Yukawa couplings y_i of the 12 fermions, the three gauge couplings g, g' and g_s, the 2 parameters describing the Higgs potential, μ and λ, the 8 mixing angles of the PMNS and CKM matrices, and the strong CP phase θ.

1.3 Strong Interaction

The existence of certain similarities between QCD and CH models makes it worthwhile to review some relevant aspects of the first theory.

1.3.1 Basic Structure

The strong interaction is described by *Quantum Chromodynamics* (QCD), which is a non-abelian gauge theory based on a local symmetry $\mathrm{SU}(3)_\mathrm{C}$. Each quark flavour constitutes a color triplet in the fundamental representation of $\mathrm{SU}(3)_\mathrm{C}$. All other particles are color singlets and do not experience strong interactions. The corresponding gauge fields (i.e. the *gluons*) transform under the complexified adjoint representation of the real Lie algebra $\mathfrak{su}(3)$, namely

$$\mathfrak{sl}(3;\mathbb{C}) \cong \mathbb{C} \otimes \mathfrak{su}(3) \tag{1.21}$$

while the gauge invariance ensures that they are massless. The QCD Lagrangian may be written as

$$\mathcal{L}_\mathrm{QCD} = -\frac{1}{4} G^A_{\mu\nu} G^{A\mu\nu} + \sum_j \bar{Q}_j (i\not{D} - m_j) Q_j \tag{1.22}$$

$$= -\frac{1}{4} G^A_{\mu\nu} G^{A\mu\nu} + \sum_j \sum_{\alpha,\beta} \bar{Q}^\alpha_j (i\gamma^\mu (\delta_{\alpha\beta}\partial_\mu + i g_s t^A_{\alpha\beta} G^A_\mu) - m_j \delta_{\alpha\beta}) Q^\beta_j \tag{1.23}$$

where $j \in \{u, d, c, s, t, b\}$ is a flavour index and $\alpha, \beta \in \{r, g, b\}$ are color indices. Here g_s is the *strong coupling constant*, t^A are the generators of $\mathrm{SU}(3)_\mathrm{C}$ related to the Gell-Mann matrices by $t^A = \lambda^A/2$, and the structure constants f_{ABC} are defined by

$$[t^A, t^B] = i f_{ABC} t^C \tag{1.24}$$

The gluon field tensor $G^A_{\mu\nu}$ is given by Eq. 1.14 while the covariant derivative is defined by

$$D_\mu = \partial_\mu + i g_s G_\mu \tag{1.25}$$

where

$$G_\mu = \sum_{A=1}^{8} G^A_\mu(x) t^A \tag{1.26}$$

is the so-called *gluon potential matrix*.

1.3.2 Asymptotic Freedom

The strong coupling constant g_s is not quite constant, but it depends on the characteristic energy scale of the processes. From the renormalization group equation, the *strong structure constant*

$$\alpha_s := \frac{g_s^2}{4\pi} \tag{1.27}$$

can be shown to have the following 1-loop scale-dependence:

$$\alpha_s(Q^2) \simeq \frac{4\pi}{\beta_0 \ln(Q^2/\Lambda^2_{\rm QCD})} \tag{1.28}$$

as a function of the *momentum transfer scale* Q^2. Here $\beta_0 = 11 - 2n_f/3$ with n_f the number of active quark flavor. Moreover, one of the striking properties of QCD is *asymptotic freedom* [3, 4] which states that

> *the strong coupling α_s increases with increasing distance or decreasing scale and decreases with decreasing distance or increasing scale.*

This strange behavior of the strong coupling has been verified in high-energy experiments to very high precision [5]. Indeed, from 1.28

$$\lim_{Q^2\to\infty} \alpha_s(Q^2) = 0 \tag{1.29}$$

hence the term asymptotic freedom. The integration constant

$$\Lambda_{\rm QCD} \simeq 250 \text{ MeV} \tag{1.30}$$

is an intrinsic scale of QCD, known as *confinement scale*. This parameter establish the scale at which non-perturbative effects take over. For energy scales much above $\Lambda_{\rm QCD}$ the theory is weakly coupled (asymptotic freedom). On the other hand, for small scales (i.e. for $Q^2 \to \Lambda^2_{\rm QCD}$) the running coupling diverges[5] and the theory is strongly coupled (confinement), signalling the breakdown of perturbation theory and any ideas of treating quarks as quasi-free particles. Consequently, a phase transition must occur when energy scale varies from higher to lower one.

The strong interaction scale $\Lambda_{\rm QCD}$ allows us to introduce the notion of *light quarks*, the ones having masses much smaller than the strong scale, and *heavy quarks*, the ones having masses much larger than strong scale. The up and down flavours are qualified for light quarks, whereas the charm, bottom, and top may be regarded as heavy. The strange quark is an exception.

1.3.3 Chiral Symmetry Breaking

Let us focus on the *massless* quark term that could be identified from the Lagrangian 1.22, namely

$$\mathcal{L}_{\rm Q}[Q_j] = \sum_j \bar{Q}_j i \not{D} Q_j \tag{1.31}$$

Any quark field Q_j can be decompose as a linear combination of its chiral components: $Q = Q_{\rm jL} + Q_{\rm jR}$. If we plug this decomposition into the QCD Lagrangian 1.31, then we can write

$$\mathcal{L}_{\rm Q}[Q_j] = \mathcal{L}_{\rm Q}[Q_{jL}] + \mathcal{L}_{\rm Q}[Q_{jR}] \tag{1.32}$$

[5] Because of this, $\Lambda_{\rm QCD}$ is also called the *Landau pole of QCD*; other terms found in the literature are the *strong interactions scale*, *QCD scale* or *hadronic mass scale*.

and the QCD interaction does not couple the left and right-handed quarks. On the other hand, as an example, let us consider just *up* and *down* quark flavours. Still under the massless assumption, we can write the quark term as

$$\mathcal{L}_{\rm Q}[u,d] = \sum_{i=u,d} \bar{Q}_{jL} i\not{D} Q_{jL} + \sum_{i=u,d} \bar{Q}_{jR} i\not{D} Q_{jR} \tag{1.33}$$

$$= \begin{pmatrix} \bar{u}_L & \bar{d}_L \end{pmatrix} i\not{D} \begin{pmatrix} u_L \\ d_L \end{pmatrix} + \begin{pmatrix} \bar{u}_R & \bar{d}_R \end{pmatrix} i\not{D} \begin{pmatrix} u_R \\ d_R \end{pmatrix} \tag{1.34}$$

and so the up and down quarks may be regarded as two independent states of a new same object, conveniently called *left* or *right chiral doublet*. The Lagrangian 1.33 is invariant under the independent rotations of left and right doublets in their respective spaces. More explicitly,

$$\begin{pmatrix} u_{L,R} \\ d_{L,R} \end{pmatrix} \mapsto U_{L,R} \begin{pmatrix} u_{L,R} \\ d_{L,R} \end{pmatrix} \tag{1.35}$$

where $U_{L,R} \in \mathrm{SU(2)_{L,R}}$. We then say that the massless quark part 1.33 of the QCD Lagrangian has a (global) *chiral symmetry*

$$G_\chi = \mathrm{SU(2)_L} \times \mathrm{SU(2)_R} \tag{1.36}$$

It turns out that non-perturbative strong effects induce the presence of quark vacuum condensates

$$\langle \Omega | \bar{u}_L^\alpha u_R^\beta | \Omega \rangle_{\rm QCD} = \langle \Omega | \bar{d}_L^\alpha d_R^\beta | \Omega \rangle_{\rm QCD} \sim -4\pi f_\pi^3 \delta_{\alpha\beta} \tag{1.37}$$

generating dynamical quark masses, even if they had zero mass in the original QCD Lagrangian. The presence of these condensates breaks spontaneously the chiral symmetry 1.36 down to the so-called *isospin subgroup*[6]

$$\mathrm{SU(2)_{L+R}} \tag{1.38}$$

which corresponds to rotations $U_L = U_R$. In fact, this is the symmetry realized in the spectrum; it is the observed *isospin symmetry*. In Eq. 1.37, $|\Omega\rangle$ is the ground state of QCD whose symmetry group is 1.38, and $f_\pi \simeq 93\,\mathrm{MeV}$ is the so-called *pion decay constant*. Note that as long as $m_u = m_d > 0$ in 1.22, the isospin symmetry is exactly conserved. According to the *Goldstone theorem*, this spontaneous breaking must leads to the appearance of massless particles in the spectrum of physical states - the Goldstone bosons - and taking place at some *chiral symmetry breaking scale* λ_χ. Indeed, they can be identified with the triplet of *pions*[7] $\pi^\pm$ and π^0 in the limit $m_u, m_d \to 0$, corresponding to pseudo-scalar mesons transforming in **3** of $\mathrm{SU(2)_{L+R}}$.

Finally, the actual small but non-zero difference between quark masses (i.e. $m_u \neq m_d > 0$) also break the chiral symmetry explicitly as well, and pions become pseudo-Nambu-Goldstone bosons (pNGBs), acquiring the small masses that we actually measure. In general, if N denotes the number of flavours presented in 1.22, then note that in the limit of equal mass quarks it possesses a global $\mathrm{SU}(N)_{\rm L+R}$ *isospin symmetry*, and in the limit of massless quarks an $\mathrm{SU}(N)_{\rm L} \times \mathrm{SU}(N)_{\rm R}$ *chiral symmetry* is present.

[6] Also called the *vector subgroup*.

[7] According to the Goldstone theorem there is one massless boson for each generator of a broken continuous symmetry. Since $\mathrm{SU(2)_L} \times \mathrm{SU(2)_R} \to \mathrm{SU(2)_{L+R}}$, then $(3+3) - 3 = 3$; hence the three pions.

1.3.4 Color Confinement

One of the prominent features of QCD at low-energy is *color-confinement*, which states that:

> *any strongly interacting system at zero temperature and density must be a color singlet at distance scales larger than* $1/\Lambda_{QCD}$.

The traditional physical interpretation of it consists in that at distances of order

$$\frac{1}{\Lambda_{\rm QCD}} \sim \mathcal{O}(10^{-15}\ \text{m}) \tag{1.39}$$

interaction of quarks becomes very strong, and as a consequence isolated free quarks cannot exist in nature (quark confinement). The color confinement of QCD is a theoretical conjecture consistent with experimental facts; it remains as one of the most difficult problems in theoretical particle physics [6].

1.3.5 QCD Phase Diagram

In summary, the essential features of hadron structure are color confinement and spontaneous chiral symmetry breaking. The former binds colored quarks interacting through coloured gluons to color-neutral hadrons; the latter brings in pions as Goldstone bosons and gives the essentially massless quarks in the QCD Lagrangian a dynamically generated effective mass.

Nevertheless, both features will come to an end when hadronic matter is brought to sufficiently high *temperatures* T or *baryon chemical potential*[8] μ_B. Indeed, putting both concepts together, we obtain a speculative *QCD phase diagram* as illustrated in Fig. (1.1); a central goal of heavy ion collision experiments is to map this phase diagram of as a function of both thermodynamic parameters [7–9]. In what follows, we proceed to comments a little about the different regions present in the diagram:

i. For low temperature and low net baryon density, we have *hadronic matter* as confined phase.

ii. For high temperature and high baryon chemical potential, deconfinement sets in and the chiral symmetry is restored, resulting in a phase consisting of unbound colored quarks and gluons, called *quark-gluon plasma* (QGP). In heavy ion collision, reducing the beam energy increases the μ_B of the QGP produced [10, 11] (principally because lower energy collisions make less entropy but also because they deposit more of their baryon number in the plasma) but it also reduces the temperatures achieved.

iii. Along the baryon chemical potential axis, and for low temperature, we are compressing cold nuclear matter and we can reach a region of color deconfinement alongside a state of broken chiral symmetry [12], i.e. *quarkyonic matter* [13–15], and whose formation requires only weak attractive interactions. In such a scenario, color deconfinement would result in a plasma of massive, unbound, and "dressed" quarks; the only role of gluons in this state would be to dynamically generate the effective quark mass, maintaining spontaneous chiral symmetry

[8] The discussion is sometimes also given in terms of *Net Baryon Density*, i.e. the density of baryons minus the density of antibaryons.

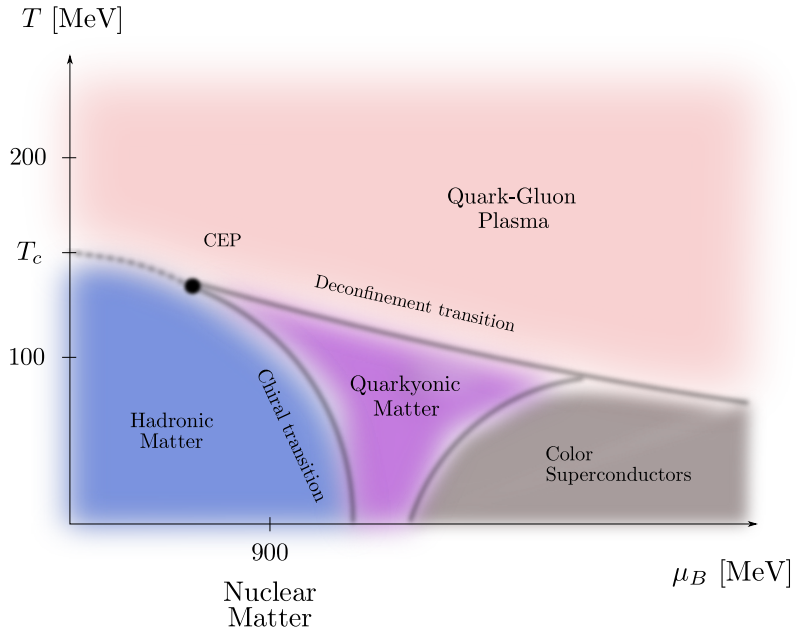

Figure 1.1: A speculative phase diagram for strongly interacting matter. The QCD vacuum in which we live, which has the familiar hadrons as its excitations, is but one phase of QCD, and far from the simplest one at that. Because of asymptotic freedom, the high temperature and high baryon density phases of QCD are more simply and more appropriately described in terms of quarks and gluons as degrees of freedom, rather than hadrons [7].

breaking. They can moreover also combine to coloured bosonic *diquarks*. Deconfinement at high density is believed to happen in the interior of neutron stars, where nuclear matter is compressed under the star's own weight to up to 10 times the normal nuclear density.

iv. At lower temperatures or higher densities, the above diquarks could condense to form a *color superconductor* [16–18]. Conversely, heating such a superconductor would "evaporate" or "melt" the condensate, just as it does for a normal superconductor, and we recover either the massive quark phase, or the conventional QGP with restored chiral symmetry. The transition between this two phases is likely first order.

v. Along the temperature axis, at zero μ_B, the phase diagram features a *crossover*[9] from QGP

[9]Roughly speaking, *crossover* is a generic term to describe a smooth transition between two separate phases of matter, upon changing some (thermal/non-thermal) parametres. The key point is that in a crossover, no canonical "phase transition" occurs, although there is a drastic change in the phase of the system. Phase transitions are classically defined à la Ehrenfest (discontinuities in the derivatives of the Free energy functional) or à la Landau (symmetry-breaking mechanisms). A crossover is thus not associated with a change of symmetry, or a discontinuity in the free energy functional, but typically it occurs in a region of the phase diagram, rather than a singular point. Microscopically, in a crossover, the ground-state of the system changes radically (so that any perturbative expansion around the original ground-state will fail to capture the new ground-state), but in a very smooth manner; i.e., without any discontinuity in the thermodynamic observables (which is the hallmark of phase transitions).

to ordinary hadronic matter as a function of decreasing T [19–21]. Increasing μ_B corresponds to doping the QGP with an excess of quarks over antiquarks, and it is an open question whether the crossover becomes a sharp first order phase transition beyond some critical point (*CEP*) [9, 22]. By increasing the temperature, the surround constituent quark cloud[10] melts away and at som critical temperature T_c, it has "evaporated", leaving pointlike quarks and gluons. Here, T_c is known as the *critical temperature transition* and it is now well established that the QCD transition is just a rapid crossover at [23–25]

$$T_c \simeq 155\,\text{MeV} \tag{1.40}$$

In this region there remains only one transition, the simultaneous onset of color deconfinement and chiral symmetry restoration. A priori there is no reason for both the (de)confinement and chiral symmetry restoration scales to be the same [26]. However, lattice studies[11] at $\mu_B = 0$ have shown that there deconfinement and chiral symmetry restoration in fact coincide [27]. Deconfinement by heating up nuclear matter is achieved by colliding heavy nuclei at enormous energies, for example at the Relativistic Heavy Ion Collider (RHIC), or at the Large Hadron Collider (LHC).

It turns out that the picture presented by lattice QCD for $T \geq 0$ and $\mu_B = 0$ cannot be easily extended to the case of nonzero μ_B. In these cases, lattice calculations become extremely difficult [28] mainly because standard Monte Carlo simulations can only be applied to the case where either $\mu_B = 0$ or it is purely imaginary. Simulations with $\mu_B \neq 0$ are hindered by the sign problem, see, for example, [28], though some mathematical extensions of lattice techniques [29–31] can probe this region[12]. Also, the scaning of the diagram (1.1) is complicated from a theoretical point of view due to the absence of first-principles theoretical calculations providing reliable guidance, as to the whether there is a critical point in the phase diagram of QCD, or its location if it does exist [7, 32] (model calculations suggest the existence of a critical point, but disagree wildly on its location in the (μ_B, T) plane).

1.4 Electroweak Interaction

1.4.1 Basic Structure

The electroweak theory is based on the gauge group $\text{SU(2)}_\text{L} \times \text{U(1)}_\text{Y}$. The Lagrangian describing the electroweak interactions is

$$\begin{aligned}\mathcal{L}_\text{EW} = &-\frac{1}{4}W^I_{\mu\nu}W^{I\mu\nu} - \frac{1}{4}B_{\mu\nu}B^{\mu\nu} \\ &+ (D_\mu H)^\dagger (D^\mu H) - \mu^2 (H^\dagger H) - \lambda (H^\dagger H)^2 \\ &+ \bar{L}_{jL} i \not{D} L_{jL} + \bar{e}_{jR} i \not{D} e_{jR} + \bar{Q}_{jL} i \not{D} Q_{jL} + \bar{u}_{jR} i \not{D} u_{jR} + \bar{d}_{jR} i \not{D} d_{jR} \\ &+ (y^e_{ij} \bar{L}_{iL} H e_{jR} + y^d_{ij} \bar{Q}_{iL} H d_{jR} + y^u_{ij} \bar{Q}_{iL} \tilde{H} u_{jR} + \text{h.c.})\end{aligned} \tag{1.41}$$

[10] A *constituent quark* is understood as a *current quark* surrounded by a cloud of virtual quarks and virtual gluons excited from the "sea". This cloud underlies the so-called *constituent quark mass*. In this way, hadrons consist of "glued" constituent quarks.

[11] *Lattice QCD* is a discretized version of QCD in the Euclidean space time which reproduces QCD when the lattice spacing goes to zero, that is in the continuum limit.

[12] Schwinger-Dyson equation techniques can also be employed to explore all region of the phase space [33, 34]

where the matrices $y_{ij}^{e,d,u}$ describe the *Yukawa couplings* between the single Higgs doublet H, and the various flavours i and j of quarks and leptons. In the above, right-handed neutrinos could be added, but since they are not necessary for the consistency of the theory, and it is not certain whether they exist or are part of the low-energy theory, we have not added them to the picture. The interactions are encoded in the covariant derivative

$$D_\mu = \partial_\mu + ig\frac{\sigma^I}{2}W_\mu^I + ig'YB_\mu \tag{1.42}$$

which for every particular case are given by

$$D_\mu Q_{iL} = \left(\partial_\mu + ig\frac{\sigma^I}{2}W_\mu^I + ig'\frac{1}{6}B_\mu\right)Q_{iL} \qquad D_\mu L_{iL} = \left(\partial_\mu + ig\frac{\sigma^I}{2}W_\mu^I - ig'\frac{1}{2}B_\mu\right)L_{iL}$$
$$D_\mu u_{iR} = \left(\partial_\mu + ig'\frac{2}{3}B_\mu\right)u_{iR} \qquad D_\mu e_{iR} = (\partial_\mu - ig'B_\mu)e_{iR}$$
$$D_\mu d_{iR} = \left(\partial_\mu - ig'\frac{1}{3}B_\mu\right)d_{iR} \qquad D_\mu H = \left(\partial_\mu + ig\frac{\sigma^I}{2}W_\mu^I + ig'\frac{1}{2}B_\mu\right)H$$

with g and g' being the $\mathrm{SU(2)_L}$ and $\mathrm{U(1)_Y}$ gauge couplings, respectively. The $\mathrm{SU(2)_L}$ generators are Pauli spin matrices obey the usual relation

$$[\sigma^I, \sigma^J] = 2i\varepsilon_{IJK}\sigma^K \tag{1.43}$$

The different transformations of the L and R fields (i.e. $\mathrm{SU(2)_L}$ is a chiral symmetry) is the origin of parity violation in the electroweak sector. This also forbids any bare mass terms for the fermions.

1.4.2 The Electroweak Symmetry Breaking

Gauge invariance does not allow mass terms in the Lagrangian neither for the gauge bosons nor for chiral fermions. However, massless gauge bosons are not acceptable for the weak interactions, which are known to be short-ranged, so that the gauge invariance must be spontaneously broken. The Standard Model incorporates the minimal mechanism for the spontaneous symmetry breaking of the electroweak sector

$$\begin{array}{c}\mathrm{SU(2)_L \times U(1)_Y}\\ \Big\downarrow \\ \mathrm{U(1)_{EM}}\end{array} \tag{1.44}$$

through the so-called *Higgs mechanism* [35–37], and which preserves the renormalizability of the gauge theory [38]. In order to achieve the EWSB, the lowest energy state (i.e. the *vacuum* of the theory, and denoted by $|\Omega\rangle$) must not respect the gauge symmetry. The breaking is triggered for the choice $\mu^2 < 0$ in the Higgs sector

$$\mathcal{L}_{\mathrm{Higgs}} = (D_\mu H)^\dagger (D^\mu H) - \mu^2 (H^\dagger H) - \lambda (H^\dagger H)^2 \tag{1.45}$$

which is clearly[13] $\mathrm{O}(4) \sim \mathrm{SU}(2)_\mathrm{L} \times \mathrm{SU}(2)_\mathrm{R}$ invariant (see 1.18). The Higgs doublet then acquires a non-zero vacuum expectation value (vev):

$$v := \langle \Omega | H | \Omega \rangle \equiv \text{constant} \tag{1.46}$$

which in turn is a function of the vev's $v_i := \langle \Omega | \phi_i | \Omega \rangle$. The vev v can be determined by rewriting the Higgs potential as

$$V(H) \to V(v_i) = \frac{1}{2}\mu^2 \left(\sum_{i=1}^{4} v_i^2 \right) + \frac{1}{4}\lambda \left(\sum_{i=1}^{4} v_i^2 \right)^2 \tag{1.47}$$

and choosing the v_i's in such a way that V is minimized; this yield the condition

$$v_1^2 + v_2^2 + v_3^2 + v_4^2 = -\frac{\mu^2}{\lambda} \tag{1.48}$$

This picks out a vacuum manifold of degenerate vacuum states (all of which have a vev equal to v), isomorphic to S^3 in four dimensions. Now, and without loss of generality, we can choice the neutral component of the Higgs doublet with a non-zero vev; to be precise $\langle \Omega | \phi_i | \Omega \rangle = 0$ for $i = 1, 2, 4$ and $\langle \Omega | \phi_3 | \Omega \rangle = v$, so that

$$\langle \Omega | H | \Omega \rangle = \frac{1}{\sqrt{2}} \begin{pmatrix} 0 \\ v \end{pmatrix} \tag{1.49}$$

and v given by $v^2 = -\mu^2/\lambda$. This vacuum is still invariant under the SO(3) rotations of the first three dimensions. This corresponds to spontaneous breaking of symmetry from SO(4) to SO(3), analogue of the isospin group. While the generators T^1, T^2, and $T^3 - Y/2$ are spontaneously broken, the generator $T^3 + Y/2$ is not, so the $\mathrm{U}(1)_\mathrm{EM}$ of electromagnetism is not broken. Thus, the electroweak $\mathrm{SU}(2)_\mathrm{L} \times \mathrm{U}(1)_\mathrm{Y}$ group is spontaneously broken to the $\mathrm{U}(1)_\mathrm{EM}$ subgroup[14]. We then redefined the neutral component by $\phi^0 = (h + v)/\sqrt{2}$, such that the physical field h (i.e. the *Higgs field*) has a vanishing vev and positive mass squared. The Lagrangian of the Higgs sector expanded around a new minimum $\mathrm{U}(1)_\mathrm{EM}$ describes three massless Nambu-Goldstone bosons (NGBs) which are "eaten" as longitudinal component to form three massive vector bosons, $W^\pm$ and Z, and a massless vector boson γ, namely

$$W_\mu^\pm = \frac{1}{\sqrt{2}} \left(W_\mu^1 \mp i W_\mu^2 \right), \qquad \begin{pmatrix} Z_\mu \\ A_\mu \end{pmatrix} = \begin{pmatrix} \cos\theta_W & -\sin\theta_W \\ \sin\theta_W & \cos\theta_W \end{pmatrix} \begin{pmatrix} W_\mu^3 \\ B_\mu \end{pmatrix} \tag{1.50}$$

plus one massive mode with mass $m_h^2 = 2\lambda v^2 = -2\mu^2$, the *Higgs boson*. The two couplings g, g' can be expressed by the weak angle θ_W and the electromagnetic charge e as

$$g = \frac{e}{\sin\theta_W}, \qquad g' = \frac{e}{\cos\theta_W} \tag{1.51}$$

Remarkably, the electric coupling is smaller than the weak one: weak interactions are weak because the mass of m_W implies a short range, not because the coupling is small. The symmetry breaking thus results in masses for vector fields

$$m_W = \frac{1}{2} g v \quad \text{and} \quad m_Z = \frac{1}{2} v \sqrt{g^2 + g'^2} \tag{1.52}$$

[13] Here, $\sim$ stands for *locally isomorphic*.

[14] Note that the $\mathrm{U}(1)_\mathrm{EM}$ would be broken as well if the ϕ^+ field were also allowed to obtain a vev.

and for fermions

$$m_f = \frac{1}{\sqrt{2}} y_f v \tag{1.53}$$

1.5 Effective Field Theories

1.5.1 Effective Lagrangians

The Standard Model of the strong and electroweak interactions has been successfully tested to a great precision. For example, the *Electroweak Precision Tests* (EWPTs) [39] performed in the last few decades have achieved great success in establishing the model 1.41 as the correct description of electroweak physics. Nevertheless, it is commonly accepted that the model does not have the trademark of a really fundamental theory which allows predictions up to arbitrary high energy scales, but it corresponds to a low energy description of a more fundamental theory just applicable up to energies not exceeding a certain scale Λ_{SM} above the EW scale. This perspective defines the SM as an *effective field theory*[15] (EFT), i.e. a theory valid at energies below some scale at which new degrees of freedom or other phenomena might manifest themselves. The basic premise of effective theories is that

> *the dynamics at low energies (or large distances) does not depend on the details of the dynamics at high energies (or short distances). As a result, low energy physics can be described using an effective Lagrangian that contains only a few degrees of freedom, ignoring additional degrees of freedom present at higher energies.*[16]

An EFT allows to consider a quantum field theory with a fundamental energy scale Λ at some energies E much smaller than Λ, so that all observables will be expanded in powers of E/Λ what allows to truncate higher energy contributions. The idea of EFTs are implicit in all descriptions of physical phenomena. In particular, they are relevant in CH models because allow to systematically investigate TeV-scale models without knowing the underlying high energy dynamics. Also, a key observation in favour of the EFT approach is that the relevant effective operators are actually much fewer than the vast possibilities of physics beyond the SM. The reduction to the Standard Model at low energies proceeds via decoupling of heavy particles with masses of order Λ_{SM} or larger; such a decoupling at the perturbative level is described by the Appelquist-Carazzone theorem. The natural criterion on whether an EFT description collapses or not is to check its unitarity. This claim bases on the fact that EFTs does not describe all of the fundamental degrees of freedom of the underlying theory. When energy is higher than the characteristic scale of the EFT, some new degrees of freedoms will be excited consequently the unitarity is lost. Fermi's theory of weak interaction is a well known example.

Effective field theories are used in two distinct ways, namely the *top-down approach* and *bottom-up approach*. In the former case, the high energy theory is well understood, but we find it useful to have a simpler theory to do low energy physics. We integrate out heavier particles and match onto

[15] See, e.g. [40–42] for detailed reviews on EFTs.

[16] Naturalness, from this perspective, is the assertion that features of this effective field theory should not be extremely sensitive to the structure of the underlying theory.

a low energy theory. This procedure yields new operators and new low energy couplings. More specifically, we expand the full Lagrangian as a sum of terms of decreasing relevance

$$\mathcal{L}_{\text{high}} \overset{\text{IR}}{\simeq} \mathcal{L}_{\text{low}} = \sum \mathcal{L}_{low}^{(n)} \tag{1.54}$$

where the sum in n is an expansion in decreasing relevance. The Lagrangians $\mathcal{L}_{\text{high}}$ and $\mathcal{L}_{\text{low}}$ will agree in the infrared (IR), but will differ in the ultraviolet (UV), and the only remnants of the high-energy dynamics are in the low-energy couplings and in the symmetries of the EFT. The desired precision tells us when to stop, i.e. how far we go with the sum on n. In the latter case, the underlying theory is unknown and we construct the EFT without reference to any other theory. Even if the underlying theory is known, we can also consider constructing the EFT from the bottom-up if the matching is difficult, for example if the matching would have to be non-perturbative in a coupling and hence is not possible analytically. Most of CH models are almost completely indifferent to the way the theory looks in the far UV. They are work in a bottom-up approach considering only composite resonances, but not the fields they are composed from. The advantage of this approach is less "model-dependence" which allows us to investigate the general idea of compositeness and its compatibility with current experimental data.

1.5.2 The Standard Model as an EFT

A search for new physics in the Higgs sector can either involve examination of specific models or the use of effective field theories respecting the symmetries of the low energy physics. If the latter approach is chosen and it is assume that the SM is a good approximation to physics at the weak scale, then the Higgs properties and its deviations from the SM can be conveniently parametrized and systematically studied by a bottom-up effective Lagrangian of the form

$$\mathcal{L}_{\text{eff}} = \mathcal{L}_{\text{EW}} + \sum_{n=1}^{\infty} \frac{c_n}{\Lambda^n} \mathcal{O}_n \tag{1.55}$$

where $\mathcal{L}_{\text{EW}}$ is given by 1.41 containing two- and four-dimensional operators only, $\mathcal{O}_n$'s are $(4+n)$-dimensional operators containing only SM fields, c_n's stand for the corresponding *Wilson Coefficients* (dimensionless coupling constants containing all information about short-distance physics above the scale Λ), and the series itself is an expansion in decreasing relevance with Λ an energy scale of $\mathcal{O}$(TeV). Here, the effective theory breaks down if the new physics contains physical states much lighter than 1 TeV, since there would not be an energy scale that distinctly separates the new physics from the SM; the dominant contributions of the new states can often be captured in a few effective operators. The Lagrangian 1.55 is then used at energy scales much below Λ, where the observed physics approximates the SM up to small corrections. While the higher dimensional operators

$$\Delta\mathcal{L}_{\text{eff}} := \sum_{n=1}^{\infty} \frac{c_n}{\Lambda^n} \mathcal{O}_n = \sum_{n=1}^{\infty} \mathcal{L}_{\text{eff}}^{(n)} \tag{1.56}$$

are generated at the new physics scale Λ, they are measured at the lower scale of the experiments. Since we are interested in extensions of the SM, then 1.55 must satisfy the following requirements

1. All effective operators $\mathcal{L}_{\text{eff}}^{(n)}$ are G_{SM}-invariant. This follows from requiring that the electroweak breaking is indeed a phenomenon connected to the electroweak scale and not to Λ, i.e. that for energies above the EW scale the complete Lagrangian is $\text{SU}(2) \times \text{U}(1)$-symmetric.

2. The theory contains the assumption that no additional fields are present, such as coloured scalars with masses $\mathcal{O}(M_W)$.

Once 1.55 is defined, the theoretical prediction for a given observable X is given by

$$X_{\text{th}}(c_n) = X_{\text{SM}} + \sum c_n X_n \tag{1.57}$$

where X_{SM} is the SM prediction including loop corrections and X_n is the correction to X from the operator $\mathcal{O}_n$. After obtaining X_{th}, we can compare the theoretical predictions with the measured value X_{ex} of X and get constraints on the coefficients c_n.

2 The SM Higgs Boson

2.1 Physics at the LHC

2.1.1 The Large Hadron Collider

The Large Hadron Collider (LHC) not only is the world's largest and most powerful particle accelerator but it is also the world's largest machine, consisting of a 27-kilometre ring of superconducting magnets with a number of accelerating structures to boost the energy of the particles along the way. The LHC is a proton-proton collider (although it also operates with collisions of proton on nuclei, and nuclei on nuclei), located approximately 100 m underground and straddling the border between France and Switzerland. The LHC occupies the tunnel formerly used for the LEP accelerator in which electrons and positrons collided at center-of-mass energies up to 209 GeV. The LHC contains 9593 magnets of different varieties and sizes which are used to direct the beams around the accelerator. These include 1232 superconducting dipole magnets 15 m in length which bend the beams, and 392 quadrupole magnets, each 5-7 metres long, which focus the beams, being capable finally of producing magnetic fields of the order of 8.4 T at a current of 11.7 kA, and a maximum proton beam energy of 7 TeV, leading to a maximum collision energy of 14 TeV. At full power, the LHC will collide 2808 proton bunches or bunch trains, each approximately 30 cm long and 16 microns in diameter and containing 1.1×10^{11} protons, designed to reach a peak luminosity of $10^{34}\,\text{cm}^{-2}\text{s}^{-1}$ or $10\,\text{nb}^{-1}\text{s}^{-1}$ and a billion proton-proton collisions per second. The spacing between the bunches is 25 ns leading to collisions occurring every 25 ns (this is called the *interbunch crossing time*); thus, at full luminosity there will be on average 25 interactions every beam crossing, most of which will be relatively uninteresting.

2.1.2 Proton-Proton Collisions

Most of the particles of the SM have short lifetimes and cannot be found by themselves in nature. This makes the study of these particles rather difficult. In order to more thoroughly understand and study the particles of the SM, it is necessary to produce them artificially. This can be done in one of several ways; however, the most common way is by colliding stable energetic particles

together that have accessible energies greater than the rest mass of the particle of interest. The available energy in a collision between two particles can be characterized by a Mandelstam variables s (a Lorentz-invariant), given by

$$s := (p_1 + p_2)^2 = (E_1 + E_2)^2 - (\vec{p}_1 + \vec{p}_2)^2 \tag{2.1}$$

where p_i is the four-momentum of incoming particle i, E_i is its energy, and $\vec{p}_i$ is its momentum vector. The total energy available for physics experiments is maximized in the centre-of-momentum frame ($\vec{p}_1 = -\vec{p}_2$), in which case the total centre-of-momentum energy is

$$E_{\mathrm{CoM}} = \sqrt{s} = E_2 + E_1 \tag{2.2}$$

The LHC collides protons because they are relatively easy to obtain, their ability to achieve high rates of collisions, and their minimal energy loss due to radiation when accelerated in a circle (i.e. the LHC tunnel), compared to electrons. However, several additional issues do arise when colliding protons. Protons are not fundamental particles, but a pretty sophisticated object. Over the last half century, an understanding of the proton has developed in which it contains three *valence quarks* embedded into a so-called *sea*, this last one defined as the collective and continuous presence of virtual quark-antiquark pairs (referred as *sea quarks*) and gluons within the interior of the proton; all of these particles -valence quarks, sea quarks and gluons- are generically referred as *partons*. The existence of the sea is allowed and governed by the uncertainty principle, which implies that they annihilate after a certain short period of time. The flavours of the three valence quarks determine many of the characteristics of the proton, but the strong force and the sea of antiquark-quark pairs are primarily responsible for its mass. Experimentally, this picture was established based on a variety of probes, one of the most important being *deep inelastic scattering* (DIS).

Every parton carry a non-negligible amount of the proton momentum. The momentum distribution functions $f_i(x,Q^2)$ of the partons within the proton are simply called *Parton Distribution Functions*[17] (PDFs) when the spin direction of the partons is not considered. They represent the probability density of finding a parton i with longitudinal momentum fraction x (or equivalently, with momentum $p = xP$) inside a proton that carries a momentum P at a energy scale Q^2. Parton distribution functions are very important in proton-proton collisions, since calculating the cross section for a specific hard parton process $\sigma(pp \to FX)$ of two protons[18] to produce a final state F or our interest, is accomplished by summing over the sub-process cross sections convoluted in each case with the parton distribution functions f_i and f_j, namely

$$\sigma_{pp\to FX} = \sum_{i,j} \int_0^1 \int_0^1 f_i(x_1, Q^2) f_j(x_2, Q^2) \sigma_{ij\to F}(x_1 P_1, x_2 P_2, Q^2)\, dx_1 dx_2 \tag{2.3}$$

where X is the inclusive scattering remnant, i, j are the possible initial state partons (gluon, up quark, etc.), P_1 and P_2 are are the initial momenta of the protons, and $\sigma_{ij\to F}$ is the cross section for the specific process, derived as a function of initial state momenta and energy scale, Q^2. Consequently, the detailed knowledge of the PDFs for the proton is an essential component in the calculation of the expected Higgs boson production rate at the LHC. Fortunately, the proton PDFs are well known and the related uncertainties on the various Higgs production cross sections are less than 10%.

[17] For an introduction to this topic, see for example [43].

[18] The discussion is generalizable to other hadrons.

2.1.3 Luminosity

Two very important parameter characterizing the performance of a particle collider are the *instantaneous luminosity* and the *integrated luminosity*. The instantaneous luminosity $\mathcal{L}$ is the number of particles passing each other per unit time through unit transverse area at the interaction point, with typical units $\mathrm{cm}^{-2}s^{-1}$. This value is a function of several beam parameters, such as the number of protons per bunch, the number of bunches, revolution frequency, as well as many other beam specific characteristics. The reaction rate R is the number of scattering events per unit time for a given process, and is given by[19]

$$R(s) = \frac{dN}{dt}(s) = \sigma(s)\mathcal{L} \tag{2.4}$$

where $\sigma(s)$ is the total scattering cross section at squared CoM energy s. In the case of two colliding beams like in the LHC, the beam density distribution is important in order to obtain an expression for $\mathcal{L}$. For the often fully justified Gaussian distributions, the luminosity is given by

$$\mathcal{L} = \frac{1}{4\pi}\frac{N_1 N_2}{\sigma_x \sigma_y} k_B f_{\mathrm{ref}} \tag{2.5}$$

where N_i is the number of particles per bunch, f_{rev} is the revolution frequency of the beams, k_B is the number of bunches, and σ_j are the standard deviations associated to the Gaussian profile distributions of the beams.

The maximum luminosity, and therefore the instantaneous number of interactions per second, is very important, but the final figure of merit is the so-called integrated luminosity. Over a period of time $\Delta t = t_2 - t_1$, the number of events of interest for the given process is simply the integral of the previous equation

$$N = \sigma \int_{t_1}^{t_2} \mathcal{L}\, dt = \sigma L \tag{2.6}$$

where the cross section can be factored out of the integral as it is independent of time. The integral

$$L := \int_{t_1}^{t_2} \mathcal{L}\, dt \tag{2.7}$$

is the *integrated luminosity*, with units of cm^{-2}, though the use of pb^{-1} or fb^{-1} (inverse pico- or femto-barns) is more common, with

$$1\,\mathrm{b} = 10^{-24}\,\mathrm{cm}^2 \simeq 2570.7\,\mathrm{GeV}^{-2} \tag{2.8}$$

Note that the integral must be taken over the sensitive time, i.e. excluding possible dead time. As we can see, the integrate luminosity is proportional to the total number of collisions collected. Thus, for example, if a detector has accumulated $100\,\mathrm{fb}^{-1}$ of integrated luminosity, one expects to find 100 events per femtobarn of cross-section within these data. The total data set obtained in 2010 at the LHC, for example, was $0.04\,\mathrm{fb}^{-1}$, compared to $5\,\mathrm{fb}^{-1}$ collected in 2011. Large integrated luminosities correspond to large data sets, which allow for the study of rare processes.

[19] There will be another factor $\epsilon < 1$ on the right-hand side, which represent the detection efficiency.

2.2 The SM Higgs Boson

Since the discovery of the Higgs boson, it has been of utmost importance to perform a detailed experimental investigation of its fundamental properties, a crucial requirement to establish the Higgs mechanism as the basic way to generate the masses of the known particles. To this end, a very precise prediction of the production cross sections and of the branching ratios for the main decay channels is mandatory. The Higgs boson couplings to the fundamental particles are set by their masses. This is a new type of interaction, very weak for ordinary particles, such as up and down quarks, and electrons, but strong for heavy particles such as the $W^{\pm}$ and Z bosons and the top quark. More precisely, the SM Higgs couplings to fundamental fermions are linearly proportional to the fermion masses, whereas the couplings to bosons are proportional to the square of the boson masses.

2.3 Higgs Decay Channels

In principle, the Higgs boson can decay to all SM particle. However, because of the proportionality of the couplings to the mass of the particles involve **??**, the largest branching ratios are to the more massive particles.

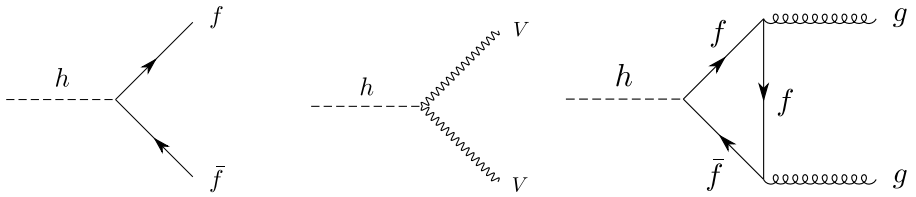

(a) Difermion Decay. (b) Divector Decay. (c) Digluon Decay.

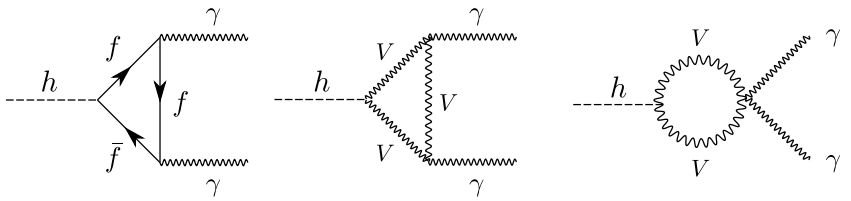

(d) Diphoton Decay.

Figure 2.1: Four relevant Higgs decay processes to be analyzed in this section.

2.3.1 Higgs Decay $h \to f\bar{f}$

The transition amplitude $\mathcal{M}(h \to f\bar{f})$ of the lowest order process (2.2) is given by

$$-i\mathcal{M}(h \to f\bar{f})(2\pi)^4\delta^4(p_1 - p_2 - p_3) = (2\pi)^4\delta^4(p_1 - p_2 - p_3)\left[\bar{u}_{s_2}(p_2)\left(-i\frac{m_f}{v}\right)v_{s_3}(p_3)\right]$$

so that

$$\mathcal{M}(h \to f\bar{f}) = \frac{m_f}{v}\bar{u}_{s_2}(p_2)v_{s_3}(p_3) \tag{2.9}$$

It follows that the average square transition amplitude is given by

$$\begin{aligned}
\langle|\mathcal{M}(h \to f\bar{f})|^2\rangle &= \sum_{\text{spin color}}\sum \mathcal{M}^*(h \to f\bar{f})\mathcal{M}(h \to f\bar{f}) \\
&= N_c \sum_{\text{spin}} \left(\frac{m_f}{m_h}\bar{v}_{s_3}(p_3)u_{s_2}(p_2)\right)\left(\frac{m_f}{m_h}\bar{u}_{s_2}(p_2)v_{s_3}(p_3)\right) \\
&= N_c \frac{m_f^2}{m_h^2}\left(\sum_{s_2}\bar{u}_{s_2}(p_2)u_{s_2}(p_2)\right)_{ji}\left(\sum_{s_3}\bar{v}_{s_3}(p_3)v_{s_3}(p_3)\right)_{ij} \\
&= N_c \frac{m_f^2}{m_h^2}\text{Tr}\left[(\not{p}_2 + m_f)(\not{p}_3 - m_f)\right] \\
&= N_c \frac{4m_f^2}{m_h^2}\left(p_2p_3 - m_f^2\right)
\end{aligned} \tag{2.10}$$

where N_c is the number of colors: 1 for leptons and 3 for quarks.

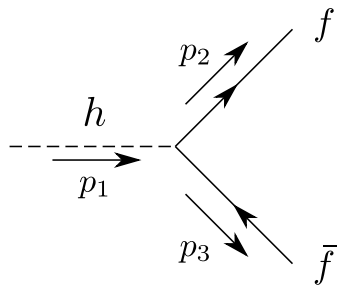

Figure 2.2: Feynman diagram describing $h \to \bar{f}f$ at lowest order.

In the COM frame, we have

$$p_1 = (m_h, \vec{0}), \quad p_2 = (E_f, \vec{p}) \quad \text{and} \quad p_3 = (E_f, -\vec{p})$$

from where

$$m_h = 2E_f \quad \text{and} \quad p_2p_3 - m_f^2 = \frac{m_h^2}{2}\left(1 - \frac{4m_f^2}{m_h^2}\right)$$

and thus 2.10 reduces to

$$\langle|\mathcal{M}(h \to f\bar{f})|^2\rangle = N_c \frac{2m_f^2m_h^2}{v^2}\left(1 - \frac{4m_f^2}{m_h^2}\right) \tag{2.11}$$

Finally, the partial decay width of the process is given by

$$\begin{aligned}\Gamma(h \to f\bar{f}) &= \frac{1}{8\pi}\frac{|\vec{p}|}{m_h^2}\langle|\mathcal{M}(h \to f\bar{f})|^2\rangle \\ &= \frac{N_c}{8\pi}\frac{m_f^2 m_h}{v^2}\left(1 - \frac{4m_f^2}{m_h^2}\right)^{3/2}\end{aligned} \tag{2.12}$$

2.3.2 Higgs Decay $h \to VV$

The transition amplitude $\mathcal{M}(h \to VV)$ of the lowest order process (2.3) is given by

$$-i\mathcal{M}(h \to VV)(2\pi)^4\delta^4(p_1 - p_2 - p_3) = (2\pi)^4\delta^4(p_1 - p_2 - p_3)\left[\epsilon_\mu^*(p_2)\left(-i\frac{2m_V^2}{v}g^{\mu\nu}\right)\epsilon_\nu^*(p_3)\right]$$

so that

$$\mathcal{M}(h \to VV) = \frac{2m_V^2}{v}\epsilon_\mu^*(p_2)\epsilon^{*\mu}(p_3) \tag{2.13}$$

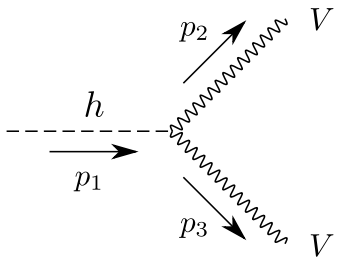

Figure 2.3: Feynman diagram describing $h \to VV$ at lowest order.

It follows that the average square transition amplitude is given by

$$\begin{aligned}\langle|\mathcal{M}(h \to VV)|^2\rangle &= \sum_{\text{spin}}\mathcal{M}^*(h \to VV)\mathcal{M}(h \to VV) \\ &= \sum_{\text{spin}}\left(\frac{2m_V^2}{v}\epsilon_\nu(p_2)\epsilon^\nu(p_3)\right)\left(\frac{2m_V^2}{v}\epsilon_\mu^*(p_2)\epsilon^{*\mu}(p_3)\right) \\ &= \frac{4m_V^4}{v^2}\left(\sum_{\text{spin}}\epsilon_\nu(p_2)\epsilon_\mu^*(p_2)\right)\left(\sum_{\text{spin}}\epsilon^\nu(p_3)\epsilon^{*\mu}(p_3)\right) \\ &= \frac{4m_V^4}{v^2}\left(-g_{\nu\mu} + \frac{p_{2\nu}p_{2\mu}}{m_V^2}\right)\left(-g^{\nu\mu} + \frac{p_3^\nu p_3^\mu}{m_V^2}\right) \\ &= \frac{4m_V^4}{v^2}\left(2 + \frac{(p_2p_3)^2}{m_V^4}\right)\end{aligned} \tag{2.14}$$

In a similar way to the previous case, we have in the CoM frame

$$p_1 = (m_h, \vec{0}), \quad p_2 = (E_V, \vec{p}) \quad \text{and} \quad p_3 = (E_V, -\vec{p})$$

from where

$$m_h = 2E_f \quad \text{and} \quad p_2 p_3 = \frac{m_h^2}{2}\left(1 - \frac{2m_V^2}{m_h^2}\right)$$

and thus 2.14 reduces to

$$\langle|\mathcal{M}(h \to VV)|^2\rangle = \frac{4m_V^4}{v^2}\left(3 + \frac{m_h^4}{4m_V^4} - \frac{m_h^2}{m_V^2}\right) \tag{2.15}$$

Finally, the partial decay width of the process is given by

$$\begin{aligned}\Gamma(h \to VV) &= \frac{\delta_V}{8\pi}\frac{|\vec{p}|}{m_h^2}\langle|\mathcal{M}(h \to VV)|^2\rangle \\ &= \frac{\delta_V}{4\pi}\frac{m_V^4}{m_h v^2}\left(1 - \frac{4m_V^2}{m_h^2}\right)^{1/2}\left(3 + \frac{m_h^4}{4m_V^4} - \frac{m_h^2}{m_V^2}\right)\end{aligned} \tag{2.16}$$

where δ_V constitutes a statistical phase factor that corrects for double-counting when there are identical particles in the final state: therefore $\delta_W = 1$ and $\delta_Z = 1/2$.

2.3.3 Higgs Decay $h \to gg$

The decay of the Higgs boson to gluons is mediated by quark loops in the SM. Despite the "loop nature" of the process, we shall see that it must be taken into consideration in view of the strong coupling between the Higgs and the top quark, which gives rise to a non-negligible decay rate contribution [44]. For every particular case, there are actually two diagrams: one as depicted in Fig. (2.4) and the other with the gluons exchanged as shown in Fig. (2.5).

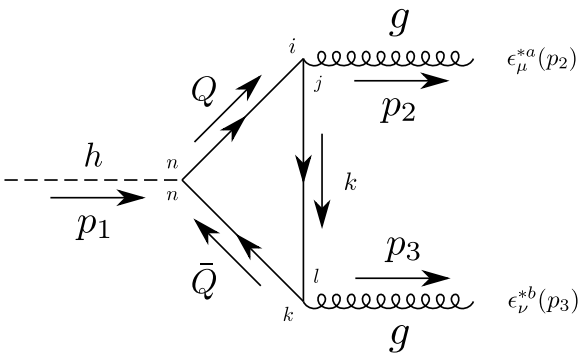

Figure 2.4: First Feynman diagram describing $h \to gg$ at lowest order.

The transition amplitude $\mathcal{M}_1(h \to gg)$ of the process shown in Fig. (2.4) is given by

$$\begin{aligned}-i\mathcal{M}_1(h \to gg)(2\pi)^4\delta^4(p_1 - p_2 - p_3) = &\int \frac{d^4q_1}{(2\pi)^4}\int \frac{d^4q_2}{(2\pi)^4}\int \frac{d^4k}{(2\pi)^4}(2\pi)^4\delta^4(p_1 - q_1 + q_2)\\ &\times (2\pi)^4\delta^4(q_1 - k - p_2)(2\pi)^4\delta^4(k - q_2 - p_3)\\ &\times (-1)\mathrm{Tr}\left[\left(-i\frac{m_Q}{v}\right)\frac{i(\not{q}_2 + m_Q)}{q_2^2 - m_Q^2}\delta_{nk}\left(-ig_s\frac{\lambda^b_{kl}}{2}\gamma^\nu\right)\right.\\ &\left.\times \frac{i(\not{k} + m_Q)}{k^2 - m_Q^2}\delta_{lj}\left(-ig_s\frac{\lambda^a_{ji}}{2}\gamma^\mu\right)\frac{i(\not{q}_1 + m_Q)}{q_1^2 - m_Q^2}\delta_{in}\right]\\ &\times \epsilon^{*a}_\mu(p_2)\epsilon^{*b}_\nu(p_3)\end{aligned} \tag{2.17}$$

where m_Q is the mass of any quark Q present in the loop, and $\epsilon^{*a}_\mu(p_2), \epsilon^{*b}_\nu(p_3)$ correspond to the transverse polarization vectors of the outcoming gluons. Also note the presence of the Kronecker deltas ensuring color conservation at every vertex. In order to simplify 2.17, first note that

$$\frac{\lambda^b_{kl}}{2}\frac{\lambda^a_{ji}}{2}\delta_{nk}\delta_{lj}\delta_{in} = \frac{1}{4}\lambda^b_{ji}\lambda^a_{ji} = \frac{1}{4}\mathrm{Tr}[\lambda^b\lambda^a] = \frac{1}{2}\delta_{ab}$$

On the other hand, we can evaluate the q_1- and q_2-integrals making use of two of the Dirac deltas present in the integrand. Finally, solving for the transition amplitude we can write

$$\mathcal{M}_1(h \to gg) = -\frac{i}{2}g_s^2\frac{m_Q}{v}\epsilon^{*a}_\mu(p_2)\epsilon^{*b}_\nu(p_3)\delta_{ab}\int \frac{d^4k}{(2\pi)^4}\frac{T^{\mu\nu}}{D} \tag{2.18}$$

where we have defined

$$T^{\mu\nu} := \mathrm{Tr}\left[\gamma^\mu(\not{k} + \not{p}_2 + m_Q)(\not{k} - \not{p}_3 + m_Q)\gamma^\nu(\not{k} + m_Q)\right] \tag{2.19}$$

$$D := (k^2 - m_Q^2)[(k + p_2)^2 - m_Q^2][(k - p_3)^2 - m_Q^2] \tag{2.20}$$

and we shall denote by $I^{\mu\nu}$ the integral presented in 2.18. In order to calculate $I^{\mu\nu}$, let us first to evaluate the spinor trace

$$\begin{aligned}T^{\mu\nu} &= \mathrm{Tr}\left[\gamma^\mu(\not{k} + \not{p}_2 + m_Q)(\not{k} - \not{p}_3 + m_Q)\gamma^\nu(\not{k} + m_Q)\right]\\ &= 4m_Q\left[p_3^\mu p_2^\nu + 4k^\mu k^\nu - 2k^\mu p_3^\nu + 2p_2^\mu k^\nu - p_2^\mu p_3^\nu + g^{\mu\nu}(m_Q^2 - p_2p_3) - k^2g^{\mu\nu}\right]\\ &\equiv 4m_Q N^{\mu\nu}\end{aligned} \tag{2.21}$$

The next task is to treat the denominator D. The usual method of Feynman parametrization

$$\frac{1}{ABC} = 2\int_0^1 dz\int_0^1 dy\int_0^1 dx\frac{\delta(x + y + z - 1)}{(Ax + By + Cz)^3} \tag{2.22}$$

can be used to combine the factors presented in D, with $A := k^2 - m_Q^2$, $B := (k + p_2)^2 - m_Q^2$ and $C := (k - p_3)^2 - m_Q^2$. Then

$$\begin{aligned}Ax + By + Cz &= (k^2 - m_Q^2)x + \left[(k + p_2)^2 - m_Q^2\right]y + \left[(k - p_3)^2 - m_Q^2\right]z\\ &= (k^2 - m_Q^2)(x + y + z) + 2k(p_2y - p_3z) + p_2^2y + p_3^2z\\ &= (k^2 - m_Q^2)(x + y + z) + 2k(p_2y - p_3z)\end{aligned} \tag{2.23}$$

where in the last step p_2^2 and p_3^2 are zero since they express the masses of the gluons which are massless. Evaluating the integral with respect to x, yield

$$\begin{aligned}\frac{1}{ABC} &= 2\int_0^1 dz \int_0^1 dy \int_0^1 dx \frac{\delta\left(x-(1-y-z)\right)}{\Big[(k^2-m_Q^2)(x+y+z)+2k(p_2y-p_3z)\Big]^3} \\ &= 2\int_0^1 dz \int_0^{1-z} dy \frac{1}{\Big[k^2-m_Q^2+2k(p_2y-p_3z)\Big]^3} \end{aligned} \tag{2.24}$$

Now, we complete the square by adding and subtracting the term $(p_2y-p_3z)^2$:

$$\begin{aligned} k^2-m_Q^2+2k(p_2y-p_3z) &= k^2-m_Q^2+2k(p_2y-p_3z)+(p_2y-p_3z)^2-(p_2y-p_3z)^2 \\ &= \left[k^2+2k(p_2y-p_3z)+(p_2y-p_3z)^2\right]-(p_2y-p_3z)^2-m_Q^2 \\ &= \left[k+(p_2y-p_3z)\right]^2-(p_2^2y^2+p_3^2z^2-2p_2p_3yz)-m_Q^2 \\ &= (k+p_2y-p_3z)^2+2p_2p_3yz-m_Q^2 \\ &= (k+p_2y-p_3z)^2-a^2 \end{aligned} \tag{2.25}$$

where we have defined $a^2 := m_Q^2-2p_2p_3yz$. Hence, our integral becomes

$$I^{\mu\nu} = \int \frac{d^4k}{(2\pi)^4}\int_0^1 dz\int_0^{1-z} dy \frac{8m_QN^{\mu\nu}}{\left[(k+p_2y-p_3z)^2-a^2\right]^3}$$

Now we take the change of variable $k\to k-p_2y+p_3z$ which yield

$$I^{\mu\nu} = \int \frac{d^4k}{(2\pi)^4}\int_0^1 dz\int_0^{1-z} dy \frac{8m_QN^{\mu\nu}}{\left(k^2-a^2\right)^3} \tag{2.26}$$

and so $N^{\mu\nu}$ must be shift to

$$\begin{aligned} N^{\mu\nu} \to\ & [p_3^\mu p_2^\nu + 4(k-p_2y+p_3z)^\mu(k-p_2y+p_3z)^\nu - 2(k-p_2y+p_3z)^\mu p_3^\nu + 2p_2^\mu(k-p_2y+p_3z)^\nu \\ & -p_2^\mu p_3^\nu + g^{\mu\nu}(m_Q^2-p_2p_3) - (k-p_2y+p_3z)^2g^{\mu\nu}\big] \\ =\ & p_3^\mu p_2^\nu + 4k^\mu k^\nu - 4k^\mu p_2^\nu y + 4k^\mu p_3^\nu z - 4p_2^\mu k^\nu y + 4p_2^\mu p_2^\nu y^2 - 4p_2^\mu p_3^\nu yz + 4p_3^\mu k^\nu z - 4p_3^\mu p_2^\nu yz \\ & + 4p_3^\mu p_3^\nu z^2 - 2k^\mu p_3^\nu + 2p_2^\mu p_3^\nu y - 2p_3^\mu p_3^\nu z + 2p_2^\mu k^\nu - 2p_2^\mu p_2^\nu y + 2p_2^\mu p_3^\nu z - p_2^\mu p_3^\nu + m_Q^2 g^{\mu\nu} \\ & - p_2p_3g^{\mu\nu} - k^2g^{\mu\nu} + p_2^2y^2g^{\mu\nu} + p_3^2z^2g^{\mu\nu} + 2kp_2yg^{\mu\nu} - 2kp_3zg^{\mu\nu} + 2p_2p_3yzg^{\mu\nu} \\ =\ & 4k^\mu k^\nu - k^2g^{\mu\nu} + p_3^\mu p_2^\nu(1-4yz) - p_2^\mu p_3^\nu(1+4yz-2y-2z) + p_3^\mu p_3^\nu(4z^2-2z) \\ & + p_2^\mu p_2^\nu(4y^2-2y) + g^{\mu\nu}(m_Q^2-p_2p_3+2p_2p_3yz) \end{aligned} \tag{2.27}$$

In the last step we have drop all terms that are linear in k^μ, since in each case, the corresponding integral will vanish (because the interval of integration is symmetric and the integrand is an odd function). Since the first two terms of $N^{\mu\nu}$ are apparently ultraviolet divergent, namely $4k^\mu k^\nu - k^2g^{\mu\nu}$, we shall need to employ dimensional regularization to perform the four-momentum integral. In view of this, let us now divide the integral into two parts

$$I^{\mu\nu} = I_1^{\mu\nu} + I_2^{\mu\nu} \tag{2.28}$$

where $I_1^{\mu\nu}$ contains the ultraviolet divergent terms and $I_2^{\mu\nu}$ contains the rest. Let us first deal with $I_1^{\mu\nu}$. In order to do this, we shall make use of the following d-dimensional integral

$$J(d;a^2;\alpha,\beta) := \int \frac{d^dk}{(2\pi)^d}\frac{(k^2)^\alpha}{(k^2-a^2)^\beta} \tag{2.29}$$

$$= \frac{i}{(4\pi)^{\frac{d}{2}}}(a^2)^{\frac{d}{2}}(-a^2)^{\alpha-\beta}\frac{\Gamma\left(\beta-\alpha-\frac{d}{2}\right)\Gamma\left(\alpha+\frac{d}{2}\right)}{\Gamma(\beta)\Gamma\left(\frac{d}{2}\right)} \tag{2.30}$$

and due Lorentz symmetry, the following property holds:

$$\int \frac{d^dk}{(2\pi)^d}\frac{(k^2)^\alpha k^\mu k^\nu}{(k^2-a^2)^\beta} = \frac{g^{\mu\nu}}{d}J(d;a^2;\alpha+1,\beta) \tag{2.31}$$

Therefore, we can write

$$\begin{aligned} I_1^{\mu\nu} &= 8m_Q\int_0^1 dz\int_0^{1-z}dy\lim_{d\to4}\int\frac{d^dk}{(2\pi)^d}\frac{\left(4k^\mu k^\nu-k^2g^{\mu\nu}\right)}{\left(k^2-a^2\right)^3} \\ &= 8m_Q\int_0^1 dz\int_0^{1-z}dy\lim_{d\to4}g^{\mu\nu}\left(\frac{4}{d}-1\right)J(d;a^2;1,3) \\ &= 8m_Q\int_0^1 dz\int_0^{1-z}dy\lim_{d\to4}\frac{ig^{\mu\nu}}{(4\pi)^{\frac{d}{2}}}\frac{d}{4}\left(\frac{4}{d}-1\right)(a^2)^{\frac{d}{2}-2}\Gamma\left(2-\frac{d}{2}\right) \end{aligned} \tag{2.32}$$

Using the change of variable $d = 4+2\epsilon$ we find

$$\begin{aligned} I_1^{\mu\nu} &= 8m_Q\int_0^1 dz\int_0^{1-z}dy\lim_{\epsilon\to0}\frac{ig^{\mu\nu}}{(4\pi)^{2+\epsilon}}\left(-\frac{\epsilon}{2}\right)(a^2)^\epsilon\Gamma(-\epsilon) \\ &= 8m_Q\int_0^1 dz\int_0^{1-z}dy\lim_{\epsilon\to0}\frac{ig^{\mu\nu}}{(4\pi)^{2+\epsilon}}\left(-\frac{\epsilon}{2}\right)(a^2)^\epsilon\left(-\frac{1}{\epsilon}+\gamma_E+\mathcal{O}(\epsilon^2)\right) \\ &= 8m_Q\int_0^1 dz\int_0^{1-z}dy\lim_{\epsilon\to0}\frac{ig^{\mu\nu}}{(4\pi)^{2+\epsilon}}(a^2)^\epsilon\left(\frac{1}{2}+\mathcal{O}(\epsilon)\right) \\ &= \frac{8im_Q}{32\pi^2}g^{\mu\nu}\int_0^1 dz\int_0^{1-z}dy \end{aligned} \tag{2.33}$$

where γ_E is the Euler-Mascheroni constant. On the other hand

$$\begin{aligned} I_2^{\mu\nu} &= 8m_Q\int_0^1 dz\int_0^{1-z}dy\left[\int\frac{d^4k}{(2\pi)^4}\frac{1}{(k^2-a^2)^3}\right][p_3^\mu p_2^\nu(1-4yz)-p_2^\mu p_3^\nu(1+4yz-2y-2z) \\ &\quad +p_3^\mu p_3^\nu(4z^2-2z)+p_2^\mu p_2^\nu(4y^2-2y)+g^{\mu\nu}(m_Q^2-p_2p_3+2p_2p_3yz)] \\ &= 8m_Q\int_0^1 dz\int_0^{1-z}dy\left[-\frac{i}{32\pi^2a^2}\right][p_3^\mu p_2^\nu(1-4yz)-p_2^\mu p_3^\nu(1+4yz-2y-2z) \\ &\quad +p_3^\mu p_3^\nu(4z^2-2z)+p_2^\mu p_2^\nu(4y^2-2y)+g^{\mu\nu}(m_Q^2-p_2p_3+2p_2p_3yz)] \\ &= -\frac{8im_Q}{32\pi^2}\int_0^1 dz\int_0^{1-z}dy\frac{1}{a^2}[p_3^\mu p_2^\nu(1-4yz)-p_2^\mu p_3^\nu(1+4yz-2y-2z) \\ &\quad +p_3^\mu p_3^\nu(4z^2-2z)+p_2^\mu p_2^\nu(4y^2-2y)+g^{\mu\nu}(m_Q^2-p_2p_3+2p_2p_3yz)] \end{aligned} \tag{2.34}$$

Therefore

$$I^{\mu\nu} = \frac{8im_Q}{32\pi^2}\int_0^1 dz\int_0^{1-z} dy\frac{1}{a^2}\left[p_3^\mu p_2^\nu(4yz-1)+p_2^\mu p_3^\nu(1+4yz-2y-2z)\right.$$
$$\left.+p_3^\mu p_3^\nu(2z-4z^2)+p_2^\mu p_2^\nu(2y-4y^2)+g^{\mu\nu}p_2p_3(1-4yz)\right] \tag{2.35}$$

This quantity will be multiplied with the polarization vectors of the gluons; but having in mind the transversality of the polarization: $\epsilon_\mu^{*a}(p_2)p_2^\mu = 0$ and $\epsilon_\nu^{*b}(p_3)p_3^\nu = 0$, some terms vanish and then the only remaining tensorial structure is

$$\begin{aligned} I^{\mu\nu} &= \frac{8im_Q}{32\pi^2}\int_0^1 dz\int_0^{1-z} dy\left[\frac{p_3^\mu p_2^\nu(4yz-1)+g^{\mu\nu}p_2p_3(1-4yz)}{a^2}\right] \\ &= \frac{8im_Q}{32\pi^2}\left(p_3^\mu p_2^\nu - g^{\mu\nu}p_2p_3\right)\left[\int_0^1 dz\int_0^{1-z} dy\,\frac{1-4yz}{m_Q^2-2p_2p_3yz}\right] \\ &= \frac{8im_Q}{32\pi^2}\left(p_3^\mu p_2^\nu - g^{\mu\nu}p_2p_3\right)\left[\frac{1}{m_Q^2}\int_0^1 dz\int_0^{1-z} dy\,\frac{1-4yz}{1-\xi_Q^{-1}yz}\right] \\ &= \frac{8i}{32\pi^2}\frac{1}{m_Q}I(\xi_Q)\left(p_3^\mu p_2^\nu - g^{\mu\nu}p_2p_3\right) \end{aligned} \tag{2.36}$$

Here, $\xi_Q := m_Q^2/2p_2p_3$ and the new function I is a *form factor* given by

$$I(\xi_Q) := \xi_Q\left[2-(4\xi_Q-1)\left[\mathrm{Li}_2\left(\frac{2}{1-\sqrt{1-4\xi_Q}}\right)+\mathrm{Li}_2\left(\frac{2}{1+\sqrt{1-4\xi_Q}}\right)\right]\right] \tag{2.37}$$

where Li_n is the polylogarithm function of order n. Finally, the transition amplitude $\mathcal{M}_1(h\to gg)$ is given by

$$\begin{aligned} \mathcal{M}_1(h\to gg) &= -\frac{i}{2}g_s^2\frac{m}{v}\epsilon_\mu^{*a}(p_2)\epsilon_\nu^{*b}(p_3)\delta_{ab}\left[\frac{8i}{32\pi^2}\frac{1}{m}I(\xi_Q)(p_3^\mu p_2^\nu - g^{\mu\nu}p_2p_3)\right] \\ &= \frac{g_s^2}{8\pi^2 v}I(\xi_Q)\epsilon_\mu^{*a}(p_2)\epsilon_\nu^{*b}(p_3)\delta_{ab}(p_3^\mu p_2^\nu - g^{\mu\nu}p_2p_3) \end{aligned} \tag{2.38}$$

We need now to calculate the transition amplitude $\mathcal{M}_2(h\to gg)$ for the second diagram. To find it, observe that if we shift in the first diagram Fig. (2.4) the variables $p_2\leftrightarrow p_3, \mu\leftrightarrow\nu, a\leftrightarrow b, i\leftrightarrow k$ and $j\leftrightarrow l$, then we get the second diagram Fig. (2.5).

Consequently, these transformations shift the transition amplitude 2.38 to

$$\begin{aligned} \mathcal{M}_2(h\to gg) &= \frac{g_s^2}{8\pi^2 v}I(\xi_Q)\epsilon_\nu^{*b}(p_3)\epsilon_\mu^{*a}(p_2)\delta_{ba}(p_2^\nu p_3^\mu - g^{\nu\mu}p_3p_2) \\ &= \frac{g_s^2}{8\pi^2 v}I(\xi_Q)\epsilon_\mu^{*a}(p_2)\epsilon_\nu^{*b}(p_3)\delta_{ab}(p_3^\mu p_2^\nu - g^{\mu\nu}p_2p_3) \end{aligned} \tag{2.39}$$

which it turns out to be exactly the same as the first one. Therefore, the two diagrams contribute equally to the total amplitude. It follows that the average square transition amplitude of the process

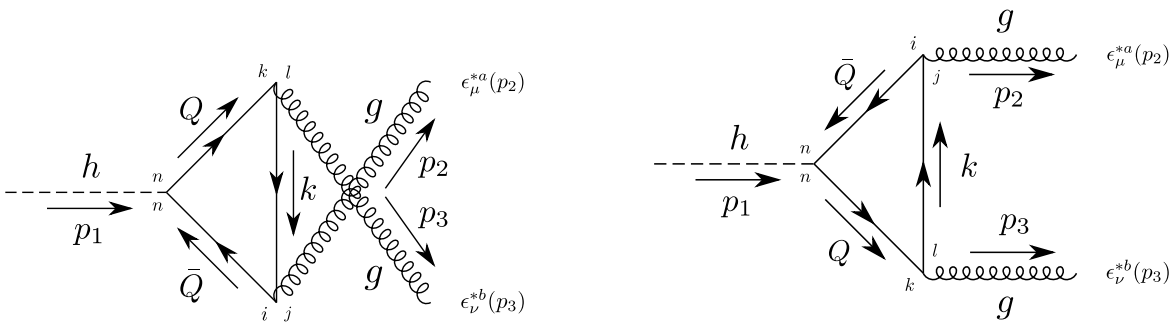

Figure 2.5: Second Feynman diagram describing $h \to gg$ at lowest order. Both left and right diagrams are topologically equivalent.

(and taking into account the contribution due to all the quarks) is given by

$$\begin{aligned}
\langle|\mathcal{M}(h\to gg)|^2\rangle &= \sum_{\text{spin color}}\sum |\sum_{\text{Q}} 2\mathcal{M}_1(h\to gg)|^2 \\
&= 4\sum_{\text{spin color}}\sum \left[\sum_{\text{Q}} \frac{g_s^2}{8\pi^2 v} I^*(\xi_Q)\epsilon_\rho^a(p_2)\epsilon_\sigma^b(p_3)\delta_{ab}(p_3^\rho p_2^\sigma - g^{\rho\sigma}p_2p_3)\right] \\
&\quad\times\left[\sum_{\text{Q}} \frac{g_s^2}{8\pi^2 v} I(\xi_Q)\epsilon_\mu^{*a}(p_2)\epsilon_\nu^{*b}(p_3)\delta_{ab}(p_3^\mu p_2^\nu - g^{\mu\nu}p_2p_3)\right] \\
&= \frac{g_s^4}{16\pi^4 v^2}|\sum_{\text{Q}} I(\xi_Q)|^2 \left[\sum_{\text{spin}} \epsilon_\mu^{*a}(p_2)\epsilon_\rho^a(p_2)\epsilon_\nu^{*b}(p_3)\epsilon_\sigma^b(p_3)\right]\left[\sum_{\text{color}}\delta_{ab}\delta_{ab}\right] \\
&\quad\times (p_3^\rho p_2^\sigma - g^{\rho\sigma}p_2p_3)\,(p_3^\mu p_2^\nu - g^{\mu\nu}p_2p_3) \\
&= \frac{g_s^4}{16\pi^4 v^2}|\sum_{\text{Q}} I(\xi_Q)|^2\,[g_{\mu\rho}g_{\nu\sigma}]\,[8]\,(p_3^\rho p_2^\sigma - g^{\rho\sigma}p_2p_3)\,(p_3^\mu p_2^\nu - g^{\mu\nu}p_2p_3) \\
&= \frac{g_s^4}{\pi^4 v^2}(p_2p_3)^2|\sum_{\text{Q}} I(\xi_Q)|^2
\end{aligned} \tag{2.40}$$

In the COM frame the four-momenta are given by

$$p_1 = (m_h, \vec{0}), \quad p_2 = (E_g, \vec{p}) \quad \text{and} \quad p_3 = (E_g, -\vec{p})$$

from where

$$m_h = 2E_g, \quad p_2p_3 = \frac{m_h^2}{2} \quad \text{and} \quad |\vec{p}| = \frac{m_h}{2}$$

and thus 2.40 reduces to

$$\langle|\mathcal{M}(h\to gg)|^2\rangle = \frac{g_s^4}{4\pi^4 v^2} m_h^4 |\sum_{\mathrm{Q}} I(\xi_Q)|^2 \tag{2.41}$$

Finally, the partial decay width of the process is given by

$$\begin{aligned}\Gamma(h\to gg) &= \frac{\frac{1}{2!}}{8\pi}\frac{|\vec{p}|}{m_h^2}\langle|\mathcal{M}(h\to gg)|^2\rangle \\ &= \frac{\alpha_s^2}{8\pi^3 v^2} m_h^3 |\sum_{\mathrm{Q}} I(\xi_Q)|^2\end{aligned} \tag{2.42}$$

where we have expressed the result in terms of the strong structure constant 1.27. Due to the form factor $I(\xi_Q)$, the heavier quarks contribute significantly to the decay rate. In the SM, the only quark that is heavy enough to make an important contribution through this decay channel is the top quark, so we expect only this quark to play an important role.

2.3.4 Higgs Decay $h \to \gamma\gamma$

Now we consider the Higgs decay into a pair of photons. The process presents a very small decay width but is of quite remarkable importance for experimental researches, since energy and momentum of γ-rays let very accurate measurements and so an accurate reconstruction of the Higgs mass. Since the photon is massless there is no coupling between the SM Higgs and the photon. Instead, this decay channel has two types of one-loop contributions at leading order: in one type of diagram fermions propagate in the loop, while in the other the W boson propagates (see Fig. 2.1d). These W loop diagrams are dominant and can interfere destructively with the subdominant top quark loop. On the one hand the contribution from the fermion loop process can be carried out complete parallel to the $h \to gg$ decay; on the other hand, the calculation of the W boson loop consists of 13 different diagrams, including apart from the W boson also ghosts and would-be Goldstone bosons. The full expression including both contributions from the fermion and W boson loops reads [45]

$$\Gamma(h\to\gamma\gamma) = \frac{\alpha_{\mathrm{EM}}^2 m_h^3}{256\pi^3 v^2}\left|\sum_f N_c Q_f^2 F_{1/2}(\tau_f) + F_1(\tau_W)\right|^2 \tag{2.43}$$

where N_c is the color factor ($N_c = 1$ for leptons, $N_c = 3$ for quarks), and Q_f is the electric charge of the fermion in the loop. The dimensionless loop factors for spin-1/2 and spin-1 particles are given by

$$F_{1/2}(\tau) = 2[\tau + (\tau-1)f(\tau)]\tau^{-2} \tag{2.44}$$

$$F_1(\tau) = -[2\tau^2 + 3\tau + 3(2\tau-1)f(\tau)]\tau^{-2} \tag{2.45}$$

and the function $f(\tau)$ is defined as

$$f(\tau) = \begin{cases} \arcsin^2\sqrt{\tau} & \text{if} \quad \tau \le 1 \\ -\frac{1}{4}\left[\ln\left(\frac{1+\sqrt{1-\tau^{-1}}}{1-\sqrt{1-\tau^{-1}}}\right) - i\pi\right]^2 & \text{if} \quad \tau > 1 \end{cases} \tag{2.46}$$

The parameters $\tau_i = m_h^2/4m_i^2$ with $i = f, W$ are defined by the corresponding masses of the heavy loop particles. The electromagnetic constant in the coupling should be taken at the scale $Q^2 = 0$ since the final state photons are real.

2.3.5 Higgs Boson Branching Ratios

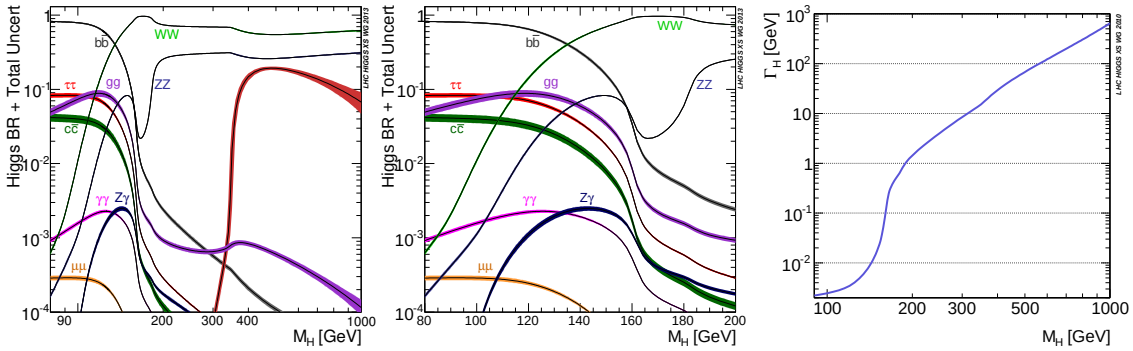

(a) SM Higgs branching ratios as a function of Higgs mass in the mass range of $90 < m_H < 1000$ GeV.

(b) SM Higgs branching ratios as a function of Higgs mass in the mass range of $80 < m_H < 200$ GeV.

(c) SM Higgs total width as a function of the Higgs mass.

Figure 2.6: Standard Model Higgs boson decay branching ratios and total width. Plots taken from [46].

2.4 Higgs Production Channels

We turn now to the production of the Higgs boson in pp collisions. At the LHC, there are essentially four mechanisms for the single production of the SM Higgs boson; they are depicted at low order in Fig. (2.7). On the experimental side, the primary production mechanism for a Higgs boson in hadronic collisions is through gluon-gluon fusion; on the theoretical side, it is the most challenging process to compute because of the quark-loop.

2.4.1 Higgs Production $gg \to h$

The primary production mechanism for a Higgs boson in hadronic collisions is through *gluon-gluon fusion*, $gg \to h$, which is shown in Fig. (2.7a). Analogously to the decay process $h \to gg$, the loop contains all quarks with mass $m_Q > 0$, and is totally dominated by the top quark because of the strong Higgs coupling with the latter. The transition amplitudes $\mathcal{M}_1(gg \to h)$ and $\mathcal{M}_2(gg \to h)$ for the production processes depicted in Fig. (2.8a) and Fig. (2.8b) are given by 2.38 and 2.39, respectively.

It follows that the average square transition amplitude of the process is given by

$$\langle|\mathcal{M}(gg \to h)|^2\rangle = \frac{g_s^4}{4\pi^4 v^2} m_h^4 |\sum_{\mathrm{Q}} I(\xi_Q)|^2 \tag{2.47}$$

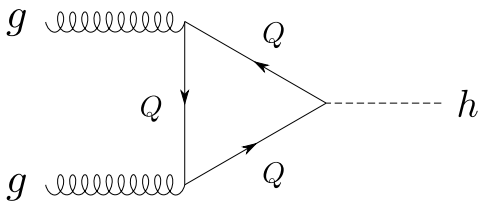

(a) Gluon-Gluon Fusion.

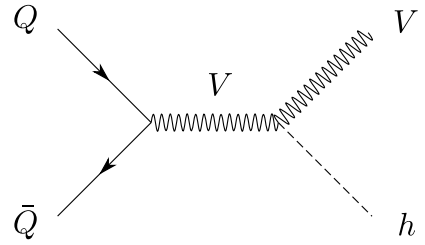

(b) Higgs Boson Bremsstrahlung.

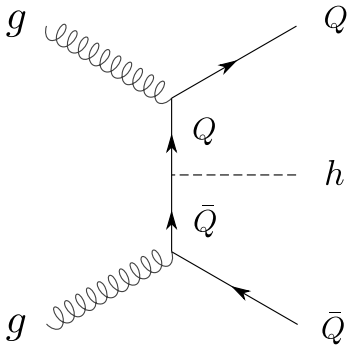

(c) Quark-Quark Fusion.

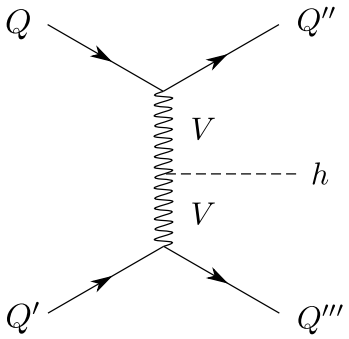

(d) Vector Boson Fusion.

Figure 2.7: The four major partonic Higgs production processes at the LHC.

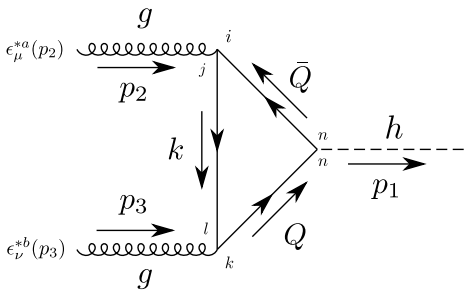

(a) First Feynman diagram describing $gg \to h$ at lowest order.

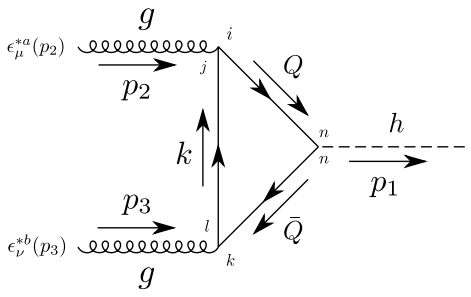

(b) Second Feynman diagram describing $gg \to h$ at lowest order.

Figure 2.8: Feynman diagram describing $gg \to h$ at lowest order.

and thus the cross section for the process is

$$\begin{aligned}\sigma(gg \to h) &= \frac{1}{2m_h^2} \int \langle |\mathcal{M}(gg \to h)|^2 \rangle \, (2\pi)^4 \delta^4(p_1 + p_2 - p_3) \frac{1}{2s} \frac{d^3\vec{p}_3}{(2\pi)^3} \\ &= \frac{\alpha_s^2}{64\pi v^2} m_h^2 |\sum_Q I(\xi_Q)|^2 \delta(s - m_h^2) \end{aligned} \tag{2.48}$$

where $\sqrt{s}$ is the energy in the gluon-gluon center-of-momentum frame and the function I is defined by 2.37. What we have calculated in 2.48 is the cross section of the lowest order process $gg \to h$ at the *partonic level*. However, at the LHC, two protons collide head-to-head and so we should be more interested in the cross section at the *hadronic level* (see Fig. 2.9).

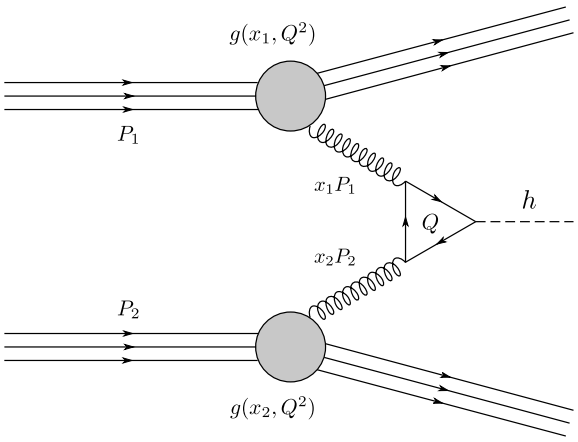

Figure 2.9: Hadronic gluon-gluon fusion process at the LHC. Here the two incoming protons carry momenta P_1 and P_2.

Therefore, in our current process the hadronic cross section $\sigma_{\text{hadronic}}(gg \to h)$ can be obtained through Eq. 2.3 by convoluting the partonic cross section 2.48 with the parton distribution functions of the gluons

$$\sigma_{\text{hadronic}}(gg \to h) = \int_0^1 dx_1 \int_0^1 dx_2 \, g(x_1, Q^2) g(x_2, Q^2) \sigma(gg \to h) \tag{2.49}$$

where x_1 and x_2 are the longitudinal momentum fractions of each proton that is carried by a gluon and $g = g(x, Q^2)$ are the PDF for the gluons. Let us analyse the cross section 2.49 for very high energies; in this limit, we can consider the proton as massless. In the hadronic center-of-momentum (HCoM), we have

$$P_1 = (|\vec{P}\,|, \vec{P}\,), \quad P_2 = (|\vec{P}\,|, -\vec{P}\,), \quad \text{and} \quad S = (P_1 + P_2)^2 = 4\vec{P}^{\,2} \tag{2.50}$$

Hence, the s variable in the partonic center-of-momentum (PCoM) can be rewritten as

$$s = (p_1 + p_2)^2 = (x_1 P_1 + x_2 P_2)^2 = x_1 x_2 S \equiv \tau S \tag{2.51}$$

In addition, define de quantity $\tau_0 := m_h^2/S$. Therefore, in the HCoM we have

$$\begin{aligned}
\sigma_{\text{hadronic}}(gg \to h) &= \frac{\alpha_s^2}{64\pi v^2} \Big| \sum_Q I(\xi_Q) \Big|^2 \int_0^1 dx_1 \int_0^1 dx_2\, g(x_1, Q^2) g(x_2, Q^2) m_h^2 \delta(s - m_h^2) \\
&= \frac{\alpha_s^2}{64\pi v^2} \Big| \sum_Q I(\xi_Q) \Big|^2 \int_0^1 dx_1 \int_0^1 dx_2\, g(x_1, Q^2) g(x_2, Q^2) m_h^2 \frac{1}{x_1 S} \delta\left(x_2 - \frac{\tau_0}{x_1}\right) \\
&= \frac{\alpha_s^2 \tau_0}{64\pi v^2} \Big| \sum_Q I(\xi_Q) \Big|^2 \int_0^1 \frac{dx_1}{x_1} \int_0^1 dx_2\, g(x_1, Q^2) g(x_2, Q^2) \delta(s - m_h^2) \\
&= \frac{\alpha_s^2 \tau_0}{64\pi v^2} \Big| \sum_Q I(\xi_Q) \Big|^2 \int_0^1 \frac{dx_1}{x_1}\, g(x_1, Q^2) g\left(\tau_0/x_1, Q^2\right)
\end{aligned} \tag{2.52}$$

which has to be integrated numerically.

2.4.2 Higgs Production $Q\bar{Q} \to Vh$

This process, depicted in Fig. (2.7b), is considered the main search mode for Tevatron but not so much at the LHC. This is because Tevatron is a $p\bar{p}$ collider and so the abundance of antiquarks in the $\bar{p}$-beam increases the probability of create a Higgs through the Higgs Strahlung channel. This is a different situation from the LHC, which is a pp collider, reducing considerably the probability of extract an antiquark from the sea.

Let us start with the case $V = Z$ depicted in Fig. (2.10a). Here, Feynman rules determine a transition amplitude $\mathcal{M}(Q\bar{Q} \to Zh)$ given by

$$\begin{aligned}
-i\mathcal{M}(Q\bar{Q} \to Zh)(2\pi)^4 \delta^4(p_1 - p_2 - p_3) = \int \frac{d^4q}{(2\pi)^4} (2\pi)^4 \delta^4(p_1 + p_2 - q)(2\pi)^4 \delta^4(q - p_3 - p_4) \\
\times \bar{v}(p_2) \left[\frac{-ig}{2\cos\theta_W} \gamma^\mu (v_Q - a_Q \gamma^5)\right] u(p_1) \\
\times \left[\frac{-i\left(g_{\mu\nu} - \frac{q_\mu q_\nu}{m_Z^2}\right)}{q^2 - m_Z^2}\right] \left(i\frac{2m_Z^2}{v}\right) \epsilon_\nu^*(p_3)
\end{aligned} \tag{2.53}$$

where v_f and a_f are the *vector* and *axial-vector coupling* for the fermion f, respectively. It follows that

$$\begin{aligned}
\mathcal{M}(Q\bar{Q} \to Zh) = -\frac{g m_Z^2}{v \cos\theta_W} \bar{v}(p_2) \gamma^\mu (v_Q - a_Q \gamma^5) u(p_1) \epsilon_\nu^*(p_3) \\
\times \left(g_{\mu\nu} - \frac{(p_3 + p_4)_\mu (p_3 + p_4)_\nu}{m_Z^2}\right) \frac{1}{(p_3 + p_4)^2 - m_Z^2}
\end{aligned} \tag{2.54}$$

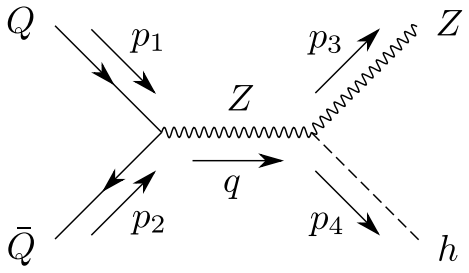

(a) First Feynman diagram contributing to $QQ \to Vh$ at lowest order.

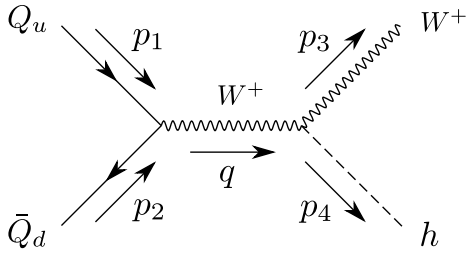

(b) Second Feynman diagram contributing to $QQ \to Vh$ at lowest order.

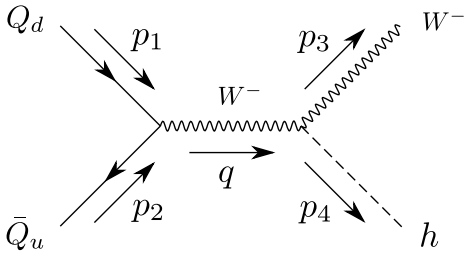

(c) Third Feynman diagram contributing to $QQ \to Vh$ at lowest order.

Figure 2.10: Feynman diagram describing $QQ \to Vh$ at lowest order.

Hence, the average square transition amplitude is given by

$$\begin{aligned}
\langle|\mathcal{M}(Q\bar{Q} \to Zh)|^2\rangle = \sum_{\text{spin}} \Bigg[& -\frac{g m_Z^2}{v \cos\theta_W} \bar{u}(p_1)\gamma^\mu (v_Q - a_Q\gamma^5) v(p_2) \epsilon_\nu(p_3) \left(g_{\mu\nu} - \frac{(p_3+p_4)_\mu (p_3+p_4)_\nu}{m_Z^2} \right) \\
& \times \frac{1}{(p_3+p_4)^2 - m_Z^2} \Bigg] \Bigg[-\frac{g m_Z^2}{v \cos\theta_W} \bar{v}(p_2)\gamma^\rho (v_Q - a_Q\gamma^5) u(p_1) \epsilon_\sigma^*(p_3) \\
& \times \left(g_{\rho\sigma} - \frac{(p_3+p_4)_\rho (p_3+p_4)_\sigma}{m_Z^2} \right) \frac{1}{(p_3+p_4)^2 - m_Z^2} \Bigg] \\
= & \frac{g^2 m_Z^4}{v^2 \cos^2\theta_W} \frac{\epsilon_\sigma^*(p_3)\epsilon_\nu(p_3)}{[(p_3+p_4)^2 - m_Z^2]^2} \left(g_{\mu\nu} - \frac{(p_3+p_4)_\mu (p_3+p_4)_\nu}{m_Z^2} \right) \\
& \times \left(g_{\rho\sigma} - \frac{(p_3+p_4)_\rho (p_3+p_4)_\sigma}{m_Z^2} \right) \text{Tr} \Big[\gamma^\mu (v_Q - a_Q\gamma^5)(\not{p}_2 + m_Q) \gamma^\rho (v_Q - a_Q\gamma^5) \\
& \times (\not{p}_1 + m_Q) \Big] \qquad (2.55)
\end{aligned}$$

In order to evaluate this last trace, we neglect the mass quark. Hence

$$\langle|\mathcal{M}(Q\bar{Q}\to Zh)|^2\rangle = \frac{g^2m_Z^4}{v^2\cos^2\theta_W}\frac{(v_Q^2+a_Q^2)}{[(p_3+p_4)^2-m_Z^2]^2}\left[p_1p_2M_Z^2+2(p_1p_3)(p_2p_3)\right] \tag{2.56}$$

For the PCoM we have

$$p_1=(|\vec{p}|,\vec{p}),\quad p_2=(|\vec{p}|,-\vec{p}),\quad p_3=(E_Z,\vec{p}')\quad\text{and}\quad p_4=(E_h,-\vec{p}')$$

and thus the cross section for the process is

$$\sigma(Q\bar{Q}\to Zh)=\frac{g^2m_Z^2}{576\pi v^2\cos^2\theta_W}\frac{(v_{Q_i}^2+a_{Q_i}^2)}{s^2(s-m_Z^2)^2}\lambda^{1/2}(s,m_h^2,m_Z^2)\left[\lambda(s,m_h^2,m_Z^2)+12sm_Z^2\right] \tag{2.57}$$

where $\lambda=\lambda(s,m_h^2,m_Z^2)$ is the so-called *Käller function*, *triangle function* or *two-particle phase space function*, and which can be written in many forms

$$\begin{aligned}\lambda(s,m_h^2,m_Z^2) &= [s-(m_h+m_Z)^2][s-(m_h-m_Z)^2] \\ &= [m_h^2-(\sqrt{s}+m_Z)^2][m_h^2-(\sqrt{s}-m_Z)^2] \\ &= [m_Z^2-(\sqrt{s}+m_h)^2][m_Z^2-(\sqrt{s}-m_h)^2] \\ &= (s-m_h^2-m_Z^2)^2-4m_h^2m_Z^2 \\ &= s+m_h^4+m_Z^4-2sm_h^2-2sm_Z^2-2m_h^2m_Z^2\end{aligned} \tag{2.58}$$

The cases $W^\pm$ depicted in Fig. (2.10b) and (2.10c) are very similar

$$\sigma(Q_u\bar{Q}_d\to W^+h)=\frac{g^2m_W^2}{576\pi v^2}\frac{|V_{Q_u\bar{Q}_d}|^2}{s^2(s-m_W^2)^2}\lambda^{1/2}(s,m_h^2,m_W^2)\left[\lambda(s,m_h^2,m_W^2)+12sm_Z^2\right] \tag{2.59}$$

and

$$\sigma(\bar{Q}_uQ_d\to W^-h)=\frac{g^2m_W^2}{576\pi v^2}\frac{|V_{\bar{Q}_uQ_d}|^2}{s^2(s-m_W^2)^2}\lambda^{1/2}(s,m_h^2,m_W^2)\left[\lambda(s,m_h^2,m_W^2)+12sm_Z^2\right] \tag{2.60}$$

which correspond to equal contributions. Here, $Q_u\equiv u,c$ and $Q_d\equiv d,s$ are considered massless (as in the previous section). Therefore, the total cross section is given by

$$\begin{aligned}\sigma(Q\bar{Q}\to W^\pm h) &= \sigma(Q_u\bar{Q}_d\to W^+h)+\sigma(Q_u\bar{Q}_d\to W^-h) \\ &= 2\sigma(Q_u\bar{Q}_d\to W^+h) \\ &= 2\sigma(\bar{Q}_uQ_d\to W^-h)\end{aligned} \tag{2.61}$$

2.4.3 Higgs Production $QQ\to QQh$

Although the gluon-gluon fusion process has the largest cross section, from the experimental perspective the vector boson fusion process $QQ\to VV\to QQh$ is also important. This is because it results in more easily identifiable final states consisting of just the decay products of the Higgs boson and two forward jets from the break-up of the collinding protons. In contrast, the gluon-gluon fusion process is accompanied by QCD radiation from the colour field, making the identification of the Higgs boson final states less easy. The Feynman diagrams describing the six lowest order processes $QQ\to ZZ\to QQh$ and $QQ\to WW\to QQh$ are shown in Fig. (A.1) and Fig. (A.2), respectively (see Appendix A).

2.4.4 Higgs Boson Production Cross Sections

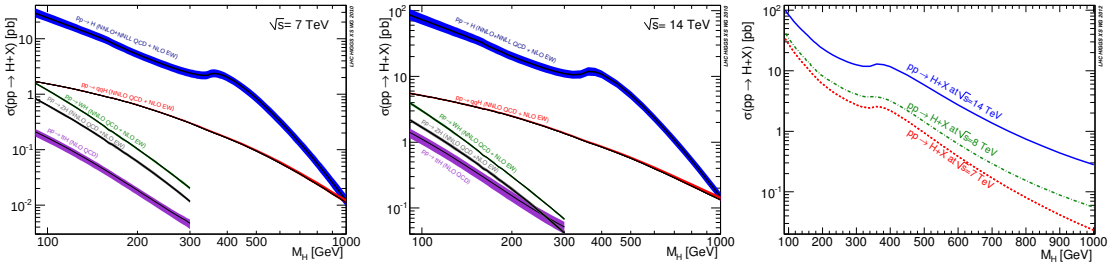

(a) Higgs production cross sections as a function of Higgs mass at $\sqrt{s} = 7$ TeV pp collisions.

(b) Higgs production cross sections as a function of Higgs mass at $\sqrt{s} = 14$ TeV pp collisions.

(c) The total Higgs cross sections for $\sqrt{s} = 7, 8$ and 14 TeV.

Figure 2.11: Higgs production cross sections and total cross section as a function of Higgs mass at different pp collision energies. Here, $pp \to h$ corresponds to gluon-gluon fusion, $pp \to QQh$ to vector boson fusion, $pp \to Vh$ to Higgs bremsstrahlung, and $pp \to tth$ to quark-quark fusion in this specific case with a top-antitop quark pair. Calculations were not performed for $m_h > 300$ GeV for the bottom three processes, as their cross sections were deemed too low. Taken from [46].

2.5 The Radiative Corrections to the Higgs Mass

At high energies, heavy particles from a not yet fully known high-energy theory might well contribute to various processes. Therefore, we assume the Standard Model valid up to some scale Λ_{SM} from where new physics shows up. At higher energies new physics takes over, which implies that we do not know how to compute loop diagrams with momenta larger than Λ_{SM}, being forced to cut such loops off at Λ_{SM}. The dominant corrections to the Higgs masses are due to the particles with the strongest couplings to the Higgs bosons. At n loops the quadratic cutoff dependence of the radiative corrections of the Higgs mass has the form [47]

$$\delta m^2_{h,\text{SM}} = \frac{\Lambda^2_{\text{SM}}}{16\pi^2} C_n(\mu) \tag{2.62}$$

where the n-loop coefficient $C_n(\mu)$ only depends on the gauge couplings g, g', the Yukawa couplings y_f and the Higgs self-coupling λ. At 1-loop, the most dangerous radiative corrections come from diagrams with the top quark, SU(2) gauge bosons, and the Higgs itself running in the loop (see Figure 2.12), and is given explicitly by [47]

$$\begin{aligned} (\delta m^2_h)_{\text{top}} &= -\frac{3y_t^2}{4\pi^2}\Lambda^2_{\text{SM}} & (\delta m^2_h)_{W^\pm} &= \frac{9g^2}{32\pi^2}\Lambda^2_{\text{SM}} \\ (\delta m^2_h)_{\text{Higgs}} &= \frac{3\lambda}{4\pi^2}\Lambda^2_{\text{SM}} & (\delta m^2_h)_{Z} &= \frac{3g'^2}{32\pi^2}\Lambda^2_{\text{SM}} \end{aligned} \tag{2.63}$$

Therefore, neglecting the numerically insignificant light fermion contributions, the 1-loop coefficient function C_1 may be written as

$$C_1 = -12y_t^2 + \frac{9}{2}g^2 + \frac{3}{2}g'^2 + 12\lambda \tag{2.64}$$

The next-order correction, first calculated in Refs. [48, 49] and confirmed in [50] read

$$\begin{aligned} C_2 = C_1 + \frac{\ln(2^6/3^3)}{16\pi^2}\Bigg[&18y_t^4 + y_t^2\left(-\frac{7}{6}g'^2 + \frac{9}{2}g^2 - 32g_s^2\right) \\ &-\frac{87}{8}g'^4 - \frac{63}{8}g^4 - \frac{15}{4}g^2g'^2 + 6\lambda(-6y_t^2 + g'^2 + 3g^2) - 24\lambda^2\Bigg] \end{aligned} \tag{2.65}$$

and numerically does not change significantly the 1-loop result.

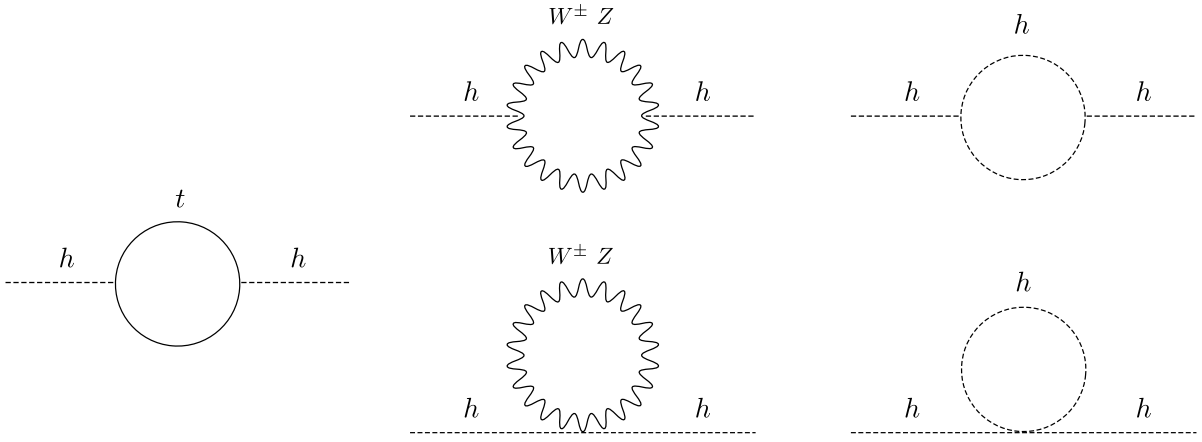

Figure 2.12: Some of the leading one-loop corrections to the SM Higgs mass squared parameter m_{H0}^2 from: the top quark, the SU(2) gauge bosons, and the Higgs boson itself.

3 The Higgs Naturalness Problem

3.1 Introduction

The Standard Model describes all particle physics experiments performed to date with remarkable success. At first sight, there seems to be no reason why it should not be the ultimate theory of nature. However, a closer look reveals that there are good reasons for expecting physics beyond the SM: the strong CP problem, neutrino oscillations, matter-antimatter asymmetry, the nature of dark matter and dark energy, gauge couplings unification, stability of the electroweak vacuum, and possibly the most important, the quantum gravity issue. Another of such motivations, the so-called *Higgs Naturalness Problem* (HNP), is the subject of this thesis.

The Higgs naturalness problem arises because the quadratically divergent 1-loop contributions 2.63 drive the Higgs mass $m_{h,\text{physical}}$ to unacceptably large values unless its bare mass parameter $m_{h,\text{bare}}$ were finely tuned in order to almost exactly cancels these 1-loop correction leaving the small electroweak scale mass that we actually observe. Such cancellation might be technically feasible, but seems ad hoc without a deeper explanation of why the cancellation terms would have such fine-tuned values. This strongly suggests that the parametrization of the electroweak symmetry breaking in terms of a fundamental scalar field is almost certainly an incomplete description, which in turn has for many years been a guiding principle in the search for physics beyond the SM, particularly for understanding the physics of electroweak symmetry breaking. This is just one reason the SM is believe to lose its predictive power on phenomena at energy scale over $\mathcal{O}(\text{TeV})$. The naturalness problem of the Higgs sector is one of the deepest questions in particle physics, and almost every one of its known solutions corresponds to a different vision of the universe. Identifying the correct answer will not just solve a conceptual puzzle, but will change the way we think about particle physics.

3.2 The Naturalness and Hierarchy Problem

3.2.1 The Gauge-Hierarchy Problem

To understand the origin of the problem, we should start by remembering why we need the Higgs in SM. The Higgs is necessary to get a renormalizable low energy effective electroweak theory [51] and it also allows the generation of mass for the $W^{\pm}$ and Z bosons and fermions in a consistent way. The $W^{\pm}$ and Z bosons violate unitarity bounds at tree-level indicating that the theory is non-perturvative at $\sim 1\,\text{TeV}$. Interestingly, one scalar particle is sufficient to solve the renormalizability problems arising form each of many different massive fields in the SM, of which each causes the problem independently of the others. Now if we go one step further and whatever the theory is beyond the SM, if it is supposed to be finite, for example if it were UV completed into string theory, or more simply if it were the effective description of some condensed matter system, then the bare mass parameter

$$m^2_{h,\text{bare}} = 2\lambda v^2 = -2\mu^2 \tag{3.1}$$

of the unrenormalized Lagrangian and the cutt-off Λ_{SM} would be both physical, and the total Higgs mass $m_{h,\text{physical}}$ could be written schematically as

$$\begin{aligned} m^2_{h,\text{physical}} &= m^2_{h,\text{bare}} + \int_0^{\Lambda_{\text{SM}}} \frac{dm_h^2}{dE}\, dE + \int_{\Lambda_{\text{SM}}}^{\infty} \frac{dm_h^2}{dE}\, dE \\ &= m^2_{h,\text{bare}} + \delta m^2_{h,\text{SM}} + \delta m^2_{h,\text{BSM}} \\ &= m^2_{h,\text{bare}} + \delta m^2_h \end{aligned} \tag{3.2}$$

with $\delta m^2_{h,\text{SM}}$ and $\delta m^2_{h,\text{BSM}}$ being the corresponding SM and beyond the SM radiative corrections, and where E should be regarded as the energy of the virtual particles that run into the loop diagrams through which $m^2_{h,\text{physical}}$ is computed. While $\delta m^2_{h,\text{BSM}}$ is a completely unknown contribution resulting from energies at and above Λ_{SM}, and so there is nothing we can tell about it before we know what the BSM theory is, it turns out that $\delta m^2_{h,\text{SM}}$ comes from virtual quanta below the cut-off and whose dynamics is by assumption well described by the SM. In consequence, the loop

corrections contributing to this last term are, in good approximation, the sum of the four loop contributions 2.63, namely

$$\delta m^2_{h,\mathrm{SM}} \simeq \frac{\Lambda^2_{\mathrm{SM}}}{16\pi^2} C_1(\mu) = \frac{3\Lambda^2_{\mathrm{SM}}}{16\pi^2}\left(-4y_t^2 + \frac{3}{2}g^2 + \frac{1}{2}g'^2 + 4\lambda\right) \tag{3.3}$$

where y_t, g, g' and λ are the top Yukawa coupling, the $\mathrm{SU}(2)_W \times \mathrm{U}(1)_Y$ gauge couplings and the quartic Higgs self-coupling, respectively. In terms of masses the above expression becomes

$$\delta m^2_{h,\mathrm{SM}} \simeq \frac{3\Lambda^2_{\mathrm{SM}}}{8\pi^2 v^2}\left(-4m_t^2 + 2m_W^2 + m_Z^2 + m_h^2\right) \tag{3.4}$$

where all the masses are determined by the well known mass-coupling relations

$$m_t^2(\mu^2) = \frac{1}{2}y_t^2(\mu^2)v^2(\mu^2) \qquad m^2_{W^\pm}(\mu^2) = \frac{1}{4}g^2(\mu^2)v^2(\mu^2) \tag{3.5}$$

$$m_h^2(\mu^2) = 2\lambda(\mu^2)v^2(\mu^2) \qquad m_Z^2(\mu^2) = \frac{1}{4}\left[g^2(\mu^2) + g'^2(\mu^2)\right]v^2(\mu^2) \tag{3.6}$$

On the one hand, the ATLAS and CMS collaborations at LHC observed a scalar boson with properties appearing well consistent with the SM Higgs based on data collected in 2011 and 2012 in the $\gamma\gamma$, ZZ^*, WW^*, $\tau\bar{\tau}$ and $b\bar{b}$ final states [52, 53]. A combination of ATLAS and CMS results for the Higgs boson mass from kinematical reconstruction has yielded [54]

$$m_{h,\mathrm{physical}} = 125.09 \pm 0.24(\mathrm{stat.}) \pm 0.11(\mathrm{syst.})\ \mathrm{GeV} \tag{3.7}$$

On the other hand, the only natural cut-off in the SM is the Planck scale $m_{\mathrm{planck}} = \sqrt{\hbar c/G}$, so that[20]

$$\Lambda_{\mathrm{SM}} \sim m_{\mathrm{planck}} \sim 10^{19}\,\mathrm{GeV} \tag{3.8}$$

and so if no new physics exists between the electroweak and Planck scales, the quantum corrections to $m_{h,\mathrm{physical}}$ would be of order $|\delta m^2_{h,\mathrm{SM}}| \sim (10^{19}\ \mathrm{GeV})^2$, dragging the dimensionful scale $m_{h,\mathrm{bare}}$ of the Higgs potential up to the Planck scale. Nevertheless, this destroy the stability of the weak scale since the physical mass 3.7 is much smaller than the cut-off of the theory. In other words, this implies that the bare mass parameter $m^2_{h,\mathrm{bare}}$ (or equivalently, λ or μ and which is absolutely free), must be a very large number

$$m^2_{h,\mathrm{bare}} \sim (10^{19}\ \mathrm{GeV})^2 \tag{3.9}$$

which means that, at least in the context of the SM, the Higgs boson mass prefers to be close to the very high scale. This raises the question: why is there such a huge hierarchy between the "natural" cut-off 3.8 of the theory and the "natural" energy scale (the observed Higgs mass) of the theory.? This is the *gauge-hierarchy problem*, also known as *big-hierarchy problem* or just the *hierarchy problem*. This set a huge hierarchy between the weak and Planck scales, yet the quadratic divergences of the Higgs sector imply that the two scales should be similar. This hierarchy puzzle can be rephrased in terms of a question about the extremely small dimensionless parameter of the theory:

$$\frac{m_{h,\mathrm{physical}}}{m_{\mathrm{planck}}} \sim 10^{-17} \tag{3.10}$$

Why is this number so small but not zero?

[20] A point particle of mass $m_{\mathrm{planck}}\sqrt{\pi}$ is a black hole with radius equal to its Compton wavelength, a situation which can not be dealt without a proper quantum theory of gravitation.

3.2.2 The Yukawa-Hierarchy Problem

Apart from the inability to understand the extreme small parameter 3.10, the SM incorporates another important hierarchy. Gauge interactions in the SM do not distinguish between the three generations of leptons or between the three generation of quarks. These families only differ by their mass values or, equivalently, their Yukawa coupling through 1.53. For example, in the quark case

$$\begin{pmatrix} y_u \sim 10^{-5} \\ y_d \sim 10^{-5} \end{pmatrix}, \quad \begin{pmatrix} y_c \sim 10^{-2} \\ y_s \sim 10^{-4} \end{pmatrix}, \quad \begin{pmatrix} y_t \sim 1 \\ y_b \sim 10^{-2} \end{pmatrix} \tag{3.11}$$

The values of the Yukawa couplings are not determined in the SM and so one could naturally assumes that all of these parameters lie in the same range of magnitude. Since the experimental evidence has shown this is not the case, one can ask: why there exist these three generations of quarks and leptons, and why the measured Yukawa couplings for the three generations of quarks and leptons display a striking hierarchy in sizes?. This is the *Yukawa-Hierarchy Problem*. As with the gauge-hierarchy problem, there must be a deeper explanation for the Yukawa-hierarchy problem, but this explanation must lie beyond the SM.

3.2.3 The Concept of Fine-Tunning

In order to see why there is also a so-called *naturalness problem* in the Higgs sector, first we must introduce a precise definition of the concept of *fine-tuning*, for which we will use a criterion introduced by R. Barbieri and G. F. Giudice [63]: consider an observable $\mathcal{O} = \mathcal{O}(p_i)$ as a function of the most general parameters p_i of the theory under study. The notion of naturalness is then interpreted as the sensitivity of the observable with respect to variations in the model parameters. To motivate the idea, define Δ_{p_i}, the amount of fine tuning associated to p_i, by

$$\frac{\delta\mathcal{O}}{\mathcal{O}} = \Delta_{p_i} \frac{\delta p_i}{p_i} \tag{3.12}$$

where $\delta\mathcal{O}$ is the change induced in $\mathcal{O}$ by a change δp_i in p_i. In terms of [64], roughly speaking the parameter $|\Delta_{p_i}^{-1}|$ measures the probability of a cancellation among terms of a given size to obtain a result which is $|\Delta_{p_i}|$ times smaller. Formally, we define the *Barbieri-Giudice fine-tuning parameter* as

$$\Delta_{BG}(\mathcal{O}; p_{\max}) := \max_{p_i} \{\, \Delta_{BG}(\mathcal{O}; p_i) \,\} \tag{3.13}$$

where

$$\Delta_{BG}(\mathcal{O}; p_i) := \left| \frac{p_i}{\mathcal{O}} \frac{\partial \mathcal{O}}{\partial p_i} \right| = \left| \frac{\partial \ln \mathcal{O}}{\partial \ln p_i} \right| \tag{3.14}$$

for every parameter p_i. The Barbieri-Giudice parameter 3.13 turns the formulation of the naturalness problem from a vague æsthetic issue to a concrete semiquantitative question. Given the above statistical interpretation of $|\Delta_{p_i}^{-1}|$, alternative variants to this parameter have also been proposed, such as [64, 65]

$$\Delta(\mathcal{O}) := \sqrt{\sum_i \Delta_{BG}(\mathcal{O}; p_i)} \tag{3.15}$$

nonetheless we will use throughout this thesis the convention 3.13. Finally, we avoid an unnatural tuning by imposing

$$\Delta_{BG}(\mathcal{O}; p_{\max}) < x \tag{3.16}$$

so that a percentage variation of any of the parameters p_i does not correspond to a percentage variation of $\mathcal{O}$ more than x-times larger. As Barbieri and Giudice did, many authors choose[21] $x = 10$ as a natural upper bound on $\Delta_{BG}(\mathcal{O}; p_{\max})$. The motivation is the subjective belief that if the discrepancies between quantities were to be natural, they must be less than of one order of magnitude; any x much greater than 10 will be classified as *fine-tuned*. Yet, as such, the choice of a number is arbitrary. Applied to our current case, we have $\mathcal{O} = m_h^2$ and $p_i = p_{\max} = \Lambda_{\rm SM}^2$, and so the Barbieri-Giudice parameter reduce to

$$\Delta_{BG}(m_h^2; \Lambda_{\rm SM}^2) = \left| \frac{\Lambda_{\rm SM}^2}{m_h^2} \frac{\partial m_h^2}{\partial \Lambda_{\rm SM}^2} \right| = \frac{|\delta m_h^2|}{m_h^2} \simeq \left(\frac{\Lambda_{\rm SM}}{450 \text{ GeV}} \right)^2 \tag{3.17}$$

The bigger is Δ_{BG}, the more precise cancellation is needed to accommodate the observed Higgs mass and the less "natural" the theory is. The above expression can also be found by rewritten equation 3.2 as

$$m_{h0}^2 = m_h^2 \left[1 + \Delta_{BG}(m_h^2; \Lambda_{\rm SM}^2) \right] \tag{3.18}$$

and so we say either "the corrections are Δ_{BG} times the Higgs mass", "a fine-tuning of one part in Δ_{BG} is required" or that "a fine-tuning of $\Delta_{BG}^{-1} \times 100$ percent is required". For example, if the Standard Model were valid up to the cut-off scale $\Lambda_{\rm SM} = 10$ TeV, a fine-tuning of about one part in 200 is required. Thus we see again a manifestation of the hierarchy problem. If we want the Standard Model to be valid up to $\Lambda_{\rm SM} = 100$ TeV, the fine-tuning required is much greater, about one part in 20000; on the other hand, around $\Lambda_{\rm SM} = 1$ TeV, the need for fine-tuning disappears completely.

3.2.4 The Concept of Naturalness

There is almost certainly a "naturalness criterion" within every branch of science. For example, in environmental sciences, it refers to the degree to which an area is pristine, free from human influence, and characterized by native species [55]. In mathematics, its meaning is associated with the intuitiveness of certain fundamental concepts, viewed as an intrinsic part of our thinking [56]. It can also be found in computer science, agriculture, in linguistics, etc. However, it is perhaps in physics that the idea has been more influential for the development of the field itself. The concept of naturalness can be funded in particle physics embedded inside two ideas.

Definition 3.1 (Structural Naturalness)**.** The first way the concept of naturalness can be found in particle physics is called *structural naturalness* and refers to the "æsthetic beauty" underlying a theory.

Structural naturalness has been a powerful guiding principle for physicists as they try to construct new theories. This may appear surprising since the final product is often a mathematically

[21] Since then, hundreds of authors have applied this criterion to various problems, from setting a naturalness contour for SUSY particle search, to the fine-tuning problem of the neutrino seesaw mechanism. Barbieri and Giudice's sensitivity criterion has been widely adopted as the doctrine of naturalness judgment.

sophisticated theory based on deep fundamental principles. However, these latter principles are often inspired by criteria of simplicity and beauty. Structural naturalness is a powerful inspirational principle but, of course, it cannot be used to validate a theory, and because of its subjective character, it cannot be quantitatively defined.

Definition 3.2 (Technical Naturalness)**.** The second way the concept of naturalness can be found in particle physics is called *numerical naturalness* or *technical naturalness*, and represents a more precise criterion that currently plays a fundamental role in the formulation of theoretical predictions for new phenomena. The technical naturalness of a theory with cut-off Λ can be assessed by different criteria:

1. A *natural parameter* ξ is one for which $\xi \sim \Lambda$. A *natural theory* is one in which all of the physical parameters are some combination of UV insensitive, natural, and symmetry-natural.

2. A *'t Hooft parameter* or *symmetry-natural parameter* is a parameter ξ for which at any scale μ the replacement $\xi(\mu) = 0$ would increase the symmetry of the system. In this case the physical parameter $\xi(\mu)$ is allowed to be very small, i.e. $\xi \ll \Lambda$, because the symmetry is weakly broken somehow. Consequently, all the parameters associated with this approximate symmetry are stable against radiative corrections, so that they do not receive significant contributions from higher-order quantum effects.

3. A *Dirac parameter* is a dimensionless parameter ξ of order 1.

4. An *unnatural parameter* is a parameter ξ for which there is a fine-tunning at the cut-off scale that produces $m \ll \Lambda$. This UV tuning somehow corrects for the large radiative corrections of the low energy theory. An *unnatural theory* is fine-tuned. This is bad, because there are no known physical mechanisms to produce fine-tuned theories. The only known explanation for fine-tuning is accidental relations in the UV parameters.

Possibly, the first formulation of a technical naturalness criterion was made by Dirac, who establishes that a physical theory is "natural" when all its dimensionless parameters are of order 1. This condition, however, is too restrictive because it would label as unnatural very successful models such as the electroweak theory (fine structure constant $\alpha \sim 10^{-2}$, electron Yukawa coupling $y_e \sim 10^{-6}$, and so on). Historically, a second criterion emerged inside the context of QFT in which the issue of the quadratic growth (divergence) in corrections to scalar masses was first raised by Kenneth G. Wilson [57]. Subsequently, in the late 1970s also Weinberg [58], Susskind [59] and Gildener [60], amongst others, identified a naturalness problem concerning the mass of a fundamental scalar field. Nonetheless, it was Gerard 't Hooft who framed this issue in terms of a principle, which he dubbed the *naturalness condition* [61, 62]; he argue that

> *at any energy scale μ, a physical parameter $\alpha(\mu)$ (or set of parameters) is allowed to be very small only if the replacement $\alpha(\mu) = 0$ would increase the symmetry of the system.*

Consequently, all the parameters associated with this approximate symmetry are stable against radiative corrections, so that they do not receive significant (i.e. $\mathcal{O}(1)$) contributions from higher-order quantum effects. Most of the parameters of the Standard Model are natural in the sense of 't Hooft. For example, the small quark and lepton masses are natural in the sense of 't Hooft despite being orders of magnitude smaller than the weak scale. This is because in the limit that

all of the quark and lepton masses vanish, the Standard Model has a large chiral global symmetry. On the other hand, there is no such recovered symmetry restoration when the Higgs mass goes to zero since the $H^\dagger H$ mass operator is invariant under all symmetries of the Standard Model and all chiral symmetries. Hence, the mass of the Higgs boson fails 't Hooft's test[22] and it is usually refer in this sense that entails a problem of naturalness.

3.2.5 The Higgs Naturalness Problem

The bare mass parameter is not predicted by the SM, but when combined with the BSM corrections loops $\delta m^2_{h,\mathrm{BSM}}$ it should largely cancel the $\delta m^2_{h,\mathrm{SM}}$ term, leaving behind the weak-scale physical mass for the Higgs 3.7. Nevertheless, just inside the SM the correct weak scale can only emerge if the tree level value $m_{h,\mathrm{bare}}$ is an extraordinarily fine-tuned parameter; indeed, if we set $\Lambda_{\mathrm{SM}} \sim 10^{19}$ GeV then note that

$$\begin{aligned} m^2_{h,\mathrm{physical}} &= m^2_{h,\mathrm{bare}} + \delta m^2_h \\ 10^4 &\sim x \cdot 10^{38} - y \cdot 10^{38} \end{aligned}$$

so that

$$x - y \sim 10^{-34} \tag{3.19}$$

and hence $m_{h,\mathrm{bare}}$ must cancels the SM 1-loop corrections with extraordinary precision in order to reproduce the small observed mass. Therefore, in this context our "true" theory formula for the observed Higgs mass requires the miraculous cancellation between the two a priori unrelated terms $m^2_{h,\mathrm{bare}}$ and δm^2_h, and being accurate up to 34 significant digits, and so each of this terms must be known with at least 34 digits accuracy even if we content ourself with an order one estimate of $m_{h,\mathrm{physical}}$. In other words, the bare mass is extremely sensitive to the scale of new physics Λ_{SM} and the parameters in the theory need to be carefully fine-tuned to keep the Higgs mass at an acceptable value of at most a few hundred GeV. Therefore, the square Higgs mass $m^2_{h,\mathrm{bare}}$ is an unnatural parameter in the theory under our previous technical naturalness criterion. This systematic cancellation of dangerous contributions can only be brought about by the type of conspiracy that is better known to physicists as a symmetry. But since in the SM there is no known such symmetry relating the various couplings, this situation is considered to be very unnatural and makes us think that there is more than just a "coincidence relation"[23]. This is the *Higgs Naturalness Problem*. There is no equivalently disquieting equation in particle physics that apparently requires such dramatic fine-tuning of quantum corrections. Only the cosmological constant has perhaps more mystery of such large discrepancies compared to expectations. Interestingly, it is argue in Ref. [47] that in the symmetric phase of the SM, the gauge-boson plus chiral-fermions sector is renormalizable without the Higgs boson and a Yukawa sector and scalars are not required at all to cure the high energy behaviour, because it is renormalizable on its own structure. Therefore, in the symmetric phase the mass-degenerate Higgs fields in the complex Higgs doublet can be as heavy as we like. Since

[22] For a more detailed discussion, see e.g. Refs. [66, 67]

[23] An interesting option was studied by M. J. G. Veltman in the context of dimensional regularization getting the one-loop condition

$$-4m_t^2 + 2m_W^2 + m_Z^2 + m_h^2 \simeq 0$$

known as *Veltman condition*. This is satisfied for a value of the Higgs mass $m_h \simeq 314$ GeV in flagrant conflict with experimental data.

unprotected by any symmetry, naturally we would expect the Higgses indeed to be very heavy. Indeed, the "origin" of the Higgs mass is very different in the broken phase, where the mass is generated by the Higgs itself 3.1 and in the symmetric phase, where is is dynamically generated by the "Planck medium".

The previous problem does not hold exclusively to the Higgs Boson. Indeed, a fine-tunning issue arises whenever the radiative corrections to the mass of a fundamental scalar particle (spin-0 particle) is calculated. In contrast, fermion and gauge boson masses do not lead to problems of this nature because there is a symmetry protecting its mass, e.g. a chiral symmetry for fermions or a gauge symmetry for gauge bosons, and so they do not have the direct quadratic sensitivity to $\Lambda_{\rm SM}$ found in Eq. 3.4. For example, radiative corrections to fermion masses are logarithmically divergent

$$\delta m_f \simeq \frac{3\alpha}{4\pi} m_f \log\left(\frac{\Lambda_{\rm SM}^2}{m_f^2}\right) \tag{3.20}$$

and so in the fermion case these corrections are small, i.e. $\delta m_f < m_f$.

3.2.6 The Little-Hierarchy Problem

We now turn the argument in the other way around. Up to what scale can we expect the SM to be valid if we suppose a fine-tuning of at most 1 part in 10 acceptable? The requirement sets an upper bound

$$\Lambda_{\rm SM} \lesssim 1.4\,\text{TeV} \tag{3.21}$$

This is generally taken as an indication that a simple extrapolation of the SM beyond a scale close to 1 TeV suffers from a naturalness problem because ultraviolet contributions to m_h^2 exceed its physical value. We should then expect to find new physics below or around this energy scale, whose presence is dictated by some symmetry and that naturally cancel the contribution from the top quark. This argument leads to an optimistic prospect, as it sets the scale of new physics on the reach of LHC. However, beginning around the year 2000, LEP experiment opened what we now known as a "little-hierarchy problem" [68–70]. It turns out that upper bounds of the type 3.21 are in a certain tension with the experimental lower bounds on the suppression scale $\Lambda_{\rm SM}$ of higher order operators, derived from fits to precision electroweak data [68,71], which typically require $\Lambda_{\rm SM} \gtrsim 10$ TeV, ruling out new strong interactions at scales below about this scale; moreover, this problem was exacerbated in the last few years by the first run of LHC experiments [72,73]. Therefore, since LEP forbade new physics close to the weak scale, there must be a little hierarchy between the weak scale and the scale of new physics; hence the name.

3.3 Some Approaches to the HNP

In the last decades, several theoretical extensions of the SM, attempting to provide a more satisfactory picture of EWSB and conjecture the structure of the theory at the TeV scale, have been proposed. In *supersymmetry*, new particles with masses at the TeV scale cancel divergent loop corrections to the Higgs mass. In theories with *extra-dimensions*, the fundamental scale of gravity is lowered from $M_{\rm planck}$ to the electroweak scale, thereby removing the hierarchy. In so-called *little Higgs* models, the SM is embedded in a larger symmetry group broken in such a way to provide

the exact amount of new physics at the TeV scale to stabilize $m_{h,\text{bare}}$. In *technicolour*, the source of the problem, i.e. the Higgs boson being a fundamental scalar, is removed since the Higgs is a fermion condensate. New particles and new (strong) interactions are predicted at the TeV scale. Another one, the *Composite Higgs* (CH) scenario, is analysed in this thesis.

3.3.1 The Technicolor Approach

Technicolor (TC) was first proposed in 1979 by S. Weinberg [58] and L. Susskind [59] as one of the first solution to the HNP. This model was inspire in QCD and replaces the Higgs boson with a new strong interaction at a scale Λ_{TC} of few TeV, which eventually triggers the electroweak breaks.

The hypothesis proposed a new asymptotically free strong gauge interaction G_{TC}, called the *technicolor gauge group*, often assumed to be[24] $\text{SU}(N_{\text{TC}})$, with its gauge coupling g_{TC} being small at very high scales ($\mathcal{O}(10^{15}$ GeV), say) and then growing to become strong and confining as we descend in energy to

$$\Lambda_{\text{SM}} \equiv \Lambda_{\text{TC}} \sim \mathcal{O}(1 \text{ TeV}) \tag{3.22}$$

Also, a new set of $\frac{1}{2}N_f$ left- and right-handed doublets of Dirac fermions (known as *technifermions*) is introduced, transforming under complex irreps. of G_{TC}

$$T_{iL,R} = \begin{pmatrix} U_i \\ D_i \end{pmatrix}_{L,R} \tag{3.23}$$

If the T_{L} are assigned to electroweak $\text{SU}(2)_{\text{L}}$ as doublets and the T_{R} as singlets, with appropriate U(1) couplings for all the technifermions, then they are massless and have a large global chiral flavour symmetry

$$G_\chi = \text{SU}(N_f)_{\text{L}} \times \text{SU}(N_f)_{\text{R}} \tag{3.24}$$

with $\text{SU}(2)_{\text{L}} \times \text{U}(1)_{\text{Y}}$ as a weakly gauged subgroup. When g_{TC} becomes strong, this triggers the production of bilinear technifermion condensates and technifermions acquire a dynamical mass (technicolor indices are suppressed here):

$$\langle\Omega|\bar{U}_{iL}U_{jR}|\Omega\rangle_{\text{TC}} = \langle\Omega|\bar{D}_{iL}D_{jR}|\Omega\rangle_{\text{TC}} \simeq -4\pi f_{\text{TC}}^3\delta_{ij} \tag{3.25}$$

where $|\Omega\rangle$ is the ground state of TC and whose symmetry group is $\text{SU}(N_f)_{\text{V}}$, the diagonal subgroup of 3.24. The formation of these condensates will generate the spontaneous symmetry breaking[25] $G_\chi \to \text{SU}(N_f)_{\text{V}}$ at the scale Λ_{TC}. In other words, the technifermion chiral symmetry and the electroweak group do not break until g_{TC} becomes large enough that condensates $\langle\bar{T}_{iL}T_{jR}\rangle_{\text{TC}}$ form. Consequently, a number of $N_f^2 - 1$ massless Goldstone bosons result with decay constant $f_{\text{TC}} = v \simeq 246$ GeV, and three linear combinations of these Goldstone bosons are absorbed as the longitudinal components of the $W^\pm$ and Z^0 weak bosons, generating the weak boson masses

$$m_W = \frac{1}{2}gf_{\text{TC}} \quad \text{and} \quad m_Z = \frac{1}{2}f_{\text{TC}}\sqrt{g^2 + g'^2} \tag{3.26}$$

[24] i.e. $\text{SU}(3)_{\text{C}} \times \text{SU}(2)_{\text{L}} \times \text{U}(1)_{\text{Y}} \times \text{SU}(N_{\text{TC}})$ is now the total gauge group.

[25] Just as happens in QCD, there should also be an infinite tower of bound states -*technihadrons*- that can be classified according to $\text{SU}(N_f)_{\text{V}}$.

Technicolor exploits our understanding of QCD dynamics, which result in an elegantly dynamical explanation for the electroweak symmetry breaking, analogous to the phenomenon that causes chiral symmetry breakdown in QCD. On the other hand, the mechanism is natural and stabilizes the weak scale far below m_{Planck}. However, while TC can explain the masses of of the W's and Z, it has no mechanics to generate mass for the ordinary quarks and leptons. The only natural possibility, if we are to avoid introducing fundamental scalars, is to enlarge G_{TC} to allow technifermions to couple to quarks and leptons. This coupling is induced by gauge bosons of the enlarged group. This approach is called *extended technicolor*[26] (ETC), and the idea is to enlarge the gauge group to

$$\text{SU}(3)_{\text{C}} \times \text{SU}(2)_{\text{L}} \times \text{U}(1)_{\text{Y}} \times \text{SU}(N_{\text{TC}} + 1) \tag{3.27}$$

in which technifermions, quarks, and leptons live in the same representations. The technicolor group will be an $\text{SU}(N_{\text{TC}})$ subgroup of the last factor. While a beautiful idea, this proposal still runs into a number of difficulties. Perhaps the most serious is the problem of flavour-changing neutral currents. In addition to four-fermion operators which generate mass, there will also be four-fermion operators involving just the ordinary quarks and leptons. These operators will not, in general, respect flavour symmetries. Prior to the Higgs discovery, other serious problems have long been noted, especially difficulties with precision studies of the Standard Model. The existence of a Higgs much lighter than 1 TeV, and with width less than a few GeV, is particularly difficult to understand in a Technicolor framework. Most proposals to understand this assume that the technicolor theory is nearly conformal over a range of scales, with a light, SM-like Higgs a consequence.

3.3.2 The Supersymmetric Approach

Supersymmetry (SUSY) not only has played a most important role in the development of theoretical physics over the last three decades, but also has strongly influenced experimental particle physics. Supersymmetry was first proposed, in the context of hadronic physics, by Hironari Miyazawa in 1966 [74]; however, Miyazawa's work was largely ignored at the time. Later, J. L. Gervais and B. Sakita (in 1971) [75], Yu. A. Golfand and E. P. Likhtman (also in 1971) [76], and D. V. Volkov and V. P. Akulov (1972) [77], independently rediscovered supersymmetry in the context of quantum field theory, as a radically new type of symmetry of spacetime and fundamental fields. It was also rediscovered in 1971 by Pierre Ramond [78] and, independently, John H. Schwarz and André Neveu [79] in the context of an early version of string theory where it was a symmetry of the two-dimensional world sheet theory. Shortly after it was realised by Wess and Zumino [80] the characteristic renormalization features of four-dimensional supersymmetric field theories, which identified them as remarkable QFTs. Since then, supersymmetry, along with its monozygotic sibling superstring theory, has become the dominant framework for formulating physics beyond the standard model[27].

Supersymmetry is a symmetry that relates bosons and fermions. Since all matter particles are fermions and all force carriers are bosons, this remarkable symmetry unifies matter and forces. In a theory with supersymmetry, bosons and fermions appear in pairs of equal mass. The particle of the Standard Model do not have this property, so supersymmetry, if it exists in nature, must be spontaneously broken. If nature is supersymmetric, the partners of the known fermions (quarks and

[26] For a detailed discussion about Technicolor and its extensions see, e.g. [81] and [82].
[27] For a historical review on supersymmetry and string theory, see [83]

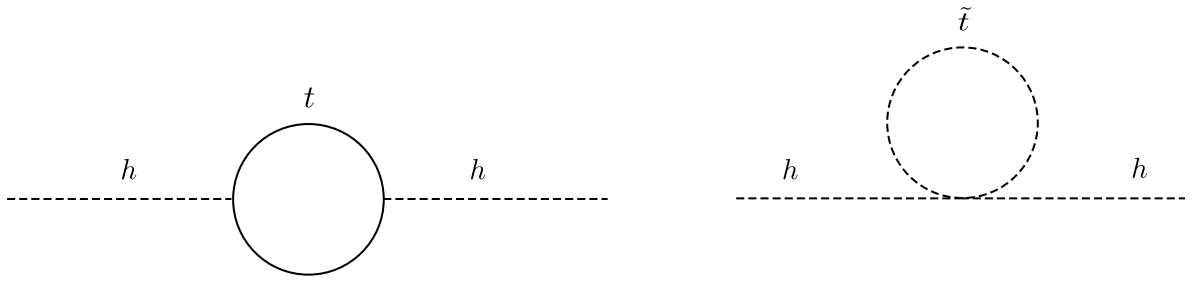

Figure 3.1: Cancellation between fermionic top quark loop (left) and scalar stop squark tadpole (right) in a supersymmetric extension of the Standard Model.

leptons) are complex scalar fields (with the same gauge charges). These particles are referred to as *squarks* and *sleptons*. The partners of the gauge bosons are the *gauginos*. The fermionic partners of the Higgs fields (supersymmetry requires a minimum of two Higgs doublets) are known as *higgsinos*.

There are several reasons why an elementary particle physicist wants to consider supersymmetric theories. An important one is that radiative corrections tend to be less important in supersymmetric theories, due to cancellations between fermion loops and boson loops; this happens because superpartner-coupling constants are related to Standard Model-coupling constants by supersymmetry, but superpartner-loops have the opposite sign from their Standard Model-partner because of opposite spin-statistics. For example, in addition to the top quark loop, there is now a loop containing a stop which tames the quadratic divergence of the Standard Model (Fig. 3.1). There are actually two types of stops, one from an electroweak doublet, one from the singlet. For simplicity, calling the mass of each of these scalars $\tilde{m}_t$, the two Feynman diagrams yield

$$\delta m_h^2 = 3\lambda_t^2 \int \frac{d^4k}{(4\pi)^4} \left(-\frac{1}{k^2 + m_t^2} + \frac{1}{k^2 + \tilde{m}_t^2} \right) \tag{3.28}$$

The leading quadratic divergence cancels, leaving only a logarithmically divergent term:

$$\delta m_h^2 = -\frac{3y_t^2}{16\pi^2} \tilde{m}_t^2 \log \left(\frac{\Lambda_{\mathrm{SM}}^2}{\tilde{m}_t^2} \right) \tag{3.29}$$

Other famous problems solved by SUSY include the vanishing or extreme smallness of the cosmological constant and the issue of renormalisation of quantum gravity. Nevertheless, it must be noted that while supersymmetry could solve most if not all of these questions, it cannot be the full answer, since we know that supersymmetry cannot be exactly realised in nature: it must be broken at experimentally accessible energies since otherwise one certainly would have detected many of the additional particles it predicts.

3.3.3 The Anthropic Principle

The last thing we should probably mention is that the apparently unnatural value of the μ parameter in the Higgs potential may also be motivated by the so-called *anthropic argument*, which states

that

> *the parameters of the universe that we observe are governed by the requirement that they must be able to support intelligent life, as otherwise we would not exist to observe our universe.*

Hence, according to the anthropic principle, a significant fine tuning in certain fundamental parameters is indeed present. If there is only one single universe, with the same laws and parameters everywhere, this is far from a satisfactory physical explanation. However, it has been realized that some physical theories can support the existence of separated domains in the universe in which different parameters and even different gauge groups are applicable. For example, in chaotic inflation [84] different domains have different Higgs vacuum expectation values, selecting different effective particle physics theories. Such domains could be regarded as, effectively, different universes. In a multiple universe theory, the anthropic requirement that we live in a universe with viable parameters is as natural as is the good fortune that we happen to live on a planet that has a temperature ideal for life [28].

4 The Composite Sector and the CCWZ Prescription

4.1 The Composite Higgs Program

As we have seen, the mass of the Higgs boson receives quadratically divergent radiative corrections making it sensitive to the energy scale of any new physics which interacts with it and thus, in the absence of cancellations, is expected to be of the same size as the highest scale in the underlying theory; this rise the question of why the Higgs mass is not, for example, of the order of the Planck mass. Composite Higgs models aim to solve this problem by postulating an scenario where the Higgs particle is not elementary but instead the bound state of some new unspecified strongly coupled constituents, being thus shielded from the UV physics by its composite nature and distinguished from other composite resonances due to the Nambu-Goldstone symmetry, and where the measured value of the Higgs mass demands in addition the existence of lighter exotic resonances. Composite Higgs models are the leading alternative to supersymmetric models for physics beyond the standard model presently tested at the LHC.

4.2 Composite Sector in Isolation

In a CH scenario, the mass of the composite Higgs would not receive corrections from the quanta of the fields at arbitrarily high energies, instead they will interact with its constituents directly. This phenomenon is realized in QCD, and we will see that CH models assemble a mechanism that shares some similarities.

We begin by postulating, in addition to the SM fermions and gauge fields, the existence of a new unspecified strongly interacting sector carryng an *ultracolor (UC) force*[29], conceptually similar

[28] For a more detailed discussion, see e.g. [85]

[29] We follow some of the terminology presented in [86].

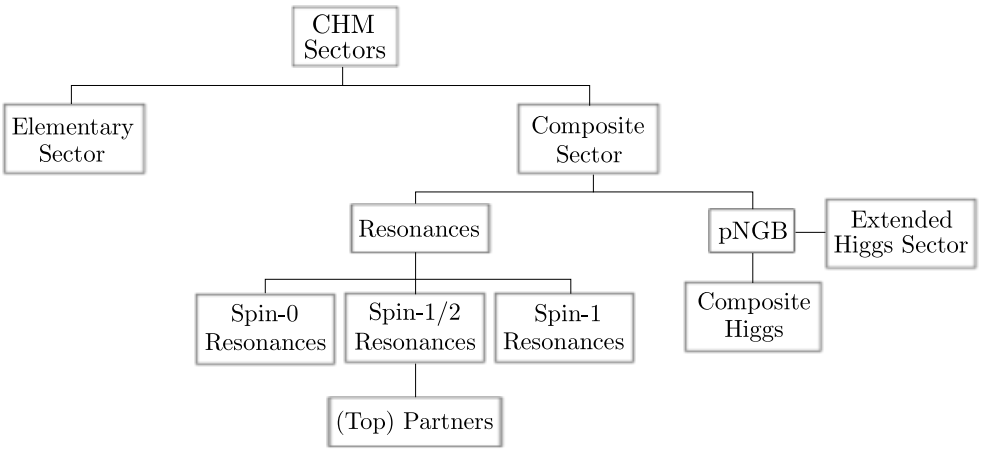

Figure 4.1: Diagram with some of the sectors that can be presented in a composite Higgs model.

to a QCD-like confining theory, and the presence of some *ultrafermions* which interact via gauge group

$$G_{\rm UC} \times {\rm SU}(2)_{\rm L} \times {\rm U}(1)_{\rm Y} \tag{4.1}$$

where $G_{\rm UC}$ is the gauge group of the new sector. This new strong sector is also endowed with a global Lie group symmetry G, which hereafter we assume to be compact, connected and semi-simple and with its low-energy regime just above the electroweak scale. The essential feature of composite Higgs being a solution of the NP is the strongly-coupled nature of the underlying UV theory, by which the Higgs mass is stabilized through dimensional transmutation generating a mass scale that is reasonably insensitive to the detailed UV physics. Then, below that mass scale the theory will appear as being hadronized into bound states whose masses are roughly given by the hadronization scale. It is also assume that when the composite sector is consider in isolation[30], strong effects induce the presence of ultrafermion vacuum condensates breaking spontaneously G down to some subgroup $H \subset G$ at the cut-off scale

$$\Lambda_{\rm SM} \equiv \Lambda_{\rm UC} \simeq 4\pi f \sim \mathcal{O}({\rm TeV}) \tag{4.2}$$

and where f is known as the *decay constant* (the analogue of the pion decay constant f_π in QCD); the currently preferred value is around $f \simeq 0.8$ TeV [87], which gives a corresponding cuttof $\Lambda_{\rm UC} \simeq 10$ TeV. The parameter 4.2 is called the *composition scale* of the new sector, and describes the scale at which the ultrafermions are confined and pNGBs, including the Higgs doublet, are produced [88]; conversely, above this scale the composite states cease to be the relevant degrees of freedom and we begin to observe their internal constituents. The $\Lambda_{\rm UC}$ is therefore an upper bound for a cut-off of our forthcoming effective description. We are not going to make a distinction between a chiral breaking scale and a composition scale as is the case with QCD at $\mu = 0$; see section (1.3.5). The mass of the composite Higgs would not receive correction from the energies which are higher than

[30] By this, we mean that we ignore the couplings of this sector with both the SM gauge fields and the SM fermions, both of which break G explicitly.

the inverse physical size ℓ_h of the Higgs:

$$\ell_h \sim \frac{1}{\Lambda_{\rm UC}} \tag{4.3}$$

i.e. the quanta of the fields at arbitrarily high energies will not interact with the Higgs as a fundamental scalar anymore, but instead they will interact with its constituents directly. The spontaneous breaking implies a number of

$$N_{\rm NGB} := \dim(G/H) = \dim(G) - \dim(H) \geq 4 \tag{4.4}$$

composite NGBs, including one with the quantum numbers of the Higgs. From them, we must be able to construct at least one $\mathrm{SU}(2)_{\rm L}$ doublet in order to identify the four real components of the SM Higgs doublet (from where the constrain ≥ 4 follows) plus possible other scalars from an enlarged Higgs sector. The breaking also introduces a *manifold of degenerate vacua*

$$\mathcal{H}_{\rm vacua} = \{\ |\Phi_0\rangle \mid \langle\Phi_0|V|\Phi_0\rangle \ \text{ is minimal}\ \} \tag{4.5}$$

of the composite sector; any of those degenerate vacua Φ_0 defines a so-called *reference vacuum orientation*, and without loss of generality, it can always be chosen at our convenience. It follows the identification

$$H := \mathrm{Stab}_G(\Phi_0) = \{\ g \in G \mid g \cdot \Phi_0 = \Phi_0\ \} \tag{4.6}$$

and referred to as the corresponding *reference invariant subgroup*.

In order to work out the theory, first of all we must introduce a reference system in the Lie algebra $\mathfrak{g}$ of G and fix some basis of generators T_A, divided into two categories

$$\{T_A\}_{A=1}^{\dim G} = \{T_a\}_{a=1}^{\dim H} \cup \{\hat{T}_{\hat{a}}\}_{\hat{a}=1}^{\dim G/H} \tag{4.7}$$

and usually normalized as

$$\mathrm{Tr}(T_A T_B) = \delta_{AB} \tag{4.8}$$

On the one hand, the unbroken generators T_a span the subalgebra $\mathfrak{h} \subset \mathfrak{g}$ of H, which are associated to fields that do not lead to physical degree of freedom when describing the NBGs of the theory. On the other hand, the broken generators $\hat{T}_{\hat{a}}$ expand the left coset space

$$G/H \cong \{\ \exp(i\alpha_{\hat{a}}\hat{T}_{\hat{a}}) \mid \alpha_{\hat{a}} \in \mathbb{R}\ \} \tag{4.9}$$

and they are associated with the physical degree of freedom describing the NGBs of the theory. Consequently, a reference vacuum Φ_0 can by fixed describing one of the degenerate vacua of the composite sector, such that[31]

$$T_a\Phi_0 = 0 \quad \text{and} \quad \hat{T}_{\hat{a}}\Phi_0 \neq 0 \tag{4.10}$$

in order to be consistent with 4.6. At first, and from the viewpoint of the composite sector alone, there is no preferred vacuum Φ_0. Therefore, the embedding 4.6 is arbitrary (i.e. any embedding

[31] Note that by the second equation, we mean that $\{T_{\hat{a}}\Phi_0\}$ constitute a linearly independent set.

of H in G by different vacua Φ_0 is completely equivalent), and so consequently the choice of generators 4.7. Nevertheless, we will see that CH models demand the embedding of the EW group

$$G_{\rm EW} := {\rm SU}(2)_{\rm L} \times {\rm U}(1)_{\rm Y} \tag{4.11}$$

in H. In fact, this is precisely what makes CH models so different from technicolor: the existence of two separate phase transitions in the theory. Namely, at some large scale one passes from a regime of free fermions to one of light bound states (including the Higgs doublet); this is followed by a second transition at the usual weak scale where the Higgs develops a VEV and breaks ${\rm SU}(2)_{\rm L} \times {\rm U}(1)_{\rm Y}$. Consequently, it is convenient to choose the T_A's in such a way that the embedding of H contains all the $G_{\rm EW}$ generators.

Finally, the phenomenology of the NGBs can be analysed by a non-linear sigma model. The general formalism will be analysed in section (4.5) through the so-called *CCWZ prescription*. Nambu-Goldstone boson fields parametrise the *angular fluctuations* $\Phi = \Phi(x)$ around any chosen reference vacuum Φ_0, and since we know that this fluctuations correspond to local transformations in the directions of the $\hat{T}_{\hat{a}}$'s, it will be convenient to perform the ansatz

$$\Phi(x) = \exp\left(i \frac{\sqrt{2}}{f} \phi_{\hat{a}} \hat{T}_{\hat{a}} \right) \Phi_0 \tag{4.12}$$

We have parametrized the NGBs

$$\phi_{\hat{a}} = \phi_{\hat{a}}(x) \tag{4.13}$$

arising from the general symmetry breaking $G \to H$ through the so-called Σ-*model field* or *Goldstone matrix*

$$\Sigma[\phi] := \exp\left(i \frac{\sqrt{2}}{f} \phi_{\hat{a}} \hat{T}_{\hat{a}} \right) \tag{4.14}$$

describing the NGBs as the fluctuations along the G/H broken directions, and which transforms in the fundamental representation of G. This matrix can be defined for any $G \to H$ breaking and it ubiquitously appears in CH models. The normalization factor $\frac{\sqrt{2}}{f}$ has been chosen to obtain a canonical kinematic term for the NGB fields. Nambu-Goldstone bosons enter in the picture through the Goldstone matrix, but eventually they form multiplets of some representation of H.

If the composite sector is still consider in isolation, then the ϕ fields are exact NGBs and hence they have no potential and their VEV's are completely arbitrary, i.e, they are *unobservable*. This is because the inherent arbitrariness in the choice of the vacuum implies any possible values in the VEV's of the NGB's, giving rise to an ambiguity in their choice. In this way, it is possible to set, in full generality, $\langle \phi_{\hat{a}} \rangle = 0$.

4.3 Vaccum Misalignment

Up to now we discussed the global symmetry of the composite sector consider in isolation and its spontaneous breaking; now we need to introduce one of its sources of explicit breaking. As we anticipated in the previous section, another important condition that is demanded in CH models is that the electroweak group 4.11 must be entirely embeddable into H. This is because in the

limit of vanishing couplings between the strong sector and the gauge bosons, the EW group should preserve the reference vacuum Φ_0, so we say that there is a *perfect alignment*, and hence whether or not the weak interactions are broken becomes an alignment question. To be honest, the strongly interacting sector G should also have an embeddable $\mathrm{SU}(3)_\mathrm{C}$ global symmetry associated to color, but this is irrelevant for our considerations and so it will not be considered in what follows. The existence of the embedding $G_\mathrm{EW} \hookrightarrow H$ will have important consequences for the phenomenology of the models built upon the symmetry breaking.

On the other hand, it turns out that the interactions of the resonances in the strong sector with the SM fields, i.e. with the gauge bosons (by gauging $G_\mathrm{SM} \subseteq H$) and fermions, explicitly break the global symmetry, leading to a Higgs potential at loop level. Consequently, some NGBs become *pseudo Nambu-Goldstone bosons* and their VEV $\langle\phi_{\hat{a}}\rangle$ is not arbitrary anymore. Moreover, their VEVs $\langle\phi_{\hat{a}}\rangle$ become observable as it can not be set to zero by an exact symmetry transformation; this uplifted the degeneracy of the vacua and fixes a *true vacuum*

$$\Omega_0 = \Sigma[\langle\phi_{\hat{a}}\rangle]\Phi_0 \tag{4.15}$$

corresponding to the EW vacuum; this phenomenon is knows as a *vacuum misalignment* (see Fig. (4.2a)). Finally, it will happen that a Coleman-Weinberg potential for the (composite) Higgs will be generated at one loop due to its gauge and fermion interactions. However, the gauge contributions are usually aligned with the EW gauge group, unlike the fermion contributions and which are expected to be large because of the large top mass. The latest will effectively provide a VEV to the Higgs field h, triggering the EWSB and the breaking SO(4) down to the custodial SO(3) group.

Since CH models are extensions of the SM, a more general subgroup $H_0 \subset G$ including the EW group could be gauged (see Fig. (4.2b)). Therefore, among the N_NGB Nambu-Goldstone bosons resulting from the spontaneous breaking $G \to H$, there will be

$$N_e := \dim(H_0) - \dim(H_0 \cap H) \geq 3 \tag{4.16}$$

of them eaten to provide the longitudinal degrees of freedom of the corresponding gauge bosons associated with the broken generators of H_0, with at least three of them, say $\phi^\pm$ and ϕ^0, giving rise to the known EW gauge bosons $W^\pm, Z^0$ (see Fig. 4.2b). The remaining NGBs ϕ become pNGBs as result of the explicit breaking. Indeed, in the forthcoming discussions we will identify H_0 with the SM electroweak group: $H_0 = G_\mathrm{SM}$.

In CH models the SM fields, apart from the Higgs, are typically considered as mostly elementary and not belonging to the new strong sector. It turns out the misalignment of the external sector G_EW with respect to H is always possible to relate it with the value of the Higgs VEV through

$$v = f \sin\langle\phi\rangle \tag{4.17}$$

where $\langle\phi\rangle$ is called the *misalignment angle*. This condition is conveniently expressed through the *fine-tuning parameter*

$$\xi := \frac{v^2}{f^2} = \sin^2\langle\phi\rangle \in (0, 1] \tag{4.18}$$

which appears ubiquitously in the study of composite Higgs in the literature. Geometrically, it determines the orientation of G_SM with respect to H in the true vacuum Ω or *degree of misalignment*

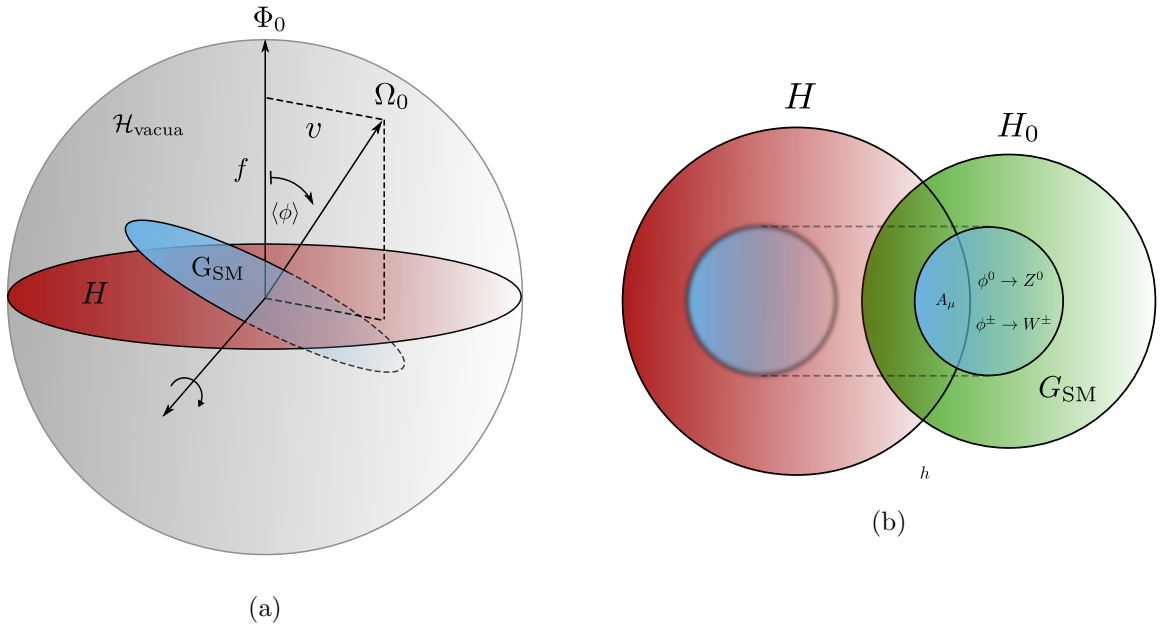

Figure 4.2: (a) Schematic representation of the gauging process of G_{SM}; it breaks G explicitly, fixes a non-zero VEV for the NGBs, and hence generates a vacuum misalignment. (b) Once G_{SM} has been gauged, the $G \to H$ spontaneous breaking gives rise to at least four NGBs, say $\phi_\pm, \phi_0$ and h, three of which are eaten as the longitudinal degrees of freedom of the EW gauge bosons $W^\pm, Z^0$. The remaining unbroken gauge boson A_μ is the photon and the uneaten NGB h remains a physical scalar.

(see Fig. (4.2a)), while algebraically it sets the size of the parametric suppression in all corrections to the precision observables. The limit $f \to \infty$ (i.e. $\xi \to 0$) with fixed v is thus a decoupling limit where the Higgs stays light and all the other resonances become infinitely heavy. On the other hand, the limit $f \to v$ (i.e. $\xi \to 1$), at fixed v, constitutes a technicolor-like scenario.

4.4 The Toy Model SO(3)/SO(2)

To illustrate some of the above general ideas and to gain a better understanding of the issues involved in realizing the Higgs as a NGB, we will consider in this section a simple toy model which incorporates the ideas presented in the previous sections.

Consider a theory with a global SO(3) symmetry spontaneously broken to an SO(2) subgroup, at a scale $\Lambda \equiv \Lambda_{\text{UC}}$. The manifold of equivalent vacua is $\mathcal{H}_{\text{vacua}} = S^2$, and for simplicity and without loss of generality, we choose a representative vacuum Φ_0 pointing along the third component

$$\Phi_0 = (0, 0, f)^T \tag{4.19}$$

and let $\Phi = \Phi(x)$ be a triplet of real scalar fields parameterizing the fluctuations around the above vacuum Φ_0. We propose the following phenomenological Lagrangian describing our toy strongly-

interacting composite sector:

$$\mathcal{L}[\Phi, \partial_\mu \Phi] = \frac{1}{2}\partial_\mu \Phi^T \partial^\mu \Phi - \frac{g_*^2}{8}(\Phi^T \Phi - f^2)^2 \tag{4.20}$$

The parameter g_* controls the interactions in our Lagrangian, and it is thus interpreted as an effective low-energy coupling of the composite sector. Given our choice of Φ_0 and taking into account the conditions 4.10, the SO(3) generators, can be conveniently chosen as

$$T = \frac{1}{\sqrt{2}} \begin{pmatrix} 0 & -i & 0 \\ i & 0 & 0 \\ 0 & 0 & 0 \end{pmatrix} \tag{4.21}$$

and

$$\hat{T}_1 = \frac{1}{\sqrt{2}} \begin{pmatrix} 0 & 0 & -i \\ 0 & 0 & 0 \\ i & 0 & 0 \end{pmatrix}, \quad \hat{T}_2 = \frac{1}{\sqrt{2}} \begin{pmatrix} 0 & 0 & 0 \\ 0 & 0 & -i \\ 0 & i & 0 \end{pmatrix} \tag{4.22}$$

which are also conveniently normalized as $\mathrm{Tr}(T_A T_B) = \delta_{AB}$. Indeed,

$$T\Phi_0 = \frac{1}{\sqrt{2}} \begin{pmatrix} 0 & -i & 0 \\ i & 0 & 0 \\ 0 & 0 & 0 \end{pmatrix} \begin{pmatrix} 0 \\ 0 \\ f \end{pmatrix} = \begin{pmatrix} 0 \\ 0 \\ 0 \end{pmatrix} \quad \text{Unbroken generator}$$

$$\hat{T}_1\Phi_0 = \frac{1}{\sqrt{2}} \begin{pmatrix} 0 & 0 & -i \\ 0 & 0 & 0 \\ i & 0 & 0 \end{pmatrix} \begin{pmatrix} 0 \\ 0 \\ f \end{pmatrix} = \frac{1}{\sqrt{2}} \begin{pmatrix} -if \\ 0 \\ 0 \end{pmatrix} \quad \text{Broken generator}$$

$$\hat{T}_2\Phi_0 = \frac{1}{\sqrt{2}} \begin{pmatrix} 0 & 0 & 0 \\ 0 & 0 & -i \\ 0 & i & 0 \end{pmatrix} \begin{pmatrix} 0 \\ 0 \\ f \end{pmatrix} = \frac{1}{\sqrt{2}} \begin{pmatrix} 0 \\ -if \\ 0 \end{pmatrix} \quad \text{Broken generator}$$

and note that the theory 4.20 is invariant, as shout it be, under SO(3) transformations

$$\Phi \mapsto \exp(i\alpha_A T_A)\Phi \tag{4.23}$$

with $A = 1, 2, 3$ and $\alpha_A \in \mathbb{R}$. Geometrically, the three generators $T, \hat{T}_1$ and $\hat{T}_2$ correspond to rotations in the xy, xz and yz planes, respectively. As we said in the previous section, in order to study the fluctuations around the vacuum Φ_0 it is convenient to perform a field redefinition and to trade the three Φ components as one radial coordinate $\sigma = \sigma(x)$ plus two angular variables $\phi_{1,2} = \phi_{1,2}(x)$ (the NGBs). We write

$$\Phi = \exp\left(i\frac{\sqrt{2}}{f}\phi_{\hat{a}}\hat{T}_{\hat{a}}\right) \begin{pmatrix} 0 \\ 0 \\ f + \sigma \end{pmatrix} = \Sigma[\phi_1, \phi_2] \begin{pmatrix} 0 \\ 0 \\ f + \sigma \end{pmatrix} \tag{4.24}$$

Note that this is not exactly the parametrization 4.12 since here we are including radial fluctuations. The Goldstone matrix in this case is explicitly given by

$$\begin{aligned}\Sigma[\phi_1,\phi_2] &= \exp\left(i\frac{\sqrt{2}}{f}\left[\frac{1}{\sqrt{2}}\begin{pmatrix}0&0&-i\phi_1\\0&0&0\\i\phi_1&0&0\end{pmatrix}+\frac{1}{\sqrt{2}}\begin{pmatrix}0&0&0\\0&0&-i\phi_2\\0&i\phi_2&0\end{pmatrix}\right]\right)\\ &= \begin{pmatrix}\frac{\phi_2^2+\phi_1^2\cos\frac{\phi}{f}}{\phi^2} & \frac{\phi_1\phi_2\left(-1+\cos\frac{\phi}{f}\right)}{\phi^2} & \frac{\phi_1}{\phi}\sin\frac{\phi}{f}\\ \frac{\phi_1\phi_2\left(-1+\cos\frac{\phi}{f}\right)}{\phi^2} & \frac{\phi_1^2+\phi_2^2\cos\frac{\phi}{f}}{\phi^2} & \frac{\phi_2}{\phi}\sin\frac{\phi}{f}\\ -\frac{\phi_1}{\phi}\sin\frac{\phi}{f} & -\frac{\phi_2}{\phi}\sin\frac{\phi}{f} & \cos\frac{\phi}{f}\end{pmatrix}\end{aligned} \tag{4.25}$$

where we have defined

$$\vec{\phi} := \begin{pmatrix}\phi_1\\ \phi_2\end{pmatrix} \in \mathbf{2} \text{ of } \mathrm{SO}(2) \tag{4.26}$$

and $\phi := \sqrt{\vec{\phi}^{\,T}\vec{\phi}}$. The above expression for Σ can be simplify as

$$\begin{aligned}\Sigma[\phi_1,\phi_2] &= \begin{pmatrix}1-\frac{\phi_1^2}{\phi^2}\left(1-\cos\frac{\phi}{f}\right) & -\frac{\phi_1\phi_2}{\phi^2}\left(1-\cos\frac{\phi}{f}\right) & \frac{\phi_1}{\phi}\sin\frac{\phi}{f}\\ -\frac{\phi_1\phi_2}{\phi^2}\left(1-\cos\frac{\phi}{f}\right) & 1-\frac{\phi_2^2}{\phi^2}\left(1-\cos\frac{\phi}{f}\right) & \frac{\phi_2}{\phi}\sin\frac{\phi}{f}\\ -\frac{\phi_1}{\phi}\sin\frac{\phi}{f} & -\frac{\phi_2}{\phi}\sin\frac{\phi}{f} & \cos\frac{\phi}{f}\end{pmatrix}\\ &= \begin{pmatrix}1_2-\frac{\vec{\phi}\,\vec{\phi}^{\,T}}{\phi^2}\left(1-\cos\frac{\phi}{f}\right) & \frac{\vec{\phi}}{\phi}\sin\frac{\phi}{f}\\ -\frac{\vec{\phi}^{\,T}}{\phi}\sin\frac{\phi}{f} & \cos\frac{\phi}{f}\end{pmatrix}\end{aligned} \tag{4.27}$$

with inverse

$$\Sigma[\phi_1,\phi_2]^{-1} = \begin{pmatrix}1_2-\frac{\vec{\phi}\,\vec{\phi}^{\,T}}{\phi^2}\left(1-\cos\frac{\phi}{f}\right) & -\frac{\vec{\phi}}{\phi}\sin\frac{\phi}{f}\\ \frac{\vec{\phi}^{\,T}}{\phi}\sin\frac{\phi}{f} & \cos\frac{\phi}{f}\end{pmatrix} \tag{4.28}$$

An analogous result is obtained in the more general spontaneous symmetry breaking pattern $\mathrm{SO}(n)\to\mathrm{SO}(n-1)$ (see Appendix B). Therefore, the field Φ becomes

$$\Phi = (f+\sigma)\begin{pmatrix}\frac{\vec{\phi}}{\phi}\sin\frac{\phi}{f}\\ \cos\frac{\phi}{f}\end{pmatrix} \tag{4.29}$$

By substituting in the Lagrangian 4.20 we obtain, term by term:

$$\begin{aligned}
\frac{1}{2}\partial_\mu\Phi^T\partial^\mu\Phi &= \frac{1}{2}\left[\frac{\vec{\phi}^{\,T}\partial_\mu\sigma}{\phi}\sin\frac{\phi}{f}+\frac{(f+\sigma)(\phi\partial_\mu\vec{\phi}^{\,T}-\vec{\phi}^{\,T}\partial_\mu\phi)}{\phi^2}\sin\frac{\phi}{f}+\frac{\vec{\phi}^{\,T}(f+\sigma)\partial_\mu\phi}{f\phi}\cos\frac{\phi}{f}\right]\\
&\times\left[\frac{\vec{\phi}\,\partial^\mu\sigma}{\phi}\sin\frac{\phi}{f}+\frac{(f+\sigma)(\phi\partial^\mu\vec{\phi}-\vec{\phi}\,\partial^\mu\phi)}{\phi^2}\sin\frac{\phi}{f}+\frac{\vec{\phi}\,(f+\sigma)\partial^\mu\phi}{f\phi}\cos\frac{\phi}{f}\right]\\
&+\frac{1}{2}\left[(\partial_\mu\sigma)\cos\frac{\phi}{f}-\frac{(f+\sigma)\partial_\mu\phi}{f}\sin\frac{\phi}{f}\right]\times\left[(\partial^\mu\sigma)\cos\frac{\phi}{f}-\frac{(f+\sigma)\partial^\mu\phi}{f}\sin\frac{\phi}{f}\right]\\
&=\frac{1}{2}\left[(\partial\sigma)^2+\frac{(f+\sigma)^2[(\partial\vec{\phi})^2-(\partial\phi)^2]}{\phi^2}\sin^2\frac{\phi}{f}+\frac{(f+\sigma)^2(\partial\phi)^2}{f^2}\right]\\
&=\frac{1}{2}(\partial\sigma)^2+\frac{1}{2}\left(1+\frac{\sigma}{f}\right)^2\left[\frac{f^2}{\phi^2}\sin^2\frac{\phi}{f}(\partial\vec{\phi})^2+\frac{f^2}{\phi^2}\left(\frac{\phi^2}{f^2}-\sin^2\frac{\phi}{f}\right)(\partial\phi)^2\right]\\
&=\frac{1}{2}(\partial\sigma)^2+\frac{1}{2}\left(1+\frac{\sigma}{f}\right)^2\left[\frac{f^2}{\phi^2}\sin^2\frac{\phi}{f}(\partial\vec{\phi})^2+\frac{f^2}{4\phi^4}\left(\frac{\phi^2}{f^2}-\sin^2\frac{\phi}{f}\right)(\partial\phi^2)^2\right]
\end{aligned}$$

where in the last line we have used the fact that $(\partial\phi^2)^2 = 4\phi^2(\partial\phi)^2$. On the other hand, the potential term yields:

$$\frac{g_*^2}{8}(\Phi^T\Phi-f^2)^2=\frac{1}{2}(g_*f)^2\sigma^2+\frac{g_*^2 f}{2}\sigma^3+\frac{g_*^2}{8}\sigma^4 \tag{4.30}$$

Putting these expressions together, the Lagrangian 4.20 becomes:

$$\begin{aligned}
\mathcal{L} &= \frac{1}{2}(\partial\sigma)^2-\frac{1}{2}(g_*f)^2\sigma^2-\frac{g_*^2 f}{2}\sigma^3-\frac{g_*^2}{8}\sigma^4\\
&+\frac{1}{2}\left(1+\frac{\sigma}{f}\right)^2\left[\frac{f^2}{\phi^2}\sin^2\frac{\phi}{f}(\partial\vec{\phi})^2+\frac{f^2}{4\phi^4}\left(\frac{\phi^2}{f^2}-\sin^2\frac{\phi}{f}\right)(\partial\phi^2)^2\right]
\end{aligned} \tag{4.31}$$

In agreement with Goldstone's theorem the ϕ's describe two massless boson associated with the two broken generators $\hat{T}_{1,2}$. The σ field has instead a mass

$$m_\sigma = g_* f \tag{4.32}$$

and in analogy with a strongly coupled sector, the σ field will be called a resonance. In fact, we will generically call a *resonance* any particle that emerges from the composite sector aside from the Goldstone bosons [89]. This mass also gives the strong sector confinement scale, conceptually similar to the chiral symmetry breaking scale λ_χ in QCD. Furthermore, in a genuine strong theory g could easily be of order 4π. Also note that every NGB is derivatively couplet. Thus, its interactions are proportional to its momentum, and as $p \to 0$ it becomes a free field. This is clear geometrically, since the potential is only a function of radial direction and not the angle, so there can be no non-derivative terms containing $\theta(x)$ in the Lagrangian. These derivative couplings of the NGBs is another general consequence of the SSB of a global symmetry, and is very important in the discussion of composite Higgs interactions.

The presence of doublet 4.26 in 4.42 evidences the realization of a SO(2)-invariance

$$\vec{\phi} \mapsto \exp(i\alpha\sigma^2)\vec{\phi} \tag{4.33}$$

which can be traced back up to one of the symmetries of the original Lagrangian 4.20, induces by the unbroken generator T:

$$\mathrm{SO}(2) = \mathrm{Stab}_{\mathrm{SO}(3)}(\Phi_0) \cong \{\, \exp(i\alpha\sigma^2) \mid \alpha \in \mathbb{R} \,\} \tag{4.34}$$

We say that 4.33 is a *linearly realized symmetry* as it acts in a linear and homogeneous way on the field variables. On the other hand, there will be two *non-linearly realized* transformations associated with the broken generators $\hat{T}_{\hat{a}}$. Since $\mathrm{SO}(2) \cong \mathrm{U}(1)$, we can switch from state space (i.e. $\mathbb{R}^2 \leftrightarrow \mathbb{C}$) by defining

$$h := \frac{1}{\sqrt{2}}(\phi_1 + i\phi_2) \tag{4.35}$$

so that

$$\phi_1 = \frac{1}{\sqrt{2}}(h + h^*) \quad \text{and} \quad \phi_2 = \frac{1}{i\sqrt{2}}(h - h^*) \tag{4.36}$$

This switch the Lagrangian 4.42 into

$$\begin{aligned}\mathcal{L} = {} & \frac{1}{2}(\partial\sigma)^2 - \frac{1}{2}(g_* f)^2\sigma^2 - \frac{g_*^2 f}{2}\sigma^3 - \frac{g_*^2}{8}\sigma^4 \\ & + \frac{1}{2}\left(1 + \frac{\sigma}{f}\right)^2 \left[\frac{f^2}{|h|^2}\sin^2\left(\frac{\sqrt{2}|h|}{f}\right)\partial_\mu h^* \partial^\mu h + \frac{f^2}{4|h|^4}\left(\frac{2|h|^2}{f^2} - \sin^2\left(\frac{\sqrt{2}|h|}{f}\right)\right)(\partial|h|^2)^2\right]\end{aligned} \tag{4.37}$$

Now that the NGBs have been obtained the last ingredient to construct the model is to gauge, with coupling strength e, the unbroken U(1) subgroup. This is achieved by replacing the derivatives in the Lagrangian 4.20 with the corresponding covariant derivative

$$\partial_\mu \Phi \to D_\mu \Phi = (\partial_\mu + ie\sqrt{2}A_\mu T)\Phi \tag{4.38}$$

where A_μ is a new U(1) gauge field with canonical kinetic term $F_{\mu\nu}F^{\mu\nu}$ and its gauge coupling with Φ are elementary/composite interaction. The resulting Lagrangian

$$\mathcal{L}[\Phi, \partial_\mu\Phi] = -\frac{1}{4}F_{\mu\nu}F^{\mu\nu} + \frac{1}{2}(D_\mu\Phi)^\dagger D^\mu\Phi - \frac{g^2}{8}(\Phi^\dagger\Phi - f^2)^2 \tag{4.39}$$

is gauge invariant provided the gauge field A_μ transform as

$$A_\mu T \mapsto U\left(A_\mu T + \frac{1}{ie}\partial_\mu\right)U^\dagger \quad \text{where } U = e^{i\alpha(x)T} \in \mathrm{U}(1) \tag{4.40}$$

The gauging, since it selects one generator among three, breaks SO(3) explicitly to SO(2). The effect of the gauging is also achieved in Lagrangian 4.42 by switching

$$\partial_\mu\vec{\phi} \to D_\mu\vec{\phi} = (\partial_\mu + ieA_\mu\sigma^2)\vec{\phi} \tag{4.41}$$

so that

$$\begin{aligned}\mathcal{L} = &-\frac{1}{4}F_{\mu\nu}F^{\mu\nu} \\ &+\frac{1}{2}(D\sigma)^2 - \frac{1}{2}(gf)^2\sigma^2 - \frac{g^2 f}{2}\sigma^3 - \frac{g^2}{8}\sigma^4 \\ &+\frac{1}{2}\left(1+\frac{\sigma}{f}\right)^2\left[\frac{f^2}{\phi^2}\sin^2\frac{\phi}{f}(D\vec{\phi})^2 + \frac{f^2}{4\phi^4}\left(\frac{\phi^2}{f^2}-\sin^2\frac{\phi}{f}\right)(\partial\phi^2)^2\right]\end{aligned} \tag{4.42}$$

and in Lagrangian 4.37 by switching

$$\partial_\mu h \to D_\mu h = (\partial_\mu + ieA_\mu)h \tag{4.43}$$

so that

$$\begin{aligned}\mathcal{L} = &\frac{1}{2}(\partial\sigma)^2 - \frac{1}{2}(g_* f)^2\sigma^2 - \frac{g_*^2 f}{2}\sigma^3 - \frac{g_*^2}{8}\sigma^4 \\ &+\frac{1}{2}\left(1+\frac{\sigma}{f}\right)^2\left[\frac{f^2}{|h|^2}\sin^2\left(\frac{\sqrt{2}|h|}{f}\right)(D_\mu h)^*(D^\mu h) + \frac{f^2}{4|h|^4}\left(\frac{2|h|^2}{f^2}-\sin^2\left(\frac{\sqrt{2}|h|}{f}\right)\right)(\partial|h|^2)^2\right]\end{aligned} \tag{4.44}$$

Now a non-vanishing potential for h is no longer forbidden, which will be radiatively generated by the gauge field loops. The potential gives in turn a non-vanishing VEV to our toy composite Higgs h and the breaking of the U(1) gauge symmetry can take place. A vacuum misalignment then take place by the now true vacuum of the theory

$$\Omega_0 = \exp\left(i\frac{\sqrt{2}}{f}\langle\phi_{\hat{a}}\rangle\hat{T}_{\hat{a}}\right)\Phi_0$$

It follows from one of the terms in 4.44 that

$$\frac{1}{2}\frac{f^2}{|h|^2}\sin^2\left(\frac{\sqrt{2}|h|}{f}\right)e^2 A_\mu A^\mu |h|^2 = \frac{1}{2}\left(ef\sin\frac{\sqrt{2}|h|}{f}\right)^2 A_\mu A^\mu \tag{4.45}$$

So, by setting the Higgs to its VEV $\langle h\rangle := V/\sqrt{2}$, the gauge boson A_μ acquires a mass

$$m_A = ef\sin\frac{V}{f} = ev \tag{4.46}$$

where $v := ef\sin(V/f)$ has been defined as the scale of the spontaneous symmetry breaking of U(1).

4.5 The CCWZ Construction

When trying to understand the low-energy and confinement regime of a strong dynamic, there are methods allowing us to work within this regime without the knowledge of the full underlying theory and all the difficulties that this would imply. One of these approaches, nowadays known as

the *Callan-Coleman-Wess-Zumino (CCWZ) prescription* [90, 91], constitute a full treatment that allows to write general low-energy effective Lagrangians for strongly or weakly coupled theories characterised by a generic $G \to H$ global symmetry breaking pattern, describing the Goldstone bosons associated with the breaking and the heavy resonances. It is readily extended to incorporate explicit symmetry breaking. Furthermore the generality of the method makes it an essential tool for the systematic study of non-minimal cosets, when trying to go beyond the custodial minimal model SO(5)/SO(4).

4.5.1 Non-linear Realization of a Symmetry

Now we proceed to derive the CCWZ prescription. Let us begin by identifying the degrees of freedom that described the NGBs, one for each broken generators as predict by Goldstone's theorem. In order to do this, we consider all the configurations that are related to some fixed representative vacuum Φ_0 by a local G transformation, namely

$$\Phi(x) = g \cdot \Phi_0 \tag{4.47}$$

and with $\cdot$ the appropriate action of G over $\mathcal{H}_{\text{vacua}}$. For every $g \in G$ we have

$$g = \exp(i\alpha_A T_A) = \exp(i\alpha_{\hat{a}}\hat{T}_{\hat{a}} + i\alpha_a T_a) \tag{4.48}$$

where T_A denotes the full set of generators of the group G, and $\hat{T}_{\hat{a}}$ and T_a are the broken and unbroken generators of G, respectively. The scalar fields $\alpha_{\hat{a}} = \alpha_{\hat{a}}(x)$ are coordinates of the coset space G/H at each point of spacetime, and the set of group elements $\exp(i\alpha_{\hat{a}}\hat{T}_{\hat{a}})$ parametrizes this coset space (see 4.9). Returning to 4.47, we note that not all of the fields α_A are physical, but some of them are redundant and they can be dropped from this ansatz. To see this, consider the well-known fact that each element $g \in G$ can be written in a unique way as a product of the form

$$g = \exp(i\theta_{\hat{a}}\hat{T}_{\hat{a}}) \exp(i\zeta_a T_a) \tag{4.49}$$

This decomposition means that once we have a parametrization $l(\theta) = \exp(i\theta_{\hat{a}}\hat{T}_{\hat{a}})$, each group element $g \in G$ can be uniquely decomposed into a product $g = lh$, where l is the representative member of the coset to which g belongs and $h(\zeta) = \exp(i\zeta_a T_a) \in H$ connects l to g within the coset. By applying 4.49 to the ansatz 4.47 we obtain

$$\Phi(x) = \Sigma[\theta]\Phi_0 \tag{4.50}$$

from where we defined, now in a natural way, the Σ-*model field* or *Goldstone matrix*:

$$\Sigma[\theta] := \exp(i\theta_{\hat{a}}\hat{T}_{\hat{a}}) \in G/H \tag{4.51}$$

with $\theta_{\hat{a}} = \theta_{\hat{a}}(x)$. Then each $\theta_{\hat{a}}$, identified as a *Nambu-Goldstone boson*, can be seen as an angular real-valued variable corresponding to an excitation around the reference vacuum Φ_0 and in a direction defined by the corresponding generator $\hat{T}_{\hat{a}}$. Nevertheless, it will be convenient sometimes to work the Goldstone matrix as

$$\Sigma[\phi] := \exp\left(i\frac{\sqrt{2}}{f}\phi_{\hat{a}}\hat{T}_{\hat{a}}\right) \tag{4.52}$$

written in terms of *canonically-normalized NGB fields*

$$\phi_{\hat{a}}(x) := \frac{f}{\sqrt{2}}\theta_{\hat{a}}(x) \tag{4.53}$$

Note that the fields associated with the unbroken generators have been dropped out from the ansatz and hence do not lead to physical degrees of freedom.

Next, we are interested in the action of the group G on the NGBs $\theta_{\hat{a}}$. In order to find this action, we consider the action of an arbitrary element $g \in G$ over the Goldstone matrix 4.51. In view of 4.49 we can decompose instead the product $g\Sigma[\theta] \in G$ in a unique way as

$$g\Sigma[\theta] = \Sigma[\theta']h \tag{4.54}$$

where we have set $\Sigma[\theta'] := \exp(i\theta'_{\hat{a}}\hat{T}_{\hat{a}})$, and clearly $\theta'_{\hat{a}} = \theta'_{\hat{a}}[\theta; g]$ and $h = h[\theta; g] = \exp(i\zeta_a[\theta; g]T_a) \in H$. Hence, from 4.54 we have

$$\Sigma[\theta'] = g\Sigma[\theta]h^\dagger \tag{4.55}$$

which defines a global transformation for every element $\Sigma[\theta] \in G/H$, namely

$$\Sigma[\theta] \overset{g\in G}{\longmapsto} \Sigma[\theta'] = g\Sigma[\theta]h^\dagger \tag{4.56}$$

Without loss of generality, we assume $\theta_{\hat{a}}$'s in the standard form. Then the non-linear realization of G on the NGBs

$$\theta_{\hat{a}} \overset{g\in G}{\longmapsto} \theta'_{\hat{a}} = \theta'_{\hat{a}}[\theta; g] \tag{4.57}$$

is given implicitly by 4.56 which is what we were looking for. From 4.55, and looking up to second order in the fields, we find

$$\theta'_{\hat{a}} = \theta_{\hat{a}} + \xi_{\hat{a}} + \cdots$$

with $g = \exp(i\xi_A T_A)$ and the dots stand for terms containing more than one power of NGBs or transformation parameter. This is precisely the symmetry transformation that forbids the NGB fields to have any potential and consequently allowing for any VEV. In accordance with 4.47, expression 4.56 induces a symmetry transformation on the ansatz $\Phi(x)$

$$\Phi(x) \overset{g\in G}{\longmapsto} \Phi'(x) = g \cdot \Phi(x) \tag{4.58}$$

In view of transformations 4.57 and 4.58, we say that the fields $\theta_{\hat{a}}$ and Φ transform in a *non-linear realization* of the group G. It it now convenient to introduce the algebra of generators of G, which decompose as

$$[T_a, T_b] = if^c_{ab}T_c + if^{\hat{c}}_{ab}\hat{T}_{\hat{c}} = (\mathrm{Ad}^{\mathfrak{h}}_a)^c{}_b T_c \tag{4.59}$$

$$[T_a, \hat{T}_{\hat{b}}] = if^c_{a\hat{b}}T_c + if^{\hat{c}}_{a\hat{b}}\hat{T}_{\hat{c}} = (R_a)^{\hat{c}}{}_{\hat{b}}\hat{T}_{\hat{c}} \tag{4.60}$$

$$[\hat{T}_{\hat{a}}, \hat{T}_{\hat{b}}] = if^c_{\hat{a}\hat{b}}T_c + if^{\hat{c}}_{\hat{a}\hat{b}}\hat{T}_{\hat{c}} \tag{4.61}$$

where the structure constants $f^{\hat{c}}_{ab}$ and $f^c_{a\hat{b}}$ vanish. Note that

$$(\mathrm{Ad}^{\mathfrak{h}}_a)^c{}_b := if^c_{ab} \tag{4.62}$$

define the adjoint representation of the Lie algebra $\mathfrak{h}$ of the subgroup H, while

$$(R_a)^{\hat{c}}_{\ \hat{b}} := i f^{\hat{c}}_{a\hat{b}} \tag{4.63}$$

form a not yet specified H representation, and denoted by R. This representation R is the one in which the NGBs transform under H. It can be identified, for any coset, by looking at the decomposition under H of the adjoint of G, namely

$$\mathrm{Ad}^G = \mathrm{Ad}^H \oplus R \tag{4.64}$$

In order to prove this, note that $\mathfrak{g} = \mathfrak{h} \oplus \mathfrak{g}/\mathfrak{h}$ as vector spaces. On the one hand, there is the adjoint representation of $\mathfrak{h}$ on the whole of $\mathfrak{g}$. On the other hand, the adjoint action of $\mathfrak{h}$ on itself is a subrepresentation, since the algebras of Lie subgroups must be Lie subalgebras. Furthermore, from Eq. 4.60 we have that $\mathfrak{g}/\mathfrak{h}$ is also closed under the action of $\mathfrak{h}$ by the Lie bracket, as it implies $[k, h] \in \mathfrak{g}/\mathfrak{h}$ for every $k \in \mathfrak{g}/\mathfrak{h}$ and every $h \in \mathfrak{h}$. Hence, the map

$$\begin{aligned} R\colon \mathfrak{h} &\to \mathrm{End}(\mathfrak{g}/\mathfrak{h}) \\ h &\mapsto [\cdot, h] \end{aligned} \tag{4.65}$$

is a subrepresentation of the total representation of $\mathfrak{h}$ on $\mathfrak{g}$. Since $\mathfrak{g} = \mathfrak{h} \oplus \mathfrak{g}/\mathfrak{h}$, we have that representation indeed decomposes as 4.64.

Contrary to the general ones, the transformations of the H subgroup act linearly on the NGBs, and hence $\theta^{\hat{a}}$'s transform in R as

$$\theta_{\hat{a}} \xmapsto{g\in H} \theta'_{\hat{a}} = \exp(i\alpha_a R_a)^{\hat{a}}_{\ \hat{b}} \theta^{\hat{b}} \tag{4.66}$$

The situation is different for the transformations along the broken generators; there is no simple way to write them explicitly, not even at the infinitesimal level, aside from particular cases. The theory that we can construct is therefore invariant under the linear realization of H, and besides the NGBs θ it can contain any H-multiplets, which we collectively denote Ψ. The NGB fields θ will play the role of the Higgs field in our description, while the Ψ will describe other fermionic and bosonic composite resonances. For the case SO(5)/SO(4) we will analyse the introduction of some of these composite resonances in Chap. 5.

Now, we would like to use the non-linear realization 4.57 of the group G to construct G-invariant Lagrangians, and derivatives are needed to construct non-trivial invariants. The problem is that, despite the fact that the symmetry is global, the non-linear realization involves the Goldstone fields and therefore is spacetime dependent. Thus, derivatives have to be transform intro covariant derivatives. Furthermore, the non-linearity of the transformation makes the transformation of $\partial_\mu \theta_{\hat{a}}$ complicate. Instead of starting with this object, we will consider the so-called *Maurer-Cartan form*

$$-\Sigma[\theta]^\dagger i\partial_\mu \Sigma[\theta] = d^{\hat{a}}_\mu[\theta]\hat{T}_{\hat{a}} + e^a_\mu[\theta]T_a =: d_\mu[\theta] + e_\mu[\theta] \tag{4.67}$$

which belongs to the Lie algebra $\mathfrak{g}$ of the G group and has simpler transformation properties. Related to the *vierbiens* $d^{\hat{a}}_\mu$ and *spin connections* e^a_μ we have introduced the shorthand notation

$$d_\mu[\theta] := d^{\hat{a}}_\mu[\theta]\hat{T}_{\hat{a}} \tag{4.68}$$

$$e_\mu[\theta] := e^a_\mu[\theta]T_a \tag{4.69}$$

Note that

$$d_\mu = \eta_{\mu\nu} d^\nu, \quad d_{\mu,\hat{a}} = d^{\hat{a}}_\mu \quad \text{and} \quad d^{\mu,\hat{a}} = d^\mu_{\hat{a}}$$

and similarly for e_μ. If the orthogonality relation $\mathrm{Tr}(T_A T_B) = \delta_{AB}$ is imposed, then $d^{\hat{a}}_\mu$ and e^a_μ can be obtain explicitly as follows:

$$d^{\hat{a}}_\mu[\theta] = -\mathrm{Tr}\Big(\Sigma[\theta]^\dagger i\partial_\mu \Sigma[\theta] \hat{T}_{\hat{a}}\Big) \tag{4.70}$$

$$e^a_\mu[\theta] = -\mathrm{Tr}\Big(\Sigma[\theta]^\dagger i\partial_\mu \Sigma[\theta] T_a\Big) \tag{4.71}$$

The Maurer-Cartan form transforms as

$$\begin{aligned} -\Sigma^\dagger i\partial_\mu \Sigma \xmapsto{g\in G} & -(g\Sigma h^\dagger)^\dagger i\partial_\mu (g\Sigma h^\dagger) \\ & = -h(\Sigma^\dagger i\partial_\mu \Sigma)h^\dagger - hi\partial_\mu h^\dagger \\ & = h d_\mu h^\dagger + h\left(e_\mu + \frac{1}{i}\partial_\mu\right) h^\dagger \end{aligned} \tag{4.72}$$

From the above expression one can easily read off the transformations of d_μ and e_μ:

$$d_\mu[\theta] \xmapsto{g\in G} h[\theta; g] d_\mu[\theta] h[\theta; g]^\dagger \tag{4.73}$$

$$e_\mu[\theta] \xmapsto{g\in G} h[\theta; g]\left(e_\mu[\theta] + \frac{1}{i}\partial_\mu\right) h[\theta; g]^\dagger \tag{4.74}$$

In particular, when rewritten in components the d_μ symbol transforms as

$$d^{\hat{a}}_\mu \hat{T}_{\hat{a}} \xmapsto{g\in G} h(d^{\hat{a}}_\mu \hat{T}_{\hat{a}})h^\dagger = d^{\hat{a}}_\mu (h\hat{T}_{\hat{a}} h^\dagger) = d^{\hat{a}}_\mu \exp(i\zeta_a R_a)^{\hat{b}}{}_{\hat{a}} \hat{T}_{\hat{b}}$$

or

$$d^{\hat{a}}_\mu[\theta] \xmapsto{g\in G} \exp(i\zeta_a R_a)^{\hat{a}}{}_{\hat{b}} d^{\hat{b}}_\mu[\theta] \tag{4.75}$$

Equations 4.73 and 4.74 show that $d_\mu[\theta]$ and $e_\mu[\theta]$ transform under a local symmetry H, and that in particular $e_\mu[\theta]$ transforms like a gauge field. It is thus possible to define a *e-covariant derivative*

$$\nabla_\mu := \partial_\mu + i e_\mu \tag{4.76}$$

for the Ψ fields and an *e-field strength tensor*

$$e_{\mu\nu} := \partial_\mu e_\nu - \partial_\nu e_\mu + i[e_\mu, e_\nu] \tag{4.77}$$

which transforms homogeneously with h in the adjoint representation

$$e_{\mu\nu} \mapsto h[\theta; g] e_{\mu\nu} h[\theta; g]^\dagger \tag{4.78}$$

Hence, the connection e_μ allows to write general G-invariant couplings to the matter fields Ψ. The d-symbol can be used to write the G-invariant leading order term

$$\mathcal{L}_{\mathrm{NGBs}} = \frac{f^2}{4} d^{\hat{a}}_\mu[\phi] d^\mu_{\hat{a}}[\phi] = \frac{1}{2}\partial_\mu \phi_{\hat{a}} \partial^\mu \phi_{\hat{a}} + \sum_{n=1}^{\infty} \mathcal{O}\left(\frac{\phi^{2n}}{f^{2n}} (\partial\phi)^2\right) \tag{4.79}$$

This is the *low energy NGB Lagrangian*, and it provides the NGB kinetic terms plus an infinite set of two-derivative interactions. Those higher order operators in 4.79 are completely fixed for a given choice of the G/H coset. Also, note that the parameter f in the above expression acquires a practical meaning: it controls the strength of the NGB interactions. In concordance with the results of section (4.4), we find that NGBs enter only with derivative coupling and no scalar potential appears; these interactions grow with the external momenta and become non-perturbative at energies $\mathcal{O}(4\pi f)$. Also, the derivative couplings of NGBs among themselves and with other composite states do not modify the mass spectrum and do not contribute to the generation of the Higgs mass.

We therefore have basically four ingredients: Σ, d_μ, ∇_μ and $e_{\mu\nu}$ on which a general $g \in G$ transformation acts as a local $h[\theta; g] \in H$ transformation belonging to the unbroken subgroup. Thus, we just have to worry about built out H-invariant operators with these building blocks and the standard group theory tools, and the full G-invariance will follow automatically. This is the *CCWZ prescription*. The reason why this result in a systematic and simple procedure is that the transformation rules are now entirely expressed in terms of the linear action of the matrix $h[\theta; g]$.

4.5.2 Gauge Sources

In order to add the description of the electroweak sector, we must generalize the situation to the case where a subgroup H_0 of the global group G is gauged. To extent the formalism, we introduce the appropriate set of gauge fields through the gauge potential matrix

$$A_\mu := A_\mu^{\tilde{a}} \widetilde{T}_{\tilde{a}} \tag{4.80}$$

where $\widetilde{T}_{\tilde{a}}$ correspond to the generators of the gauge subgroup H_0. The gauge potential matrix 4.80 transforms in the standard way

$$A_\mu \xmapsto{p(x)\in H_0} p(x)\left(A_\mu + \frac{1}{i}\partial_\mu\right)p(x)^\dagger \tag{4.81}$$

under a local transformation $p(x) \in H_0$. It turns out that instead of gauging just $H_0 \subseteq G$, it is often convenient to gauge formally all the fields (i.e. $\widetilde{T}_{\tilde{a}} \equiv T_A$), promote them to a full multiplet in the adjoint representation of G, couple it to the strong sector and eventually decouple the unwant ones by an infinite kinetic term, which correspond to vanishing coupling strength. Therefore, some of them will be made dynamical by the kinetic terms and the others will be regarded as non-dynamical and eventually set to zero at the end of the calculation.

In this *generalized CCWZ prescription*, NGBs still transform implicitly according to 4.56 with $g \in G$ being a local element, and the Maurer-Cartan form is generalized to

$$-\Sigma[\theta]^\dagger i D_\mu \Sigma[\theta] = d_\mu^{\hat{a}}[\theta; A]\hat{T}_{\hat{a}} + e_\mu^a[\theta; A]T_a =: d_\mu[\theta; A] + e_\mu[\theta; A] \tag{4.82}$$

with

$$D_\mu := \partial_\mu + iA_\mu \tag{4.83}$$

The above transforms as

$$\begin{aligned} -\Sigma^\dagger i D_\mu \Sigma \xmapsto{g\in G} & -(g\Sigma h^\dagger) i(\partial_\mu + iA_\mu)(g\Sigma h^\dagger) \\ &= -h\Big(\Sigma^\dagger i D_\mu \Sigma\Big)h^\dagger - hi\partial_\mu h^\dagger \\ &= h d_\mu h^\dagger + h\left(\partial_\mu + \frac{1}{i}e_\mu\right)h^\dagger \end{aligned}$$

and hence the generalized d_μ and e_μ symbols transform as before:

$$d_\mu[\theta;A] \xmapsto{g\in G} h[\theta;g]d_\mu[\theta;A]h[\theta;g]^\dagger \tag{4.84}$$

$$e_\mu[\theta;A] \xmapsto{g\in G} h[\theta;g]\left(e_\mu[\theta;A] + \frac{1}{i}\partial_\mu\right)h[\theta;g]^\dagger \tag{4.85}$$

Analogously, if $\mathrm{Tr}(T_A T_B) = \delta_{AB}$ is imposed then

$$d_\mu^{\hat{a}}[\theta;A] = -\mathrm{Tr}\Big(\Sigma[\theta]^\dagger i D_\mu \Sigma[\theta]\hat{T}_{\hat{a}}\Big) \tag{4.86}$$

$$e_\mu^{a}[\theta;A] = -\mathrm{Tr}\Big(\Sigma[\theta]^\dagger i D_\mu \Sigma[\theta] T_a\Big) \tag{4.87}$$

and Eq. 4.76 is generalized to

$$\nabla_\mu := D_\mu + ie_\mu \tag{4.88}$$

Two new covariant structures can be constructed from the field strength of the external gauge fields as follows

$$\begin{aligned} f_{\mu\nu}[\theta;A] &:= \Sigma^\dagger[\theta]F_{\mu\nu}\Sigma[\theta] \\ &= (f^+_{\mu\nu})^a T_a + (f^-_{\mu\nu})^{\hat{a}}T_{\hat{a}} \\ &= f^+_{\mu\nu} + f^-_{\mu\nu} \end{aligned} \tag{4.89}$$

which transform as

$$f^\pm_{\mu\nu}[\theta;A] \mapsto h[g;\theta]f^\pm_{\mu\nu}[\theta;A]h^\dagger[g;\theta] \tag{4.90}$$

Finally, the 2-derivative non-linear sigma-model 4.79 trivially generalizes to

$$\mathcal{L}_{\mathrm{NGBs}} = \frac{f^2}{4}d_\mu^{\hat{a}}[\phi,A]d^\mu_{\hat{a}}[\phi,A] \tag{4.91}$$

containing now not only NGB kinetic terms and derivative self-coupling, but also interactions involving the gauge fields, which are all dictated by the local G-invariance and predicted in terms of the scale f. Finally, and according to the formalism introduced in Ref. [90,91], the most general Lagrangian invariant under a non-linearly realized group G, spontaneously broken to a linearly realized subgroup H, should be written using the components d_μ and the covariant derivative ∇_μ introduced before, that act on matter fields in representations of H.

4.6 The CCWZ for the Minimal Coset SO(5)/SO(4)

The minimal choice we can think is $H = G_{\rm EW} = \mathrm{SU}(2)_{\rm L} \times \mathrm{U}(1)_{\rm Y}$. Accordingly, it follows from equation 4.4 that the minimal choice of the global symmetry is $G = \mathrm{SU}(3)$; indeed, SU(3) contains an SU(2) and an additional U(1) that we can try to identify with the EW group. However it must be discarded because of the lack of custodial protection that ensures that the corrections to certain electroweak observables are sufficiently suppressed[32]. We will refer to this model as the *non-custodial minimal model*. To have a custodial symmetry, the subgroup H has to be extended to

$$H = \mathrm{SO}(4) \sim \mathrm{SU}(2)_L \times \mathrm{SU}(2)_R \tag{4.92}$$

which contains both the gauge group $\mathrm{SU}(2)_L$, as well as the custodial group $\mathrm{SU}(2)_R$. In this case the minimal choice is

$$G = \mathrm{SO}(5) \tag{4.93}$$

Thus, the SO(5)/SO(4) symmetry breaking pattern constitutes the true minimal implementation of a CH model [92]. We interpret the $\mathrm{SU}(2)_L$ factor as the SM one and we identify the hypercharge with the third $\mathrm{SU}(2)_R$ generator. We refer to this latest model as the *custodial minimal model* or *minimal composite Higgs (MCH) model* in the sense that delivers the minimal number of NGBs fields and relies on the minimal number of symmetry generators but still obey custodial symmetry. Nevertheless, in order to reproduce the correct hypercharge, one must enlarge the global symmetry by including an extra unbroken $\mathrm{U}(1)_X$ factor and define the hypercharge as

$$Y := T_{3R} + X \tag{4.94}$$

where T_{3R} is the third $\mathrm{SU}(2)_R$ generator of SO(5). Therefore the coset is actually

$$\mathrm{SO}(5) \times \mathrm{U}(1)_X / \mathrm{SO}(4) \times \mathrm{U}(1)_X \tag{4.95}$$

The SU(4)/Sp(4) coset is usually considered as the next to minimal MCH model. However this is a minimal choice when considering a description in terms of bound states of fermions [93, 94].

In the MCH model, a number equal to

$$N_{\rm NGB} = \dim \mathrm{SO}(5)/\mathrm{SO}(4) = 4$$

of NGBs arise, while

$$N_e = \dim G_{\rm EW} - \dim H \cap G_{\rm EW} = 4 - 1 = 3$$

of them will be eaten as longitudinal components giving rise to the massive $W_\mu^\pm$ and Z_μ^0 gauge bosons of the EW sector. As result, the composite sector does not contain composite resonances, but only the pNGB Higgs 1.18 as a complex doublet of composite scalars of $\mathrm{SU}(2)_{\rm L} \times \mathrm{U}(1)_{\rm Y}$ and the SM gauge fields. The generators of SO(5) and their convenient split into generators of SO(4) and the broken ones can be found in Appendix (B.5). The manifold of equivalent vacua is $\mathcal{H}_{\rm vacua} = S^4$ and the chosen representative vacuum configuration points along the fifth component

$$\Phi_0 = (0, 0, 0, 0, f)^T$$

[32] This non-custodial minimal model, for example, derives in large corrections to the Peskin-Takeuchi T parameter.

The five real components of Φ are conveniently parametrized with one radial coordinate $\sigma = \sigma(x)$ plus the four angular variables $\phi_{\hat{a}} = \phi_{\hat{a}}(x)$ (the Nambu-Goldstone fields), as

$$\Phi = \Sigma[\phi] \begin{pmatrix} \vec{0} \\ f + \sigma \end{pmatrix} = (f + \sigma) \begin{pmatrix} \frac{\vec{\phi}}{\phi} \sin \frac{\phi}{f} \\ \cos \frac{\phi}{f} \end{pmatrix} \tag{4.96}$$

with the Goldstone matrix given by

$$\Sigma[\phi] = \begin{pmatrix} 1_4 - \frac{\vec{\phi}\,\vec{\phi}^{\,T}}{\phi^2}\left(1 - \cos\frac{\phi}{f}\right) & \frac{\vec{\phi}}{\phi}\sin\frac{\phi}{f} \\ -\frac{\vec{\phi}^{\,T}}{\phi}\sin\frac{\phi}{f} & \cos\frac{\phi}{f} \end{pmatrix} \tag{4.97}$$

and where we have defined the quadruple

$$\vec{\phi} := (\phi_1, \phi_2, \phi_3, \phi_4)^T \tag{4.98}$$

living in the **4** of the unbroken SO(4). In view of the local isomorphism 4.92, the above NGBs transform equivalently as a $(\mathbf{2}, \mathbf{2})$ of $\mathrm{SU}(2)_L \times \mathrm{SU}(2)_R$, and so they can be expressed in terms of the two Higgs doublet components ϕ^+ and ϕ^0 of 1.18 as

$$\vec{\phi} = \frac{1}{\sqrt{2}} \begin{pmatrix} \phi^+ + \phi^{+*} \\ i(\phi^{+*} - \phi^+) \\ \phi^0 + \phi^{0*} \\ i(\phi^{0*} - \phi^0) \end{pmatrix} \tag{4.99}$$

The symmetry content of the theory consist on the linearly-realized action of the unbroken generators T_a, and the four non-linearly realized transformations associated with the broken generators $\hat{T}_{\hat{a}}$.

Let us now turn to the determination of the d_μ and e_μ symbols. Those are defined in equations 4.86 and 4.87, respectively, one for each of the 10 generators of SO(5). As expected, only a subset of those sources will be eventually made physical setting the unnecessary fields to zero. The physical sources are the ones in the EW group, i.e $H_0 = G_{\mathrm{EW}}$. Thus, we split the A_μ^A's in unbroken and broken components

$$\{A_\mu^A\} = \{\, A_\mu^a = \{\, A_{\mu,L}^\alpha, A_{\mu,R}^\alpha \,\}, A_\mu^{\hat{a}} = 0 \,\} \tag{4.100}$$

and already setting the latter ones to zero. We make the identification:

$$\{A_{\mu,L}^\alpha\} = \{\, gW_\mu^1, gW_\mu^2, gW_\mu^3 \,\} \tag{4.101}$$

$$\{A_{\mu,R}^\alpha\} = \{\, 0, 0, g'B_\mu \,\} \tag{4.102}$$

Therefore, the gauge potential matrix A_μ will be

$$\begin{aligned} A_\mu &= gW_\mu^1 T_1^L + gW_\mu^2 T_2^L + gW_\mu^3 T_3^L + g'B_\mu T_3^R \\ &= \frac{g}{\sqrt{2}} W_\mu^+ (T_1^L + iT_2^L) + \frac{g}{\sqrt{2}} W_\mu^- (T_1^L - iT_2^L) \\ &\quad + g(\cos\theta_W Z_\mu + \sin\theta_W A_\mu) T_3^L + g'(\cos\theta_W A_\mu - \sin\theta_W Z_\mu) T_3^R \end{aligned}$$

where the second equality is written in terms of the mass eigenstates $W^{\pm}_{\mu}, Z^{0}_{\mu}$, and θ_W denote the *Weinberg angle*. The d_μ and e_μ connections are given by

$$d^{\hat{a}}_{\mu} = \sqrt{2}\left(\frac{1}{f} - \frac{1}{\phi}\sin\frac{\phi}{f}\right)\frac{\vec{\phi}^{\ T}\cdot D_\mu\vec{\phi}}{\phi^2}\phi_{\hat{a}} + \frac{\sqrt{2}}{\phi}\sin\frac{\phi}{f}D_\mu\phi_{\hat{a}} \tag{4.103}$$

$$e^{\alpha}_{\mu,L} = -A^{\alpha}_{\mu,L} + \frac{4i}{\phi^2}\sin^2\frac{\phi}{2f}\vec{\phi}^{\ T}t^{\alpha}_{L}D_\mu\vec{\phi} \tag{4.104}$$

$$e^{\alpha}_{\mu,R} = -A^{\alpha}_{\mu,R} + \frac{4i}{\phi^2}\sin^2\frac{\phi}{2f}\vec{\phi}^{\ T}t^{\alpha}_{R}D_\mu\vec{\phi} \tag{4.105}$$

where

$$D_\mu\vec{\phi} = (\partial_\mu + iA^{\alpha}_{\mu,L}t^{\alpha}_{L} + iA_{\mu,R}t^{\alpha}_{R})\vec{\phi} \tag{4.106}$$

Now that the basic objects are known we can straightforwardly apply the general CCWZ machinery. In particular, the non-linear sigma-model Lagrangian 4.91 is given by

$$\begin{aligned}\mathcal{L}_{\text{pNGB}} &= \frac{f^2}{4}\text{Tr}\Big(\Sigma[\theta]^\dagger i D_\mu\Sigma[\theta]\hat{T}_{\hat{a}}\Big)\text{Tr}\Big(\Sigma[\theta]^\dagger i D^\mu\Sigma[\theta]\hat{T}_{\hat{a}}\Big)\\ &= \frac{f^2}{2|H|^2}\sin^2\frac{\sqrt{2}|H|}{f}(D_\mu H)^\dagger(D^\mu H) + \frac{f^2}{8|H|^4}\left(2\frac{|H|^2}{f^2} - \sin^2\frac{\sqrt{2}|H|}{f}\right)(\partial|H|^2)^2\end{aligned} \tag{4.107}$$

By going to the unitary gauge, defined as usual by

$$H = \frac{1}{\sqrt{2}}\begin{pmatrix}0\\ \langle h\rangle + h(x)\end{pmatrix} \tag{4.108}$$

where $\langle h\rangle$ denotes the Higgs VEV and $h(x)$ describes the physical Higgs fluctuations, the above Lagrangian is surprisingly simple

$$\mathcal{L}_{\text{pNGB}} = \frac{1}{2}(\partial_\mu h)^2 + \frac{g^2}{4}f^2\sin^2\frac{\langle h\rangle + h}{f}\left(|W_\mu|^2 + \frac{1}{2\cos^2\theta_W}Z^2_\mu\right) \tag{4.109}$$

from which we immediately read two consequences:

1. In general, to compute the Higgs couplings in models where the Higgs is a pNGB, it is important to note that $\langle h\rangle$ is not the same as the SM Higgs vacuum expectation value of $v \simeq 246\,\text{GeV}$. Instead,

$$\xi := \frac{v^2}{f^2} = \sin^2\frac{\langle h\rangle}{f} \tag{4.110}$$

out of which we can extracted the definition of the physical EWSB scale v and its relation with the Higgs VEV $\langle h\rangle$. The vector boson masses W and Z masses are then given by

$$m_W = \cos\theta_W m_Z = \frac{1}{2}gf\sin\frac{\langle h\rangle}{f} \equiv \frac{1}{2}gv \tag{4.111}$$

and the misalignment angle $\langle\phi\rangle$ can be identify as

$$\langle\phi\rangle = \frac{\langle h\rangle}{f} \tag{4.112}$$

2. The Lagrangian 4.109 also contains an infinite set of local interactions involving two gauge bosons and an arbitrary number of Higgs fields. By Taylor-expanding around $h = 0$ we have

$$\begin{aligned} f^2 \sin^2\left(\frac{\langle h\rangle + h}{f}\right) &= f^2 \sin^2\frac{\langle h\rangle}{f} + fh \sin\frac{2\langle h\rangle}{f} + h^2\cos\frac{2\langle h\rangle}{f} - \frac{2h^3}{3f}\sin\frac{2\langle h\rangle}{f} - \cdots \\ &= v^2 + fh2\sin\frac{\langle h\rangle}{f}\cos\frac{\langle h\rangle}{f} + h^2\left(1 - 2\sin^2\frac{\langle h\rangle}{f}\right) - \frac{2h^3}{3f}2\sin\frac{\langle h\rangle}{f}\cos\frac{\langle h\rangle}{f} - \cdots \\ &= v^2\left(1 + 2\sqrt{1-\xi}\frac{h}{v} + (1-2\xi)\frac{h^2}{v^2} - \frac{4}{3}\xi\sqrt{1-\xi}\frac{h^3}{v^3} - \cdots\right) \end{aligned}$$

and so we can easily compute the first few interaction terms:

$$\frac{g^2}{4}v^2\left(|W_\mu|^2 + \frac{1}{2\cos^2\theta_W}Z_\mu^2\right)\left(2\sqrt{1-\xi}\frac{h}{v} + (1-2\xi)\frac{h^2}{v^2} - \frac{4}{3}\xi\sqrt{1-\xi}\frac{h^3}{v^3} - \cdots\right) \tag{4.113}$$

In particular, this means that the SM couplings to the gauge bosons $V \equiv W_\mu^\pm, Z_\mu^\pm$ are modified as follows

$$g_{VVh} = g_{VVh}^{\text{SM}}\sqrt{1-\xi} \tag{4.114}$$

$$g_{VVhh} = g_{VVhh}^{\text{SM}}(1-2\xi) \tag{4.115}$$

In addition, we see that high-dimensional vertices with more than 2 Higgs arise, which could might trigger new phenomena.

5 The Elementary and Resonance Sectors

5.1 The Elementary Sector

Up to now, we have not introduced the SM fermions in the picture neither their interactions with the Higgs nor their mass generation. Standard Model gauge bosons and fermions constitute what we will call the *elementary sector*, since we assume it to be neutral under the interactions of the strong sector. The Lagrangian of this sector will be

$$\begin{aligned} \mathcal{L}_{\text{elem}}^{r\mathcal{O}} = &-\frac{1}{4}W_{\mu\nu}^I W^{I\mu\nu} - \frac{1}{4}B_{\mu\nu}B^{\mu\nu} \\ &+ \bar{L}_{jL}i\not{D}L_{jL} + \bar{e}_{jR}i\not{D}e_{jR} + \bar{Q}_{jL}i\not{D}Q_{jL} + \bar{u}_{jR}i\not{D}u_{jR} + \bar{d}_{jR}i\not{D}d_{jR} \end{aligned} \tag{5.1}$$

The analysis of the following sections is largely insensitive to the structure of light quarks and lepton couplings because in most CH scenarios these couplings are too weak to contribute to the resonances' collider phenomenology (e.g. top partner's phenomenology); hence we will be mainly interested only in the third generation of quarks. As we will see, by the *partial compositeness hypothesis* the fields of this sector must be though as the real elementary states of the theory; consequently we will refer to them as *elementary fields*. This is in contrast to what we will called *SM fermions*, which correspond to the fermions observed experimentally and constitute linear superpositions of the above elementary fermions and *resonances*. In general, elementary fields will be embedded in representations of G as a consequence of the partial compositeness hypothesis and the embedding of composite operators. Henceforth in the thesis we will focus only in the minimal CH model SO(5)/SO(4).

5.2 The Resonance Sector

5.2.1 Landscape of the Resonance Sector

Depending on the global symmetry of the strongly interacting sector, there may be additional light pNGB scalars (i.e. kaon-like particles) arising from the strong sector, giving rise to an *extended Higgs sector*. On the other hand, at the scale $\Lambda_{\rm UC} = 4\pi f$ the strong sector condenses and it generates, on top of the pNGB Higgs, a set of resonances with typical mass

$$m_* = g_* f \tag{5.2}$$

with $g_* \in [1, 4\pi]$, and usually assumed to be the only ones below the cut-off of the model as shown in Fig. 5.1. We will generically called a *resonances* any (composite) particle arising from the composite sector aside from the Goldstone bosons (see Fig. 4.1). The SM gauge and fermion fields are then considered as *external sources*. The spectrum of resonances is important not only for the study of their on-shell production at the LHC, but also for assessing the compatibility of the theory with EWPT, since loops of the new fermions contribute to the electroweak observables. The upper bound on g_* ensures that the loop expansion parameter $(g_*/4\pi)^2$ is less than unity, while the limit $g_* = 4\pi$ corresponds to a maximally strongly coupled theory in the spirit of naive dimensional analysis. Is in this sense that the coupling g_* measures how strong the coupling of the model can become before it is replaced by a more fundamental description.

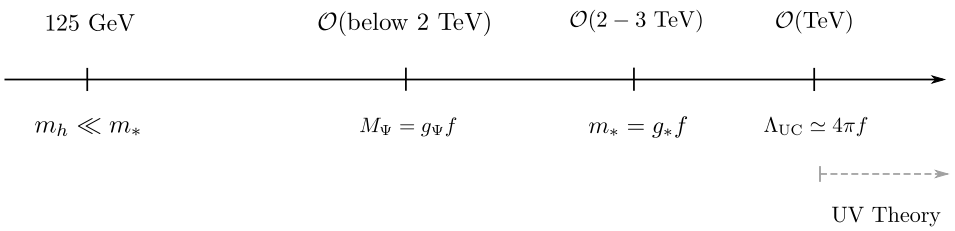

Figure 5.1: Schematic picture of the spectrum in a CH model and a top partners-resonances interplay. Resonance and top partner masses are depicted by $m_* = m_\rho, m_\eta$ and M_Ψ, respectively.

It turns out that any realistic realization of a CH model will assume the existence of a whole spectrum of these kind of hadrons coming from the new strong sector. They will play an important role by means of the partial compositeness hypothesis, through which the generation of fermion masses can be achived. It is due this hypothesis, in conjunction with the measured value of the Higgs mass, that the existence of lighter exotic resonances in the theory is demanded. Concretely, it will be necessary the presence of colored composite spin-1/2 resonances with a mass below 2 TeV [95–99], one for each SM fermion, mixing with the SM fermions.

5.2.2 Partial Fermion Compositeness

Standard Model gauge field are coupled to the composite sector by gauging $G_{\rm SM} \subset G$, but coupling SM fermions to this same strong sector could not be so intuitive, and in fact more than one

possibility can be found in the literature. One way to go would be to write down bilinear couplings to composite operators, of the form

$$\mathcal{L}_{\text{mix}} = y^t \bar{Q}_L \mathcal{O}_S^t t_R + y^b \bar{Q}_L \mathcal{O}_S^b b_R + \text{h.c.} \tag{5.3}$$

where $Q_L = (t_L, b_L)^T$, t_R and d_R are usually taken only as the third generation of quarks in the SM since they play the most prominent role, and the dimensionless parameters $y_i^{t,b}$ defines how strong the external perturbation is. The operator $\mathcal{O}_S$ is a Lorentz scalar composite operator constituted of strong sector fields forming Yukawa-like couplings. This mechanism for fermion mass generation was adopted first in the context of Technicolor theories, and also in the first realizations of a composite Higgs. For example, in minimal technicolor we have

$$(\mathcal{O}_S)^i{}_j = \psi_R^i \psi_{L,j} \tag{5.4}$$

where $\psi_{L,R}$ are the chiral techniquark fields, endowed with flavor indices $i, j = 1, 2$ in $\text{SU}(2)_L \times \text{SU}(2)_R$. This mechanism, however, typically suffers from a severe flavor problem [100].

As a second possibility we introduce the so-called *partial compositeness hypothesis*, originally proposed by D. B. Kaplan [101], and which constitutes nowadays in CH models the most appealing way to break the Goldstone symmetry and generate the Higgs mass and the Yukawa couplings of the elementary sector, through a mixing between these elementary states and operators of the strong sector (i.e. with fermionic resonances), and without introducing too large flavour-violating effects. The mechanism of partial compositeness postulates the existence of new elementary fermions with the same quantum numbers to SM quarks and leptons, and that in the UV Lagrangian (i.e. above the G-symmetry breaking scale) each chirality of these fermion couples linearly to a different *composite fermionic operator* $\mathcal{O}_{L,R}$ made of the composite fermions Ψ and the pNGB's of the strong sector

$$\mathcal{L}_{\text{mix}} = y_L^Q \bar{Q}_L \mathcal{O}_{Q,R} + y_R^t \bar{t}_R \mathcal{O}_{t,L} + y_R^b \bar{b}_R \mathcal{O}_{b,L} + \text{h.c.} \tag{5.5}$$

where we have written the terms that concern just to a third family of elementary fermions, namely $Q_L = (t_L, b_L)$, t_R and b_R. Since the elementary sector does not respect the full global symmetry G, once the composite and elementary sectors are coupled, the 1-loop effective potential generated by the elementary-composite interactions will allow the Higgs to have a mass and fix its vacuum expectation value in a G_{SM}-breaking direction, where the *proto-Yukawa couplings* $y_{L,R}$ can be viewed as spurions parameterizing the effects of the explicit breaking and which constitute matrices in flavour space. This is very interesting as contrary to the SM case, where the Higgs potential is some ad hoc term in the Lagrangian. Thus, in these models we have a dynamical explanation of the electroweak symmetry breaking and the Higgs mass.

5.2.3 (Top) Partners

After the linear mixings in the fermion sector 5.5 are diagonalized, we will find that the resulting physical *SM states* are a linear combination of elementary and composite degrees of freedom [89], namely

$$|\text{Physical}\rangle_i = \cos\theta_i \, |\text{Elemental}\rangle_i + \sin\theta_i \, |\text{Resonance}\rangle_i \tag{5.6}$$

The effects of the strong dynamics are encoded in terms of the form factors of these SM states in momentum space, in analogy with the form factors of the nucleons in low-energy QCD. It is

expected, and for each family, there will be at least one spin-1/2 resonance for each gauge-invariant composite local operator $\mathcal{O}_{L,R}$ presented in 5.5. These kind of resonances are called *partners*. The following are some of their fundamental characteristics:

1. Partners are multiplets of the unbroken symmetry H which in turn, as expected, should contain the custodial symmetry $\mathrm{SU}(2) \times \mathrm{SU}(2)$ extending the electroweak symmetry $\mathrm{SU}(2) \times \mathrm{U}(1)$.

2. Partners must carry QCD color because the composite fermionic operators must come in color triplets in order to be consistently coupled with the quarks. Hence, due their coloured nature, partners can be copiously produced at hadron colliders by QCD interactions.

3. The Partner's mass originates from the strong sector confinement regardless of the breaking of the EW symmetry. If they are charged, then they must thus be endowed with a Dirac mass term, which means that both chiralities must be present with the same quantum numbers. Following Eq. 5.2, the typical mass of the top partners will be represented by M_Ψ and so the corresponding coupling g_Ψ is defined through

$$g_\Psi = \frac{M_\Psi}{f} \tag{5.7}$$

4. The naturalness of electroweak symmetry breaking will depend on the mass of the top-partners. That is in close analogy with the supersymmetric case, where naturalness is largely controlled by the mass of the bosonic top partners, the stops. The common feature of all scenarios is that the top partners need to be light for a reasonably natural theory, but the way the tuning scales with the top-partners' mass is instead different in each case [102].

In general, the Higgs potential is largely determined by the dynamics associated with the top quark and the partners it mixes to, which are specifically called *top partners*. As expected, top partners will play a prominent role.

In the MCH model context, top partner fields Ψ must have well-defined transformation properties under the unbroken SO(4) group. We will consider three cases: Ψ transforming in the

$$r_\Psi = \mathbf{1}, \quad r_\Psi = \mathbf{4}, \quad \text{and} \quad r_\Psi = \mathbf{9} \tag{5.8}$$

of SO(4). Since partners are excited from the vacuum by the operators $\mathcal{O}_{iL,jR}$, it follows for corresponding top partners $\Psi_{\mathbf{4}}$ and $\Psi_{\mathbf{1}}$ that

$$\langle 0|\mathcal{O}_L|\Psi_{\mathbf{4}}\rangle \neq 0 \quad \text{and} \quad \langle 0|\mathcal{O}_R|\Psi_{\mathbf{1}}\rangle \neq 0 \tag{5.9}$$

It is worth mentioning that fourth-generation quarks with SM-like chiral couplings are excluded as they contribute through loops to the couplings of the Higgs boson, altering the Higgs boson production cross-sections to values incompatible with observation [103, 104]. These constraints on chiral quarks can be evaded by heavy *vector-like quarks* (VLQs) [105]: hypothetical spin-1/2 coloured particles that, unlike to fermions in the SM, both of their chiralities share the same electroweak coupling; hence the qualification *vector-like*. Vector-like quarks are materialised in CH

models as resonances discussed just above. Unlike other models[33] predicting VLQs, it is perhaps in CH models where they have their most crucial stand due their role stabilizing the loop-induced Higgs potential and keeping the Higgs mass light [98,106]. Not only of theoretical interest due their roles played in many BSM, VLQs constitute one active area of experimental search, such as the carried out by both the ATLAS [107] and CMS [108] collaborations at the LHC. Since top partners are heavy fermions coupled to top and bottom, the experimental searches for 4th family quarks present a somewhat similar phenomenology, and can be used to derive bounds on particular CH models [102].

5.3 Embeddings

5.3.1 Embedding Composite Operators

We now return to our problem of identifying suitable representations for the fermionic operators. In order to simplify the possible choices, we focus on those that transform linearly under the whole group SO(5). Apart from this, is an operator of the strong sector that transforms in some representation $r_{\mathcal{O}}$ of $\mathrm{SO}(5)\times\mathrm{U}(1)_X$ and whose choice is, to some extent, free. Minimality and the aim of reproducing explicit models considered in the literature, led us to consider two cases[34]

$$r_{\mathcal{O}} = \mathbf{5}_{2/3} \quad \text{and} \quad r_{\mathcal{O}} = \mathbf{14}_{2/3} \tag{5.10}$$

The choice of a specific embedding for the composite operators will have two immediate consequences. On the one hand, the embedding of the elementary sector will be immediately set. On the other hand, the decomposition of these SO(5) embeddings under SO(4) will motivate the corresponding embedding of the (top) partners.

Finally, we analyze the form of the composite operators. Let us suppose the elementary sector is embedded into $r_{\mathcal{O}}$-multipletes. Since the fermion resonances Ψ sit in representations r_Ψ of H only, then this implies that [96]

$$\mathcal{O} \propto \Sigma\Psi \tag{5.11}$$

from where it follows that

$$\mathcal{O} \mapsto (g\Sigma h^\dagger)(h\Psi) = g\mathcal{O} \tag{5.12}$$

By dimensional analysis the proportionality constant is chosen to be f, the decay constant of the strong sector and the characteristic energy scale of it. Hence, the composite operators will have the form

$$\mathcal{O}^{r_{\mathcal{O}},r_\Psi}_{L,R} := f\Sigma\Psi_{L,R} \tag{5.13}$$

Notice that the embedded $Q_{L,R}$ can not be contracted directly with Ψ because they live in different spaces. The former transforms linearly under SO(5) as reported in 5.18 and 5.22, while Ψ transforms under the non-linear representations of SO(4). For this reason one insertion of the Goldstone matrix, transforming according to Eq. 4.56, is needed. Therefore the resonances $\Psi_{L,R}$, besides being embedding in r_Ψ of H, must be "uplifted" to the representation $r_{\mathcal{O}}$ of G in order to be

[33] VLQs also play a useful role in other models, like supersymmetry [109–111], and their phenomenology can be studied in effective models, independently of the theoretical framework they come from (see, for instance, [112–117]).

[34] The phenomenology of the case $r_{\mathcal{O}} = \mathbf{10}$ is, in addition to those presented here, studied in Ref. [118].

correctly coupled to the elemental states through 5.5. On the other hand if, for example, the elementary sector is now embedded into a two-indices symmetric traceless tensor representation, then the composite operators will have the form

$$\mathcal{O}^{r_\mathcal{O},r_\Psi}_{L,R} := f\Sigma\Psi_{L,R}\Sigma^\dagger \tag{5.14}$$

which can be used to construct the following G-invariant quantity:

$$\begin{aligned}\mathrm{Tr}[\mathcal{O}] = \mathrm{Tr}[f\Sigma\Psi\Sigma^\dagger] &\mapsto \mathrm{Tr}[f(g\Sigma h^\dagger)(h\Psi h^\dagger)(g\Sigma h^\dagger)^\dagger] \\ &= \mathrm{Tr}[f\Sigma\Psi\Sigma^\dagger]\end{aligned} \tag{5.15}$$

In this sense, any representation r_Ψ can be "dressed" with the matrices Σ to get representations of G.

5.3.2 The Elementary Embedding $r_\mathcal{O} = \mathbf{5}$

As we have said, the embedding choice of the composite operators sets the embedding of the elementary sector. Our first case is the fundamental **5** representation, where both chiralities Q^5_L and Q^5_R of the elementary states (in this case, just top quark-like states) have representatives couplings y_L and y_R to the strong sector, respectively. We write these interactions

$$\mathcal{L}^{5,r_\Psi}_{\mathrm{mix}} = y^{5,r_\Psi}_L \bar{Q}^5_L \mathcal{O}^{5,r_\Psi}_R + y^{5,r_\Psi}_R \bar{Q}^5_R \mathcal{O}^{5,r_\Psi}_L + \mathrm{h.c.} \tag{5.16}$$

where we have defined the "incomplete" five-plets [118]

$$Q^5_L := \frac{1}{\sqrt{2}}\begin{pmatrix} ib_L \\ b_L \\ it_L \\ -t_L \\ 0 \end{pmatrix}, \quad Q^5_R := \begin{pmatrix} 0 \\ 0 \\ 0 \\ 0 \\ t_R \end{pmatrix} \tag{5.17}$$

with suitable transformation properties

$$Q^5_{L,R} \mapsto g Q^5_{L,R} \quad \text{or} \quad (Q^5_{L,R})^i \mapsto g^i{}_j (Q^5_{L,R})^j \tag{5.18}$$

$$Q^5_{L,R} \mapsto \bar{Q}^5_{L,R} g^{-1} \quad \text{or} \quad (\bar{Q}^5_{L,R})_i \mapsto (\bar{Q}^5_{L,R})_j (g^{-1})^j{}_i \tag{5.19}$$

under $g \in G$. The $\mathrm{U}(1)_X$ charge for each five-plet is equal to $2/3$.

5.3.3 The Elementary Embedding $r_\mathcal{O} = \mathbf{14}$

The second case correspond to a **14** embedding. The partial composite sector reads

$$\mathcal{L}^{14,r_\Psi}_{\mathrm{mix}} = a_\Psi \mathrm{Tr}\left[y^{14,r_\Psi}_L \bar{Q}^{14}_L \mathcal{O}^{14,r_\Psi}_R + y^{14,r_\Psi}_R \bar{Q}^{14}_R \mathcal{O}^{14,r_\Psi}_L \right] + \mathrm{h.c.} \tag{5.20}$$

with $a_\Psi = \sqrt{5}/2, \sqrt{2}, 1$ for $r_\Psi = \mathbf{1}, \mathbf{4}, \mathbf{9}$, respectively, and where we have defined the fourteen-plets [118]

$$Q_L^{14} := \frac{1}{\sqrt{2}} \begin{pmatrix} 0 & 0 & 0 & 0 & ib_L \\ 0 & 0 & 0 & 0 & b_L \\ 0 & 0 & 0 & 0 & it_L \\ 0 & 0 & 0 & 0 & -t_L \\ ib_L & b_L & it_L & -t_L & 0 \end{pmatrix}, \quad Q_R^{14} := \frac{1}{2\sqrt{5}} \begin{pmatrix} -t_R & 0 & 0 & 0 & 0 \\ 0 & -t_R & 0 & 0 & 0 \\ 0 & 0 & -t_R & 0 & 0 \\ 0 & 0 & 0 & -t_R & 0 \\ 0 & 0 & 0 & 0 & 4t_R \end{pmatrix} \tag{5.21}$$

with suitable transformation properties

$$Q_{L,R}^{14} \mapsto g Q_{L,R}^{14} g^{-1} \quad \text{or} \quad (Q_{L,R}^{14})^{ij} \mapsto g^i{}_k g^j{}_l (Q_{L,R}^{14})^{kl} \tag{5.22}$$

$$\bar{Q}_{L,R}^{14} \mapsto g \bar{Q}_{L,R}^{14} g^{-1} \quad \text{or} \quad (\bar{Q}_{L,R}^{14})_{ij} \mapsto (\bar{Q}_{L,R}^{14})_{kl} (g^{-1})^k{}_i (g^{-1})^l{}_j \tag{5.23}$$

under $g \in G$. The $\mathrm{U}(1)_X$ charge is equal to $2/3$.

5.3.4 Decomposing r_Ψ

The decomposition of $r_\mathcal{O}$ of SO(5) under representations of SO(4) will allow us to identify the resonances that can coupled and how they should be embedded. Indeed, note that

$$\mathbf{5}_{2/3} = \mathbf{1}_{2/3} \oplus \mathbf{4}_{2/3} \tag{5.24}$$

$$\mathbf{14}_{2/3} = \mathbf{1}_{2/3} \oplus \mathbf{4}_{2/3} \oplus \mathbf{9}_{2/3} \tag{5.25}$$

Therefore, in both cases we expect to find a $\mathbf{1}_{2/3}$ and/or a $\mathbf{4}_{2/3}$ in the low-energy spectrum. In the last case this implies that, in addition to four-plets and singlets, the elementary states can also mix with fermionic resonances that transform as nine-plets under SO(4). We proceed to analyse the above cases in the next subsections.

5.3.5 The Resonance Embedding $r_\Psi = \mathbf{1}$

The *singlet* representation $r_\Psi = \mathbf{1}$ allows the introduction of a single exotic top-like partner, denoted here through

$$\Psi_1 := \tilde{T} \tag{5.26}$$

and whose Lagrangian is given by

$$\mathcal{L}_{\Psi_1} = \bar{\Psi}_1 i \not{D} \Psi_1 - M_1 \bar{\Psi}_1 \Psi_1 \tag{5.27}$$

Since it is a singlet of $H = \mathrm{SO}(4)$, it does not transform under CCWZ. The corresponding composite operators are given by

$$\mathcal{O}_{L,R}^{5,1} = f \Sigma \Psi_{1L,R}^5 \tag{5.28}$$

$$\mathcal{O}_{L,R}^{14,1} = f \Sigma \Psi_{1L,R}^{14} \Sigma^\dagger \tag{5.29}$$

where we have introduced the following **5** and **14** embeddings of SO(5) for this singlet partner

$$\Psi_1^5 := \begin{pmatrix} 0_{4\times 1} \\ \Psi_1 \end{pmatrix} \tag{5.30}$$

$$\Psi_1^{14} := \mathrm{diag}(0_{1\times 4}, \Psi_1) \tag{5.31}$$

Table 5.1: Charges for the different states found in the models $r_{\mathcal{O}} = \mathbf{5}$ and $\mathbf{14}$. The conventions $Q = I_3 + Y$ and $Y = T_{3R} + X$ are used.

	Q	I_3	Y	T_{3R}	X
$\tilde{T}$	2/3	0	2/3	0	2/3
$X_{5/3}$	5/3	1/2	7/6	1/2	2/3
$X_{2/3}$	2/3	−1/2	7/6	1/2	2/3
T	2/3	1/2	1/6	−1/2	2/3
B	−1/3	−1/2	1/6	−1/2	2/3
$U_{8/3}$	8/3	1	5/3	1	2/3
$U_{5/3}$	5/3	0	5/3	1	2/3
$U_{2/3}$	2/3	−1	5/3	1	2/3
$Y_{5/3}$	5/3	1	2/3	0	2/3
$Y_{2/3}$	2/3	0	2/3	0	2/3
$Y_{-1/3}$	−1/3	−1	2/3	0	2/3
$Z_{2/3}$	2/3	1	−1/3	−1	2/3
$Z_{-1/3}$	−1/3	0	−1/3	−1	2/3
$Z_{-4/3}$	−4/3	−1	−1/3	−1	2/3

5.3.6 The Resonance Embedding $r_\Psi = \mathbf{4}$

The *four-plet* representation $r_\Psi = \mathbf{4}$ allows the introduction of top partners encoded through

$$\Psi_4 := \frac{1}{\sqrt{2}} \begin{pmatrix} iB - iX_{5/3} \\ B + X_{5/3} \\ iT + iX_{2/3} \\ -T + X_{2/3} \end{pmatrix} \tag{5.32}$$

where the subscripts denote the electric charge. It transforms under CCWZ as

$$\Psi_4 \mapsto h\Psi_4 \quad \text{or} \quad (\Psi_4)^i \mapsto h^i{}_j (\Psi_4)^j = \exp\left(i\zeta_a R_a\right)^i{}_j (\Psi_4)^j \tag{5.33}$$

$$\bar{\Psi}_4 \mapsto \bar{\Psi}_4 h^{-1} \quad \text{or} \quad (\bar{\Psi}_4)_i \mapsto (\bar{\Psi}_4)_j (h^{-1})^j{}_i \tag{5.34}$$

for a generic element $h[\phi; g] \in \mathrm{SO}(4)$. This four-plet Ψ_4 is decomposable into two doublets of $\mathrm{SU}(2)_L$, namely

$$\Psi_4 \supset \begin{pmatrix} T \\ B \end{pmatrix}, \begin{pmatrix} X_{5/3} \\ X_{2/3} \end{pmatrix} \tag{5.35}$$

of hypercharge 1/6 and 7/6, respectively. The former has the same quantum numbers as the doublet (t_L, b_L), whilst the latter contains a state of exotic charge 5/3 plus another top-like quark $X_{2/3}$. The Lagrangian of this four-plet Ψ_4 of top partners is given by

$$\mathcal{L}_{\Psi_4} = \bar{\Psi}_4 i \not{\nabla} \Psi_4 - M_4 \bar{\Psi}_4 \Psi_4 \tag{5.36}$$

with $\not{\nabla} = \gamma^\mu \nabla_\mu$ given by

$$\nabla_\mu \Psi_4 = \left(\partial_\mu + \frac{2}{3} i g' B_\mu + i e_\mu\right) \Psi_4 \tag{5.37}$$

The corresponding composite operators are given by

$$\mathcal{O}^{5,4}_{L,R} = f \Sigma \Psi^5_{4L,R} \tag{5.38}$$

$$\mathcal{O}^{14,4}_{L,R} = f \Sigma \Psi^{14}_{4L,R} \Sigma^\dagger \tag{5.39}$$

where we have introduced the following **5** and **14** embeddings of SO(5) for this four-plet of partners

$$\Psi^5_4 := \begin{pmatrix} \Psi_4 \\ 0 \end{pmatrix} \tag{5.40}$$

$$\Psi^{14}_4 := \mathrm{diag}(\Psi_4, 0) \tag{5.41}$$

5.3.7 The Resonance Embedding $r_\Psi = \mathbf{9}$

The *nine-plet* representation $r_\Psi = \mathbf{9}$ allows the introduction of top partners encoded through symmetric, traceless 2-contravariant tensor field [119] (elements in the upper diagonal have been omitted for clarity)

$$\Psi_9 := \tag{5.42}$$

$$\frac{1}{2}\begin{pmatrix} -U_{8/3} + Y_{2/3} - Z_{\text{-}4/3} & & & \\ i Z_{\text{-}4/3} - i U_{8/3} & U_{8/3} + Y_{2/3} + Z_{\text{-}4/3} & & \\ \frac{U_{5/3}}{\sqrt{2}} - \frac{Y_{\text{-}1/3}}{\sqrt{2}} + \frac{Y_{5/3}}{\sqrt{2}} - \frac{Z_{\text{-}1/3}}{\sqrt{2}} & \frac{iU_{5/3}}{\sqrt{2}} + \frac{iY_{\text{-}1/3}}{\sqrt{2}} + \frac{iY_{5/3}}{\sqrt{2}} + \frac{iZ_{\text{-}1/3}}{\sqrt{2}} & -U_{2/3} - Y_{2/3} - Z_{2/3} & \\ -\frac{iY_{5/3}}{\sqrt{2}} + \frac{iY_{\text{-}1/3}}{\sqrt{2}} + \frac{iY_{5/3}}{\sqrt{2}} - \frac{iZ_{\text{-}1/3}}{\sqrt{2}} & \frac{U_{5/3}}{\sqrt{2}} + \frac{Y_{\text{-}1/3}}{\sqrt{2}} - \frac{Y_{5/3}}{\sqrt{2}} - \frac{Z_{\text{-}1/3}}{\sqrt{2}} & i U_{2/3} - i Z_{2/3} & U_{2/3} - Y_{2/3} + Z_{2/3} \end{pmatrix}$$

and transforming under CCWZ as

$$\Psi_9 \mapsto h \Psi_9 h^{-1} \quad \text{or} \quad (\Psi_9)^{ij} \mapsto h^i{}_k h^j{}_l (\Psi_9)^{kl} \tag{5.43}$$

$$\bar{\Psi}_9 \mapsto h \bar{\Psi}_9 h^{-1} \quad \text{or} \quad (\bar{\Psi}_9)_{ij} \mapsto (\bar{\Psi}_9)_{kl} (h^{-1})^k{}_i (h^{-1})^l{}_j \tag{5.44}$$

This nine-plet Ψ_9 is decomposable into three triplets of the SM gauge group $\mathrm{SU}(2)_L$, namely

$$\Psi_9 \supset \begin{pmatrix} U_{8/3} \\ U_{5/3} \\ U_{2/3} \end{pmatrix}, \begin{pmatrix} Y_{5/3} \\ Y_{2/3} \\ Y_{\text{-}1/3} \end{pmatrix}, \begin{pmatrix} Z_{2/3} \\ Z_{\text{-}1/3} \\ Z_{\text{-}4/3} \end{pmatrix} \tag{5.45}$$

separated according to their $T^3_R = 1, 0, -1$ for U's, Y's, and Z's, respectively. The subscripts denote the electric charge, and their hypercharge correspond to $5/3$, $2/3$ and $-1/3$ for each family. The Lagrangian of this four-plet Ψ_9 is given by

$$\mathcal{L}_{\Psi_9} = \mathrm{Tr}\left[\bar{\Psi}_9 i \not{\triangle} \Psi_9\right] - \mathrm{Tr}\left[M_9 \bar{\Psi}_9 \Psi_9\right] \tag{5.46}$$

with $\not{\triangle} = \gamma^\mu \triangle_\mu$ given by

$$\triangle_\mu \Psi_9 := \nabla_\mu \Psi_9 + i \Psi_9 e_\mu = \left(\partial_\mu + \frac{2}{3} i g' B_\mu + i e_\mu\right) \Psi_9 + i \Psi_9 e_\mu \tag{5.47}$$

The corresponding composite operator is given by

$$\mathcal{O}^{14,9}_{L,R} = f\Sigma\Psi^{14}_{9L,R}\Sigma^\dagger \tag{5.48}$$

where we have introduced the following **14** embedding of SO(5) for this nine-plet of partners

$$\Psi^{14}_9 := \mathrm{diag}(\Psi_9, 0) \tag{5.49}$$

5.4 Interaction Between Partners

It is possible to construct interaction terms between the previous partners using SO(4)-invariant objects at our disposal, namely Ψ_1, Ψ_4, Ψ_9 and d^i_μ. The following correspond to the terms of lowest possible order:

1. Between Ψ_1 and Ψ_4 we have

$$\mathcal{L}_{\Psi_{1,4}} = ic_{1,4}(\bar{\Psi}_4)_i\gamma^\mu d^i_\mu\Psi_1 + \text{h.c.} \tag{5.50}$$

   Indeed,

$$\begin{aligned} ic_{1,4}(\bar{\Psi}_4)_i\gamma^\mu d^i_\mu\Psi_1 &\mapsto ic_{1,4}(\bar{\Psi}_4)_k(h^{-1})^k{}_i\gamma^\mu h^i{}_l d^l_\mu\Psi_1 \\ &= ic_{1,4}(\bar{\Psi}_4)_k\delta^k_l\gamma^\mu d^l_\mu\Psi_1 \\ &= ic_{1,4}(\bar{\Psi}_4)_l\gamma^\mu d^l_\mu\Psi_1 \end{aligned}$$

2. Between Ψ_1 and Ψ_9 we have

$$\mathcal{L}_{\Psi_{1,9}} = i\frac{c_{1,9}}{f}(\bar{\Psi}_9)_{ij}d^i_\mu d^{\mu,j}\Psi_1 + \text{h.c.} \tag{5.51}$$

3. Between Ψ_4 and Ψ_9 we have

$$\mathcal{L}_{\Psi_{4,9}} = ic_{4,9}(\bar{\Psi}_9)_{ij}\gamma^\mu d^i_\mu(\Psi_4)^j + \text{h.c.} \tag{5.52}$$

4. Between Ψ_1, Ψ_4 and Ψ_9 we have

$$\mathcal{L}_{\Psi_{1,4,9}} = i\frac{c_{1,4,9}}{f^{3/2}}(\bar{\Psi}_9)_{ij}\gamma^\mu d^i_\mu(\Psi_4)^j\Psi_1 + \text{h.c.} \tag{5.53}$$

The dimensionless coefficients $c_{i,j}$ and $c_{1,4,9}$ are expected of order unity from power counting arguments [120].

5.5 The Models $\mathrm{M}_{\mathcal{O}}$

5.5.1 Identifying the Models

Finally, depending on whether the composite operators are embedded in $\mathbf{5}_{2/3}$ or the $\mathbf{14}_{2/3}$ of $\mathrm{SO}(5)\times\mathrm{U}(1)_X$, this will give rise to the corresponding models

$$\mathrm{M}_{\mathcal{O}} \in \{\,\mathrm{M}_5, \mathrm{M}_{14}\,\} \tag{5.54}$$

Taking into account all the information of the previous chapters, the Lagrangian $\mathcal{L}_{\mathrm{M}_{\mathcal{O}}}$ of each one of the two previous models will be written as

$$\mathcal{L}_{\mathrm{M}_{\mathcal{O}}} := \mathcal{L}^{r_{\mathcal{O}}}_{\mathrm{elem}} + \mathcal{L}^{r_{\mathcal{O}}}_{\Psi} + \mathcal{L}^{r_{\mathcal{O}}}_{\mathrm{mix}} \tag{5.55}$$

We proceed to detail each one of the previous Lagrangians:

1. $\mathcal{L}^{r_{\mathcal{O}}}_{\mathrm{elem}}$ correspond to the elementary sector Lagrangian 5.1 with $Q_{L,R}$ embedded into the representation $r_{\mathcal{O}}$ of $\mathrm{SO}(5)$.

2. $\mathcal{L}^{r_{\mathcal{O}}}_{\Psi}$ is the Lagrangian of the partners:

   2.1 For $r_{\mathcal{O}} = \mathbf{5}$ the Lagrangian is given by

$$\begin{aligned}\mathcal{L}^{5}_{\Psi} &:= \mathcal{L}_{\Psi_1} + \mathcal{L}_{\Psi_4} + \mathcal{L}_{\Psi_{1,4}} \\ &= \bar{\Psi}_1 i\not{D}\Psi_1 - M_1\bar{\Psi}_1\Psi_1 + \bar{\Psi}_4 i\not{\nabla}\Psi_4 - M_4\bar{\Psi}_4\Psi_4 + \left(ic_{1,4}(\bar{\Psi}_4)_i\gamma^\mu d^i_\mu\Psi_1 + \mathrm{h.c.}\right)\end{aligned} \tag{5.56}$$

   2.2 For $r_{\mathcal{O}} = \mathbf{14}$ the Lagrangian is given by

$$\begin{aligned}\mathcal{L}^{14}_{\Psi} &:= \mathcal{L}_{\Psi_1} + \mathcal{L}_{\Psi_4} + \mathcal{L}_{\Psi_9} + \mathcal{L}_{\Psi_{1,4}} + \mathcal{L}_{\Psi_{1,9}} + \mathcal{L}_{\Psi_{4,9}} + \mathcal{L}_{\Psi_{1,4,9}} \\ &= \bar{\Psi}_1 i\not{D}\Psi_1 - M_1\bar{\Psi}_1\Psi_1 + \bar{\Psi}_4 i\not{\nabla}\Psi_4 - M_4\bar{\Psi}_4\Psi_4 + \mathrm{Tr}\left[\bar{\Psi}_9 i\not{\Delta}\Psi_9\right] - \mathrm{Tr}\left[M_9\bar{\Psi}_9\Psi_9\right] \\ &\quad + \Bigg(ic_{1,4}(\bar{\Psi}_4)_i\gamma^\mu d^i_\mu\Psi_1 + i\frac{c_{1,9}}{f}(\bar{\Psi}_9)_{ij}d^i_\mu d^{\mu,j}\Psi_1 + ic_{4,9}(\bar{\Psi}_9)_{ij}\gamma^\mu d^i_\mu(\Psi_4)^j \\ &\quad + i\frac{c_{1,4,9}}{f^{3/2}}(\bar{\Psi}_9)_{ij}\gamma^\mu d^i_\mu(\Psi_4)^j\Psi_1 + \mathrm{h.c.}\Bigg)\end{aligned} \tag{5.57}$$

3. $\mathcal{L}^{r_{\mathcal{O}}}_{\mathrm{mix}}$ is the corresponding compositness Lagrangian:

   3.1 For $r_{\mathcal{O}} = \mathbf{5}$ the Lagrangian is given by

$$\mathcal{L}^{5}_{\mathrm{mix}} := \mathcal{L}^{5,1}_{\mathrm{mix}} + \mathcal{L}^{5,4}_{\mathrm{mix}} \tag{5.58}$$

   where

$$\begin{aligned}\mathcal{L}^{5,1}_{\mathrm{mix}} &= y^{5,1}_L\bar{Q}^5_L f\Sigma\Psi^5_{1R} + y^{5,1}_R\bar{Q}^5_R f\Sigma\Psi^5_{1L} + \mathrm{h.c.} \\ &= y^{5,1}_L f(\bar{Q}^5_L)_I\Sigma^I{}_5\Psi_{1R} + y^{5,1}_R f\bar{t}_R\Sigma^5{}_5\Psi_{1L} + \mathrm{h.c.}\end{aligned} \tag{5.59}$$

   and

$$\begin{aligned}\mathcal{L}^{5,4}_{\mathrm{mix}} &= y^{5,4}_L\bar{Q}^5_L f\Sigma\Psi^5_{4R} + y^{5,4}_R\bar{Q}^5_R f\Sigma\Psi^5_{4L} + \mathrm{h.c.} \\ &= y^{5,4}_L f(\bar{Q}^5_L)_I\Sigma^I{}_i(\Psi_{4R})^i + y^{5,4}_R f\bar{t}_R\Sigma^5{}_i(\Psi_{4L})^i + \mathrm{h.c.}\end{aligned} \tag{5.60}$$

3.2 For $r_{\mathcal{O}} = \mathbf{14}$ the Lagrangian reads

$$\mathcal{L}^{14}_{\text{mix}} := \mathcal{L}^{14,1}_{\text{mix}} + \mathcal{L}^{14,4}_{\text{mix}} + \mathcal{L}^{14,9}_{\text{mix}} \tag{5.61}$$

where

$$\begin{aligned}\mathcal{L}^{14,1}_{\text{mix}} &= \frac{\sqrt{5}}{2}\text{Tr}\left[y^{14,1}_L \bar{Q}^{14}_L f\Sigma\Psi^{14}_{1R}\Sigma^\dagger + y^{14,1}_R \bar{Q}^{14}_R f\Sigma\Psi^{14}_{1L}\Sigma^\dagger\right] + \text{h.c.} \\ &= \frac{\sqrt{5}}{2}\left(y^{14,1}_L f(\bar{Q}^{14}_L)_{IJ}\Sigma^I{}_5\Sigma^J{}_5\Psi_{1R} + y^{14,1}_R f(\bar{Q}^{14}_R)_{IJ}\Sigma^I{}_5\Sigma^J{}_5\Psi_{1L} + \text{h.c.}\right)\end{aligned} \tag{5.62}$$

and

$$\begin{aligned}\mathcal{L}^{14,4}_{\text{mix}} &= \sqrt{2}\text{Tr}\left[y^{14,4}_L \bar{Q}^{14}_L f\Sigma\Psi^{14}_{4R}\Sigma^\dagger + y^{14,4}_R \bar{Q}^{14}_R f\Sigma\Psi^{14}_{4L}\Sigma^\dagger\right] + \text{h.c.} \\ &= \sqrt{2}\left(y^{14,4}_L f(\bar{Q}^{14}_L)_{IJ}\Sigma^I{}_i\Sigma^J{}_5(\Psi_{4R})^i + y^{14,4}_R f(\bar{Q}^{14}_R)_{IJ}\Sigma^I{}_i\Sigma^J{}_5(\Psi_{4L})^i + \text{h.c.}\right)\end{aligned} \tag{5.63}$$

and

$$\begin{aligned}\mathcal{L}^{14,9}_{\text{mix}} &= \text{Tr}\left[y^{14,9}_L \bar{Q}^{14}_L f\Sigma\Psi^{14}_{9R}\Sigma^\dagger + y^{14,9}_R \bar{Q}^{14}_R f\Sigma\Psi^{14}_{9L}\Sigma^\dagger\right] + \text{h.c.} \\ &= y^{14,9}_L f(\bar{Q}^{14}_L)_{IJ}\Sigma^I{}_i\Sigma^J{}_j(\Psi_{9R})^{ij} + y^{14,9}_R f(\bar{Q}^{14}_R)_{IJ}\Sigma^I{}_i\Sigma^J{}_i(\Psi_{9L})^{ij} + \text{h.c.}\end{aligned} \tag{5.64}$$

5.5.2 The Models $\mathbf{M_5}$ and $\mathbf{M_{14}}$

Finally, we present the Lagrangians of the two models 5.54. On the one hand, the Lagrangian of the model M_5 including the lowest order interaction between the partners Ψ_1 and Ψ_4 is given by

$$\begin{aligned}\mathcal{L}_{\text{M}_5} &= \mathcal{L}^5_{\text{elem}} + \mathcal{L}^5_\Psi + \mathcal{L}^5_{\text{mix}} \\ &= -\frac{1}{4}W^I_{\mu\nu}W^{I\mu\nu} - \frac{1}{4}B_{\mu\nu}B^{\mu\nu} + \bar{Q}^5_L i\not{D}Q^5_L + \bar{t}_R i\not{D}t_R \\ &\quad + \bar{\Psi}_1 i\not{D}\Psi_1 - M_1\bar{\Psi}_1\Psi_1 + \bar{\Psi}_4 i\not{\nabla}\Psi_4 - M_4\bar{\Psi}_4\Psi_4 + \left(ic_{1,4}(\bar{\Psi}_4)_i\gamma^\mu d^i_\mu\Psi_1 + \text{h.c.}\right) \\ &\quad + \left(y^{5,1}_L f(\bar{Q}^5_L)_I\Sigma^I{}_5\Psi_{1R} + y^{5,1}_R f\bar{t}_R\Sigma^5{}_5\Psi_{1L} + \text{h.c.}\right) \\ &\quad + \left(y^{5,4}_L f(\bar{Q}^5_L)_I\Sigma^I{}_i(\Psi_{4R})^i + y^{5,4}_R f\bar{t}_R\Sigma^5{}_i(\Psi_{4L})^i + \text{h.c.}\right)\end{aligned} \tag{5.65}$$

where $I = 1,\dots,5$ and $i = 1,\dots,4$, and all terms carrying dimension-4 operators. On the other hand, the Lagrangian of the model M_{14} including the lowest order interaction terms between the

partners Ψ_1, Ψ_4 and Ψ_9 is given by

$$\begin{aligned}
\mathcal{L}_{\mathrm{M}_{14}} &= \mathcal{L}^{14}_{\mathrm{elem}} + \mathcal{L}^{14}_{\Psi} + \mathcal{L}^{14}_{\mathrm{mix}} \\
&= -\frac{1}{4}W^I_{\mu\nu}W^{I\mu\nu} - \frac{1}{4}B_{\mu\nu}B^{\mu\nu} + \bar{Q}_L i\not{D} Q_L + \bar{t}_R i\not{D} t_R \\
&\quad + \bar{\Psi}_1 i\not{D}\Psi_1 - M_1\bar{\Psi}_1\Psi_1 + \bar{\Psi}_4 i\not{\nabla}\Psi_4 - M_4\bar{\Psi}_4\Psi_4 + \mathrm{Tr}\left[\bar{\Psi}_9 i\not{\Delta}\Psi_9\right] - \mathrm{Tr}\left[M_9\bar{\Psi}_9\Psi_9\right] \\
&\quad + \Big(ic_{1,4}(\bar{\Psi}_4)_i\gamma^\mu d^i_\mu\Psi_1 + i\frac{c_{1,9}}{f}(\bar{\Psi}_9)_{ij}d^i_\mu d^{\mu,j}\Psi_1 + ic_{4,9}(\bar{\Psi}_9)_{ij}\gamma^\mu d^i_\mu(\Psi_4)^j \\
&\quad + i\frac{c_{1,4,9}}{f^{3/2}}(\bar{\Psi}_9)_{ij}\gamma^\mu d^i_\mu(\Psi_4)^j\Psi_1 + \mathrm{h.c.}\Big) \\
&\quad + \frac{\sqrt{5}}{2}\left(y^{14,1}_L f(\bar{Q}^{14}_L)_{IJ}\Sigma^I{}_5\Sigma^J{}_5\Psi_{1R} + y^{14,1}_R f(\bar{Q}^{14}_R)_{IJ}\Sigma^I{}_5\Sigma^J{}_5\Psi_{1L} + \mathrm{h.c.}\right) \\
&\quad + \sqrt{2}\left(y^{14,4}_L f(\bar{Q}^{14}_L)_{IJ}\Sigma^I{}_i\Sigma^J{}_5(\Psi_{4R})^i + y^{14,4}_R f(\bar{Q}^{14}_R)_{IJ}\Sigma^I{}_i\Sigma^J{}_5(\Psi_{4L})^i + \mathrm{h.c.}\right) \\
&\quad + \left(y^{14,9}_L f(\bar{Q}^{14}_L)_{IJ}\Sigma^I{}_i\Sigma^J{}_j(\Psi_{9R})^{ij} + y^{14,9}_R f(\bar{Q}^{14}_R)_{IJ}\Sigma^I{}_i\Sigma^J{}_j(\Psi_{9L})^{ij} + \mathrm{h.c.}\right)
\end{aligned} \tag{5.66}$$

where $I, J = 1, \ldots, 5$ and $i = 1, \ldots, 4$, and with all terms, except $\mathcal{L}_{\Psi_{1,9}}$ and $\mathcal{L}_{\Psi_{1,4,9}}$, carrying dimension-4 operators.

5.6 The Sub-Models $\mathrm{M}_{\mathcal{O},\Psi}$

It turns out that sometimes it is possible and convenient to develop a simplified description of the previous models in order to study the phenomenology of the production of specific top-partner sectors. Any of these simplified models should capture the robust features of the above complete constructions $\mathrm{M}_{\mathcal{O}}$. In particular, robust and crucial features are the pNGB nature of the Higgs and the selection rules associated with the small breaking of the corresponding global symmetry. Depending on whether the composite operators are embedded into $r_{\mathcal{O}} = \mathbf{5}_{2/3}$ or $\mathbf{14}_{2/3}$, and partners are in $r_\Psi = \mathbf{1}_{2/3}$, $\mathbf{4}_{2/3}$ or $\mathbf{9}_{2/3}$ of the unbroken SO(4), this will give rise to five *sub-models*. We denote them by

$$\mathrm{M}_{\mathcal{O},\Psi} \in \{\, \mathrm{M}_{5,1}, \mathrm{M}_{5,4}, \mathrm{M}_{14,1}, \mathrm{M}_{14,4}, \mathrm{M}_{14,9} \,\} \tag{5.67}$$

and their classification is summarized in Table (5.2). Taking into account the information of the previous sections, the Lagrangian $\mathcal{L}_{\mathrm{M}_{\mathcal{O},\Psi}}$ of each one of the previous sub-models can be divided as

$$\mathcal{L}_{\mathrm{M}_{\mathcal{O},\Psi}} := \mathcal{L}^{r_{\mathcal{O}}}_{\mathrm{elem}} + \mathcal{L}_{\Psi_{r_\Psi}} + \mathcal{L}^{r_{\mathcal{O}},r_\Psi}_{\mathrm{mix}} \tag{5.68}$$

Table 5.2: The five sub-models shaped by the choices of the representations r_Ψ and $r_{\mathcal{O}}$.

	$r_\Psi = \mathbf{1}$	$r_\Psi = \mathbf{4}$	$r_\Psi = \mathbf{9}$
$r_{\mathcal{O}} = \mathbf{5}$	$\mathrm{M}_{5,1}$	$\mathrm{M}_{5,4}$	–
$r_{\mathcal{O}} = \mathbf{14}$	$\mathrm{M}_{14,1}$	$\mathrm{M}_{14,4}$	$\mathrm{M}_{14,9}$

As an example, the Lagrangian of the sub-model $\mathrm{M}_{5,4}$ would be

$$\begin{aligned}\mathcal{L}_{\mathrm{M}_{5,4}} &= \mathcal{L}^5_{\mathrm{elem}} + \mathcal{L}_{\Psi_4} + \mathcal{L}^{5,4}_{\mathrm{mix}} \\ &= -\frac{1}{4}W^I_{\mu\nu}W^{I\mu\nu} - \frac{1}{4}B_{\mu\nu}B^{\mu\nu} + \bar{Q}^5_L i\not{D} Q^5_L + \bar{t}_R i\not{D} t_R \\ &\quad + \bar{\Psi}_4 i\not{\nabla}\Psi_4 - M_4\bar{\Psi}_4\Psi_4 \\ &\quad + \left(y^{5,4}_L f(\bar{Q}^5_L)_I \Sigma^I{}_i(\Psi_{4R})^i + y^{5,4}_R f\bar{t}_R\Sigma^5{}_i(\Psi_{4L})^i + \mathrm{h.c.}\right)\end{aligned} \tag{5.69}$$

A detailed discussion of the sub-model $\mathrm{M}_{5,1}, \mathrm{M}_{5,4}, \mathrm{M}_{14,1}$ and $\mathrm{M}_{14,4}$ can be found in Ref. [102]. Nevertheless, in this Ref. authors consider the right-handed top quark t_R emerging as a chiral bound state of the strong dynamics, and so t_R must belong to a complete multiplet of the unbroken subgroup SO(4); moreover, since they do not want extra massless states, it must be a singlet. In this context, the above Lagrangian will change to

$$\begin{aligned}\mathcal{L}_{\mathrm{M}_{5,4}} &= -\frac{1}{4}W^I_{\mu\nu}W^{I\mu\nu} - \frac{1}{4}B_{\mu\nu}B^{\mu\nu} + \bar{Q}^5_L i\not{D} Q^5_L \\ &\quad + \bar{\Psi}_4 i\not{\nabla}\Psi_4 - M_4\bar{\Psi}_4\Psi_4 + \bar{t}_R i\not{D} t_R + \left(ic_{\mathbf{4},R}(\bar{\Psi}_4)_i\gamma^\mu d^i_\mu t_R + \mathrm{h.c.}\right) \\ &\quad + \left(y^{5,4}_L f(\bar{Q}^5_L)_I \Sigma^I{}_i(\Psi_{4R})^i + y^{5,R}_R f(\bar{Q}^5_L)_I\Sigma^I{}_5 t_R + \mathrm{h.c.}\right)\end{aligned} \tag{5.70}$$

6 Extra Resonances

6.1 Spin-1 and Spin-0 Resonances

Since pNGB transform as a **4** of SO(4), other resonances must fall in one of the following representations

$$\mathbf{4}\otimes\mathbf{4} = \mathbf{1}\oplus\mathbf{6}\oplus\mathbf{9} \tag{6.1}$$

of SO(4). Therefore, the resonances can be equivalently encoded by one of the $\mathrm{SU}(2)_L \times \mathrm{SU}(2)_R$-representations

$$(\mathbf{1},\mathbf{1})\oplus(\mathbf{3},\mathbf{1})\oplus(\mathbf{1},\mathbf{3})\oplus(\mathbf{3},\mathbf{3}) \tag{6.2}$$

and so symmetry implies that the possible spin assignments are

1. A spin-0 state $\eta \equiv (\mathbf{1},\mathbf{1})$
2. Two spin-1 states $\rho_L \equiv (\mathbf{3},\mathbf{1})$ and $\rho_R \equiv (\mathbf{1},\mathbf{3})$
3. A spin-0 state $\Delta \equiv (\mathbf{3},\mathbf{3})$

We will focus our analysis in the first two cases.

6.1.1 Spin-1 Resonances

On the one hand, and in view of Eq. 6.2, the existence of spin-1 resonances $\rho^\mu_L = (\mathbf{3},\mathbf{1})$ and $\rho^\mu_R = (\mathbf{1},\mathbf{3})$, below the cut-off of the theory at $\Lambda_{\mathrm{UC}} = 4\pi f$, can be assume. They are parametrized by a mass $m_{\rho_\chi} = g_{\rho_\chi} f$ and a coupling $1 < g_{\rho_\chi} < 4\pi$, which controls both the interactions among

the resonances and the resonance-pion interactions (here $\chi \in \{L, R\}$). This scenario has been considered in [95]. Their description as triplet representations of $\mathrm{SU}(2)_L \times \mathrm{SU}(2)_R$ follows the vector formalism presented in [121], where the fields transform non-linearly as

$$\rho^\mu_\chi = \rho^\mu_{a\chi} T_{a\chi} \ , \qquad \rho^\mu_\chi \mapsto h \rho^\mu_\chi h^\dagger + \frac{i}{g_{\rho_\chi}} (h \partial^\mu_\chi h^\dagger)_\chi \tag{6.3}$$

under a transformation $g \in \mathrm{SO}(5)$, with $h = h[\phi; g]$ and the unbroken generators $T_{a\chi}$ are defined in Appendix (B.5). At leading order in derivatives, the most general Lagrangian allowed by Eq. 6.3 has the form [122]

$$\begin{aligned} \mathcal{L}_\rho &= \sum_{\chi=L,R} \mathcal{L}^{\mathrm{kin}}_{\rho_\chi} + \mathcal{L}_{\rho_\chi/\mathrm{pNGB}} + \mathcal{L}_{\rho_\chi/\mathrm{M}} \\ &= \sum_{\chi=L,R} -\frac{1}{4 g^2_{\rho_\chi}} \rho^{\mu\nu}_\chi \rho_{\chi\mu\nu} + \frac{m^2_{\rho_\chi}}{2 g_{\rho_\chi}} (\rho^\mu_\chi - e^\mu_\chi)^2 + \mathcal{L}_{\mathrm{M}+\rho_\chi} + \mathcal{L}^{\mathrm{mag}}_{\mathrm{M}+\rho_\chi} \end{aligned} \tag{6.4}$$

where

$$\mathcal{L}_{\mathrm{M}+\rho_\chi} = \frac{1}{\sqrt{2}} \alpha_{\chi i} J^\mu_{i\chi} (\rho_{\mu\chi} - e_{\mu\chi}) + \mathrm{h.c.} \tag{6.5}$$

$$\mathcal{L}^{\mathrm{mag}}_{\mathrm{M}+\rho_\chi} = \frac{1}{f} \beta_{i\chi} J^{\mu\nu}_{i\chi} \rho_{\mu\nu\chi} + \mathrm{h.c.} \tag{6.6}$$

The e_μ symbol is given by Eqs. 4.104 and 4.105, and the field strength is defined as

$$\rho^{\mu\nu}_\chi = \partial^\mu \rho^\nu_\chi - \partial^\nu \rho^\mu_\chi + [\rho^\mu, \rho^\nu] \tag{6.7}$$

Lagrangian 6.5 encodes fermion currents coupled to the spin-1 resonances, whereas Lagrangian 6.6 contains tensors of the 2nd rank made out of fermions and coupled to the resonance strength field. The set of fermion currents and 2nd rank tensors constructable for the four first sub-models in the list 5.67 can be found in Ref. [95].

6.1.2 Spin-0 Resonances

On the other hand, and again in view of Eq. 6.2, the existence of a spin-0 resonance $\eta = (\mathbf{1}, \mathbf{1})$, below the cut-off of the theory at $\Lambda_{\mathrm{UC}} = 4\pi f$, can be assume. It is parametrized by a mass $m_\eta = g_\eta f$ and a coupling $1 < g_\eta < 4\pi$, which controls both the interactions among the resonances and the resonance-pion interactions. As done for the ρ resonances, we write the effective Lagrangian by focussing on the leading operators in a derivative expansion ∂/Λ that are relevant for $\pi\pi$ scattering. The Lagrangian that is found reads [122, 123]

$$\mathcal{L}_\eta := \mathcal{L}^{\mathrm{kin}}_\eta + \mathcal{L}_{\eta/\mathrm{pNGB}} + \mathcal{L}_{\eta/\mathrm{M}} \tag{6.8}$$

where

1. $\mathcal{L}^{\mathrm{kin}}_\eta$ in the kinetic and mass term

$$\mathcal{L}^{\mathrm{kin}}_\eta = \frac{1}{2} (\partial_\mu \eta)^2 - \frac{1}{2} m^2_\eta \eta^2 \tag{6.9}$$

2. $\mathcal{L}_{\eta/\text{pNGB}}$ is the Lagrangian coupling the pNGB sector and the η-sector

$$\mathcal{L}_{\eta/\text{pNGB}} = \frac{f^2}{4}\left(2a_\eta\frac{\eta}{f} + b_\eta\frac{\eta^2}{f^2}\right)\text{Tr}[d_\mu d^\mu] \tag{6.10}$$

where cubic and quartic self-interactions for η have been omitted, and $a_\eta, b_\eta \lesssim \mathcal{O}(1)$.

3. $\mathcal{L}_{\eta/\text{M}}$ is the Lagrangian relating the $\text{M}_\mathcal{O}$ sector and the η-sector

$$\mathcal{L}_{\eta/\text{M}} := \mathcal{L}^{\text{der}}_{\eta/\text{M}} + \mathcal{L}^{\text{tri}}_{\eta/\text{M}} \tag{6.11}$$

where

3.1 $\mathcal{L}^{\text{der}}_{\eta/\text{M}}$ generates the *derivative couplings*

$$\mathcal{L}^{\text{der}}_{\eta/\text{M}} = \frac{\alpha_i}{f\sqrt{2}}J_i^\mu\partial_\mu\eta + \text{h.c.} \tag{6.12}$$

where the fermionic currents J_i^μ with $i \in \{\, Q, \Psi, Q\Psi \,\}$ are summarized in Tables 6.1 and 6.2. We have divided for convenience the currents into the sub-models $\text{M}_{\mathcal{O},\Psi}$, but for every model $\text{M}_\mathcal{O}$ we should sum the currents over the corresponding partners Ψ.

3.2 $\mathcal{L}^{\text{tri}}_{\eta/\text{M}}$ generates the *trilinear fermion-fermion-scalar couplings*

$$\mathcal{L}^{\text{tri}}_{\eta/\text{M}_{5,1}} = \left(y^{5,1}_{L,\eta}(\bar{Q}^5_L)_I\Sigma^I{}_5\Psi_{1R} + y^{5,1}_{R,\eta}\bar{t}_R\Sigma^5{}_5\Psi_{1L} + \text{h.c.}\right)\eta \tag{6.13}$$

$$\mathcal{L}^{\text{tri}}_{\eta/\text{M}_{5,4}} = \left(y^{5,4}_{L,\eta}(\bar{Q}^5_L)_I\Sigma^I{}_i(\Psi_{4R})^i + y^{5,4}_{R,\eta}\bar{t}_R\Sigma^5{}_i(\Psi_{4L})^i + \text{h.c.}\right)\eta \tag{6.14}$$

$$\mathcal{L}^{\text{tri}}_{\eta/\text{M}_{14,1}} = \frac{\sqrt{5}}{2}\left(y^{14,1}_{L,\eta}(\bar{Q}^{14}_L)_{IJ}\Sigma^I{}_5\Sigma^J{}_5\Psi_{1R} + y^{14,1}_{R,\eta}(\bar{Q}^{14}_R)_{IJ}\Sigma^I{}_5\Sigma^J{}_5\Psi_{1L} + \text{h.c.}\right)\eta \tag{6.15}$$

$$\mathcal{L}^{\text{tri}}_{\eta/\text{M}_{14,4}} = \sqrt{2}\left(y^{14,4}_{L,\eta}(\bar{Q}^{14}_L)_{IJ}\Sigma^I{}_i\Sigma^J{}_5(\Psi_{4R})^i + y^{14,4}_{R,\eta}(\bar{Q}^{14}_R)_{IJ}\Sigma^I{}_i\Sigma^J{}_5(\Psi_{4L})^i + \text{h.c.}\right)\eta \tag{6.16}$$

Table 6.1: Fermionic current for the sub-model $\mathrm{M}_{5,1}$ and $\mathrm{M}_{5,4}$.

$\mathrm{M}_{5,1}$	$\mathrm{M}_{5,4}$
$J^\mu_{Q_L} = \bar{Q}^5_L \gamma^\mu Q^5_L$	$J^\mu_{Q_L} = \bar{Q}^5_L \gamma^\mu Q^5_L$
$J^\mu_{Q_R} = \bar{Q}^5_R \gamma^\mu Q^5_R$ $= \bar{t}_R \gamma^\mu t_R$	$J^\mu_{Q_R} = \bar{Q}^5_R \gamma^\mu Q^5_R$ $= \bar{t}_R \gamma^\mu t_R$
$J^\mu_{\Psi_1} = \bar{\Psi}^5_1 \gamma^\mu \Psi^5_1$ $= \bar{\Psi}_1 \gamma^\mu \Psi_1$	$J^\mu_{\Psi_4} = \bar{\Psi}^5_4 \gamma^\mu \Psi^5_4$ $= (\bar{\Psi}_4)_i \gamma^\mu (\Psi_4)^i$
$J^\mu_{Q_L\Psi_1} = \bar{Q}^5_L \Sigma \gamma^\mu \Psi^5_{1L}$ $= (\bar{Q}^5_L \Sigma)_5 \gamma^\mu \Psi_{1L}$	$J^\mu_{Q_L\Psi_4} = \bar{Q}^5_L \Sigma \gamma^\mu \Psi^5_{4L}$ $= (\bar{Q}^5_L \Sigma)_i \gamma^\mu (\Psi_{4L})^i$
$J^\mu_{Q_R\Psi_1} = \bar{Q}^5_R \Sigma \gamma^\mu \Psi^5_{1R}$ $= \bar{t}_R \Sigma^5{}_5 \gamma^\mu \Psi_{1R}$	$J^\mu_{Q_R\Psi_4} = \bar{Q}^5_R \Sigma \gamma^\mu \Psi^5_{4R}$ $= \bar{t}_R \Sigma^5{}_i \gamma^\mu (\Psi_{4R})^i$

Table 6.2: Fermionic current for the sub-model $\mathrm{M}_{14,1}$, $\mathrm{M}_{14,4}$ and $\mathrm{M}_{14,9}$.

$\mathrm{M}_{14,1}$	$\mathrm{M}_{14,4}$	$\mathrm{M}_{14,9}$
$J^\mu_{Q_L} = \mathrm{Tr}\left[\Sigma^T \bar{Q}^{14}_L \Sigma \gamma^\mu \Sigma^T Q^{14}_L \Sigma\right]$	$J^\mu_{Q_L} = \mathrm{Tr}\left[\Sigma^T \bar{Q}^{14}_L \Sigma \gamma^\mu \Sigma^T Q^{14}_L \Sigma\right]$	$J^\mu_{Q_L} = \mathrm{Tr}\left[\Sigma^T \bar{Q}^{14}_L \Sigma \gamma^\mu \Sigma^T Q^{14}_L \Sigma\right]$
$J^\mu_{Q_R} = \mathrm{Tr}\left[\Sigma^T \bar{Q}^{14}_R \Sigma \gamma^\mu \Sigma^T Q^{14}_R \Sigma\right]$	$J^\mu_{Q_R} = \mathrm{Tr}\left[\Sigma^T \bar{Q}^{14}_R \Sigma \gamma^\mu \Sigma^T Q^{14}_R \Sigma\right]$	$J^\mu_{Q_R} = \mathrm{Tr}\left[\Sigma^T \bar{Q}^{14}_R \Sigma \gamma^\mu \Sigma^T Q^{14}_R \Sigma\right]$
$J^\mu_{\Psi_1} = \mathrm{Tr}\left[\bar{\Psi}^{14}_1 \gamma^\mu \Psi^{14}_1\right]$	$J^\mu_{\Psi_4} = \mathrm{Tr}\left[\bar{\Psi}^{14}_4 \gamma^\mu \Psi^{14}_4\right]$	$J^\mu_{\Psi_9} = \mathrm{Tr}\left[\bar{\Psi}^{14}_9 \gamma^\mu \Psi^{14}_9\right]$
$J^\mu_{Q_L\Psi_1} = \mathrm{Tr}\left[\Sigma^T \bar{Q}^{14}_L \Sigma \gamma^\mu \Psi^{14}_{1L}\right]$	$J^\mu_{Q_L\Psi_4} = \mathrm{Tr}\left[\Sigma^T \bar{Q}^{14}_L \Sigma \gamma^\mu \Psi^{14}_{4L}\right]$	$J^\mu_{Q_L\Psi_9} = \mathrm{Tr}\left[\Sigma^T \bar{Q}^{14}_L \Sigma \gamma^\mu \Psi^{14}_{9L}\right]$
$J^\mu_{Q_R\Psi_1} = \mathrm{Tr}\left[\Sigma^T \bar{Q}^{14}_R \Sigma \gamma^\mu \Psi^{14}_{1R}\right]$	$J^\mu_{Q_R\Psi_4} = \mathrm{Tr}\left[\Sigma^T \bar{Q}^{14}_R \Sigma \gamma^\mu \Psi^{14}_{4R}\right]$	$J^\mu_{Q_R\Psi_9} = \mathrm{Tr}\left[\Sigma^T \bar{Q}^{14}_R \Sigma \gamma^\mu \Psi^{14}_{9R}\right]$

6.2 Bringing Together the Sectors

6.2.1 The Models $\mathbf{M}_{r_\mathcal{O}}$ and $\mathbf{M}_{r_\mathcal{O}, r_\Psi}$ Coupled to Spin-1 or Spin-0 Resonances

We can now joint the elementary sector, the resonance sector and the pNGB sector in order to construct a composite Higgs model with all the above characteristics. The Lagrangian of these models read

$$\mathcal{L}^*_\mathcal{O} := \mathcal{L}_{\mathrm{pNGB}} + \mathcal{L}_{\mathrm{M}_\mathcal{O}} + \mathcal{L}_* \tag{6.17}$$

where $\mathcal{L}_{\mathrm{pNGB}}$ is given by 4.107, $\mathcal{L}_{\mathrm{M}_\mathcal{O}}$ correspond either to 5.65 or 5.66, and $\mathcal{L}_*$ is either 6.8 or 6.4. Similarly, we can work with any of the four models 5.67. The Lagrangian of these sub-models then read

$$\mathcal{L}^*_{\mathcal{O},\Psi} := \mathcal{L}_{\mathrm{pNGB}} + \mathcal{L}_{\mathrm{M}_{\mathcal{O},\Psi}} + \mathcal{L}_* \tag{6.18}$$

where $\mathcal{L}_{\mathrm{M}_{\mathcal{O},\Psi}}$ is now given by 5.68. For example, the Lagrangian of the sub-model $\mathrm{M}_{5,4}$ coupled to a spin-0 resonance η reads

$$\begin{aligned}
\mathcal{L}^{\eta}_{5,4} &= \mathcal{L}_{\mathrm{pNGB}} + \mathcal{L}_{\mathrm{M}_{5,4}} + \mathcal{L}_{\eta} \\
&= \frac{f^2}{2|H|^2}\sin^2\frac{\sqrt{2}|H|}{f}(D_\mu H)^\dagger(D^\mu H) + \frac{f^2}{8|H|^4}\left(2\frac{|H|^2}{f^2} - \sin^2\frac{\sqrt{2}|H|}{f}\right)(\partial|H|^2)^2 \\
&\quad - \frac{1}{4}W^I_{\mu\nu}W^{I\mu\nu} - \frac{1}{4}B_{\mu\nu}B^{\mu\nu} + \bar{Q}^5_L i\not{D} Q^5_L + \bar{t}_R i\not{D} t_R \\
&\quad + \bar{\Psi}_4 i\not{\nabla}\Psi_4 - M_4\bar{\Psi}_4\Psi_4 \\
&\quad + \left(y^{5,4}_L f(\bar{Q}^5_L)_I\Sigma^I{}_i(\Psi_{4R})^i + y^{5,4}_R f\bar{t}_R\Sigma^5{}_i(\Psi_{4L})^i + \mathrm{h.c.}\right) \\
&\quad + \frac{1}{2}(\partial_\mu\eta)^2 - \frac{1}{2}m^2_\eta\eta^2 + \frac{f^2}{4}\left(2a_\eta\frac{\eta}{f} + b_\eta\frac{\eta^2}{f^2}\right)\mathrm{Tr}[d_\mu d^\mu] + \left(\frac{\alpha_i}{f\sqrt{2}}J^\mu_i\partial_\mu\eta + \mathrm{h.c.}\right) \\
&\quad + \left(y^{5,4}_{L,\eta}(\bar{Q}^5_L)_I\Sigma^I{}_i(\Psi_{4R})^i + y^{5,4}_{R,\eta}\bar{t}_R\Sigma^5{}_i(\Psi_{4L})^i + \mathrm{h.c.}\right)\eta
\end{aligned} \tag{6.19}$$

7 Phenomenology of a Specific CH Model with a Spin-0 Resonance

7.1 Introduction

Here, we show the basic result presented in Ref. [123] where the author of this thesis participated. The work was realized under slightly different assumptions to the ones presented in the previous sections. It explores the low energy effects from the interplay among an elementary, partner-resonances and spin-0 resonance sectors in a SO(5)/SO(4) CH model framework. Such interactions are encoded via derivative couplings of the scalar resonance η, assumed to be a singlet of SO(4), with a complete set of SO(5)-invariant fermionic current. The elementary sector is embedded into the cases $r_{\mathcal{O}} = \mathbf{5}$ and $\mathbf{14}$. In the former scenario, the embedding 5.17 is used, while in the latter one the right-handed top quark t_R emerges as a chiral bound state of the strong dynamics and must thus belong to a complete multiplet of the unbroken subgroup SO(4), and given we do not want extra massless states, it must be a singlet

$$Q^{14}_L = \frac{1}{\sqrt{2}}\begin{pmatrix} 0 & 0 & 0 & 0 & ib_L \\ 0 & 0 & 0 & 0 & b_L \\ 0 & 0 & 0 & 0 & it_L \\ 0 & 0 & 0 & 0 & -t_L \\ ib_L & b_L & it_L & -t_L & 0 \end{pmatrix}, \quad Q^{14}_R = t_R \tag{7.1}$$

Finally, the decomposition 5.24 and 5.25 are taken into account in order to generate the four model $\mathrm{M}_{5,1}, \mathrm{M}_{5,4}, \mathrm{M}_{14,1}$ and $\mathrm{M}_{14,4}$, where the the case $r_\Psi = \mathbf{9}$ was dropped. The top partners are encoded by 5.26 and 5.32.

7.2 Spin-0 Production and Decay

7.2.1 Spin-0 Branching Ratios

All the quark partners are colored, hence their pair-production at hadron colliders is QCD-driven, being completely model-independent and insensitive to the degrees of compositeness of the associated SM quarks. Qualitatively, the top partner production is independent on whether both or only one multiplet is present in the effective theory.

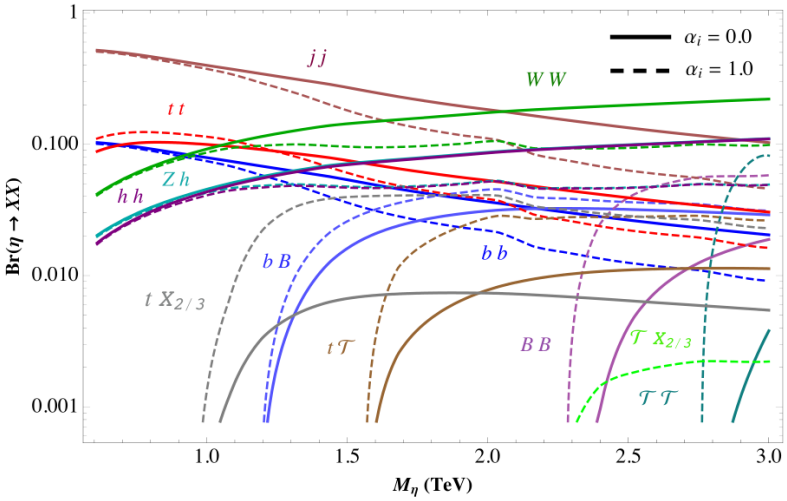

Figure 7.1: All branching ratios for the different η-decay modes at $M_{5,4}$ by setting $\xi = 0.2$ and $a_\eta = 1/2$, and accounting for no currents, i.e $\alpha_i = 0$, as well as their constribution when $\alpha_i = 1$ (thick and dashed curves). Taken from Ref. [95].

Decays of the heavy resonance η may occur into single and double top partner's final states (the former accompanied by an associated SM quark), as well as into gauge and Higgs channels, e.g. $\eta \to \{hh, WW, Zh\}$. Fig. 7.1 gathers the branching ratios for two different cases $\alpha = 0, 1$ (thick-dashed curves) at $M_{5,4}$ with $\xi = 0.2$ and by setting $a_\eta = 1/2$ at 6.10, whose involved effective term is responsible for the gauge and Higgs channels. Generically, these modes will be more relevant rather than the fermionic channels as a consequence of the involve kinematics of both initial and final states. It is worth noting that:

- No fermion-resonance currents ($\alpha_i = 0$) entails dominant dijet, top-pair and gauge, Higgs channels, while sub-dominant single-double partners final states. The dijet channel is the dominant one for $M_\eta \lesssim 2\,\text{TeV}$, becoming sub-dominant with respect the W-pair for a higher mass value.

- The scenario is altered after switching extra fermion-resonance couplings on ($\alpha_i = 01$. Indeed, the dijet, top-pair and gauge, Higgs channels qualitatively diminish, with a notorious enhancement for all the single and double partner final states in contrast. Despite this, the former modes are still relatively the dominant ones.

- The enhancement occurring at the partner final states, may be a slight departure, as in the case of the mode bB, or even an rough increase of one or two orders of magnitude for the $tX_{2/3}$ and TT channels.

Analogous comments apply for the product of the scalar resonance production cross section times the corresponding branching ratio. Once the scalar resonance are produced, their decays can generate, aside from the gauge and Higgs channels, either a single or double quark partner in the final states. A fuller top partner production mechanism is triggered by bringing QCD, EW and Higgs-mediated interactions onto the stage.

7.2.2 Spin-0 Cross Sections

The role of spin-0 and spin-1 resonances on the pNGB scattering has been studied in [122], and their experimental searches were explored for $\xi = 0.1$ in [124, 125]. Associated production cross sections through the process $pp \to \eta$ where computed by using MadGraph 5. Fig. 7.2 displays all the spin-0 production cross sections as a functions of the parameter M_η in the benchmark mass range $M_\eta \in [0.6, 3]$ TeV, for all the models at $\sqrt{s} = 14$ TeV, and setting $\alpha_i = 1$ for $\xi = 0.1, 0.2$. The resonance production is slightly altered when the fermion-resonance current interactions of 6.12 are included, therefore the situation $\alpha_i = 0$ coincides with the one in Fig. 7.2.

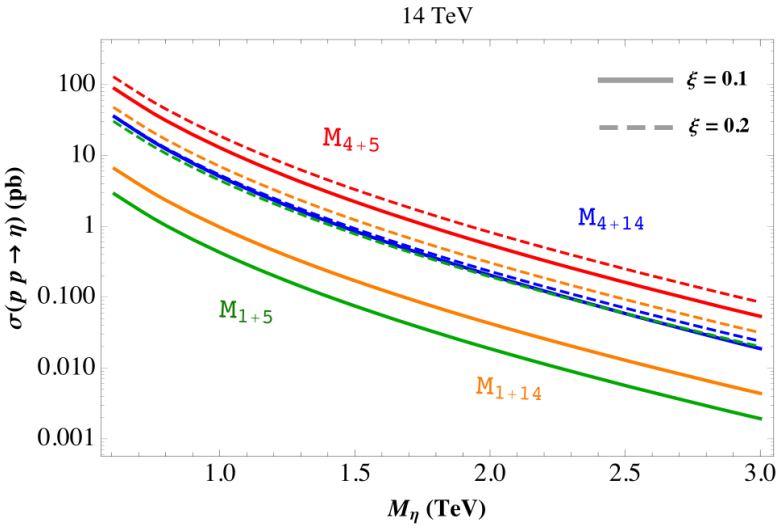

Figure 7.2: Production cross section for η in all four models at 14 TeV, for $\xi = 0.1, 0.2$ (thick and thin curves), and by setting $\alpha_i = 1$. Taken from Ref. [95].

Keeping the SM top quark mass at its experimental observed value requires the proto-Yukawa couplings $y_{L,R}^{5,r_\Psi}$ to be properly set, either through its predicted value and by implementing relations. The scalar heavy resonances is predominantly yielded at the model $M_{5,4}$ as it can be seen from Fig. 7.2. In addition, a higher ξ-value enhances all the productions, although at $M_{14,4}$ the production is slightly increased. Notice that whether the elementary fermions are **5** or **14**-embeddings, the four-plet scenario favours higher production values rather than the singlet one. The scalar resonance is

mainly yielded at $M_{5,4}$, reaching rough cross section values of ~ 150 pb (0.1 pb) at $M_\eta \sim 0.6$ TeV (3 TeV) for $\xi = 0.2$. Posterior decays of the heavy resonance may occur into single and double top partner's final states (the former accompanied by an associated SM quark), as well as into gauge and Higgs channels, e.g. $\eta \to hh, WW, Zh$.

7.3 Partner Production

7.3.1 Double Partner Production

The production of double-partner final states receives contributions from QCD as well as SM gauge, Higgs, and η-mediated processes. Fig. 7.3 collects double-partner production cross sections only for neutral final states, where we have constructed the pair cross sections for each value of the mass parameter $M_4 = M_1 = M_\Psi$ by interpolation using MadGraph 5 simulations, at 14 TeV LHC in all the models for $\xi = 0.2$, and for a fixed scalar mass $M_\eta \sim 1.25$ TeV.

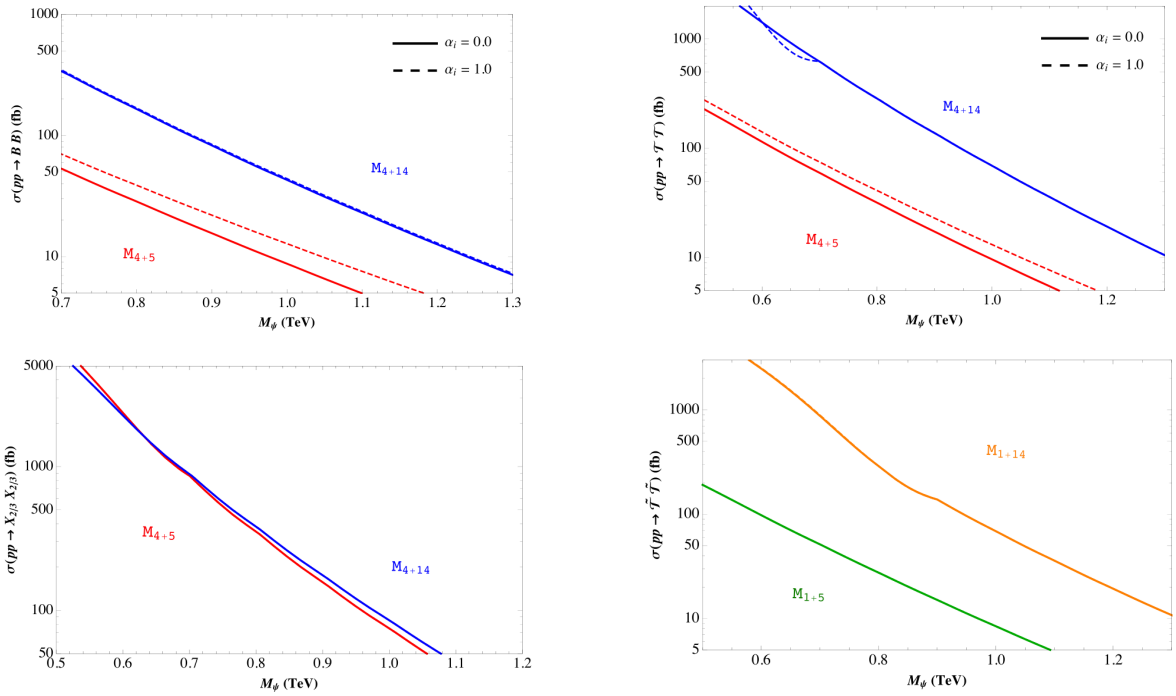

Figure 7.3: Double-partner production cross sections at 14 TeV for $\xi = 0.2$, only for neutral final states. Two different situations $\alpha_i = 0, 1$ (thick-dashed curves) are plotted to compare the impact on the production from the fermion-resonance Lagrangian 6.12. Taken from Ref. [95].

Two different situations $\alpha_i = 0, 1$ (thick-dashed curves) display the impact on the production from the additional fermion-resonance effects regarded here. Slight enhancements occurs at $M_{5,4}$, whereas vanishing-tiny contributions are induced at the rest of the models due to the implied f-suppressed derivative couplings of 6.12. The final states TT and BB are dominantly produced via pp collisions in $M_{14,4}$ as the involved quark partner masses are smaller than the corresponding ones

at $M_{5,4}$. The final state $X_{2/3}X_{2/3}$ does not distinguish the elementary embeddings representation as the involved partner masses are equal at both models. The same comments apply qualitatively and quantitatively for the channel $X_{5/3}X_{5/3}$ as the involved partner masses are degenerate with the corresponding one for $X_{2/3}$. Generically, producing pairs either of $X_{2/3}$ or $X_{5/3}$ will be kinematically favoured with respect to the double production of both T and B, because their relatively higher masses. Likewise, the pair production of the singlet $\tilde{T}$ (Fig. 7.3) is favoured at $M_{14,1}$, as the involved masses result smaller at **14**-elementary embeddings compared with the one at **5**-scenario.

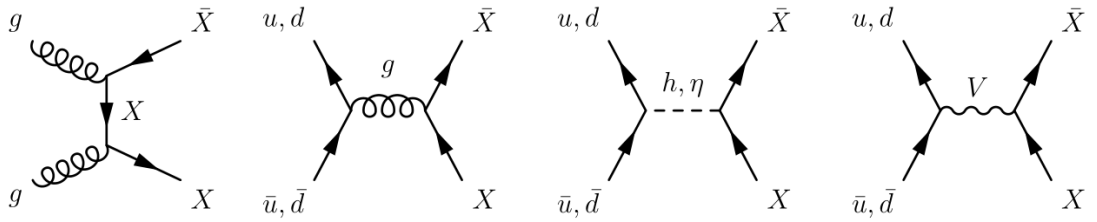

Figure 7.4: Feynman diagram contributing to the double partner production, where $V = Z, \gamma$ and with $X \in \{ T, B, X_{2/3}, X_{5/3}, \tilde{T} \}$. Taken from Ref. [95].

7.3.2 Single Partner Production

QCD induces the production of single-partner final states, together with the SM gauge, Higgs and η-mediated processes for the case of neutral final states respectively, Fig. 7.5. These channels are gathered in Fig. 7.7 and Fig. 7.3.

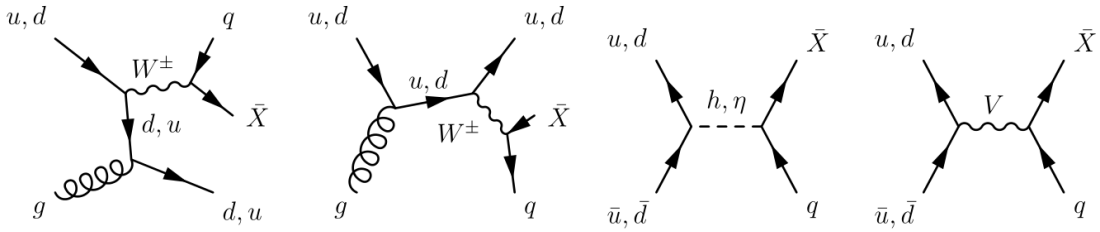

Figure 7.5: Feynman diagram contributing to the single partner production, where $V = Z, \gamma$ and with q standing for any up down-like quark conveniently couple to $X \in \{ T, B, X_{2/3}, X_{5/3}, \tilde{T} \}$. Taken from Ref. [95].

Notice that the departures induced by the extra fermion-scalar couplings in 6.12 are only exhibited at the neutral final states as they are sensitive to the mediation of the scalar resonance η via derivative couplings at 6.12. Cross section values are generically increased by the presence of the latter couplings, becoming notoriously enhanced at the channels $tX_{2/3}$ and $t\tilde{T}$ for the models $M_{5,4}$ and $M_{14,1}$ respectively.

The kinematic of less massive final states at the models $M_{14,4}$ and $M_{14,1}$ is responsible for the relative dominance of the former with respect $M_{5,4}$ and of the latter compared with $M_{5,1}$ at

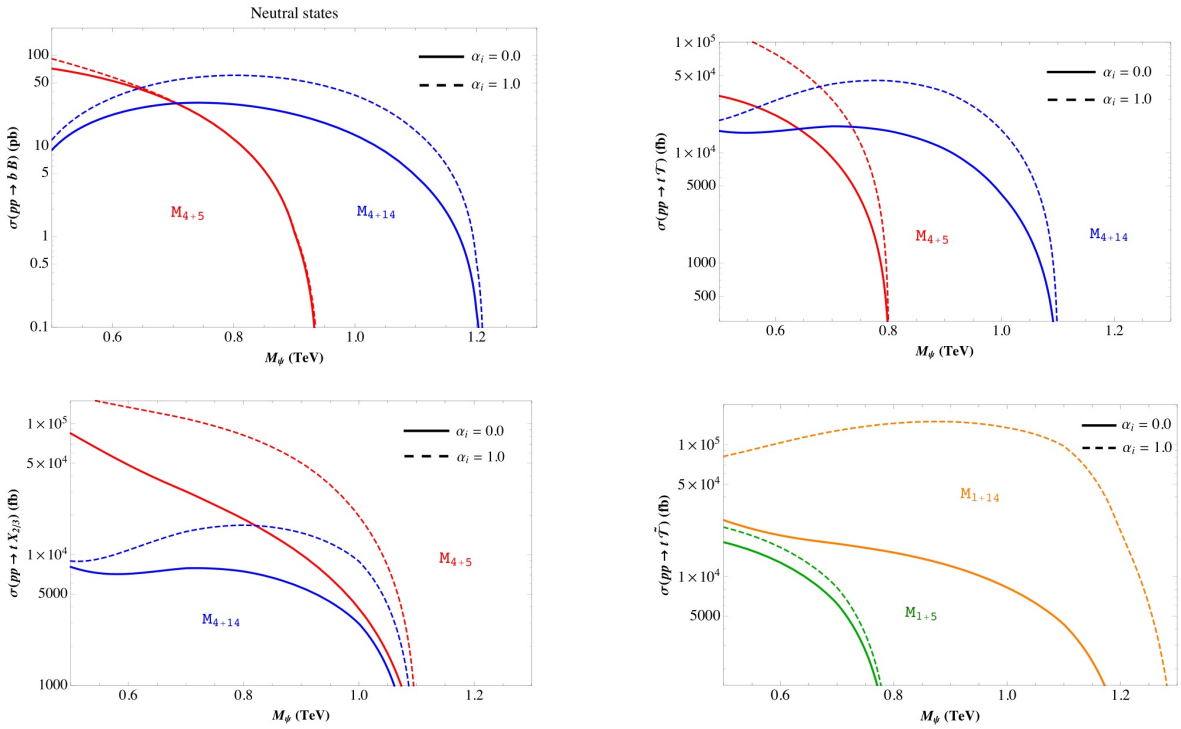

Figure 7.6: Single-partner production cross sections at 14 TeV for $\xi = 0.2$ and for the neutral final states. Two different situations $\alpha_i = 0, 1$ (thick-dashed curves) are plotted to compare the impact on the production from the fermion-resonance Lagrangian 6.12. Taken from Ref. [95].

the neutral channels $bB, tT, t\tilde{T}$, and at the charged final states $bX_{2/3}, b\tilde{T}$ as well. Although some cases do not obey this, like the mode $tX_{2/3}$ and $tX_{5/3}$, where the combined effect of fermion diagonalization effects roughly suppress the induced contributions from the additional interactions of 6.12. Despite the absence of the flavour-changing neutral couplings in the charge 1/3 sector [102], and of the $B \to hb$ channel at $M_{5,4}$, the final state bB is still possible at the four-plet models via derivative couplings of 6.12 as it can be seen from Fig. 7.7. Yielding the singlet $\tilde{T}$ at the **14**-elementary embeddings results dominantly favoured rather than at the **5**-scenario as the involved masses result smaller at the former model.

7.4 Parameter Spaces

It has been derived here the parameter spaces allowed by the recent available LHC partner searches, in terms of ξ and the mass scales M_η and M_Ψ. CMS has released [108] the results of searches for vector-like quarks, 2/3 and $-4/3$ electrically charged, that are pair produced in pp interactions at $\sqrt{s} = 13\,\text{TeV}$, and decaying exclusively via the Wb channel. Events were selected requiring a lepton and neutrino from one W, and a quark-antiquark pair from the other boson gauge. The selection requires a muon or electron, significant missing transverse momentum, and at least four jets. A kinematic fit assuming a pair production of 2/3 or $-4/3$ electrically charged vector-like quarks was

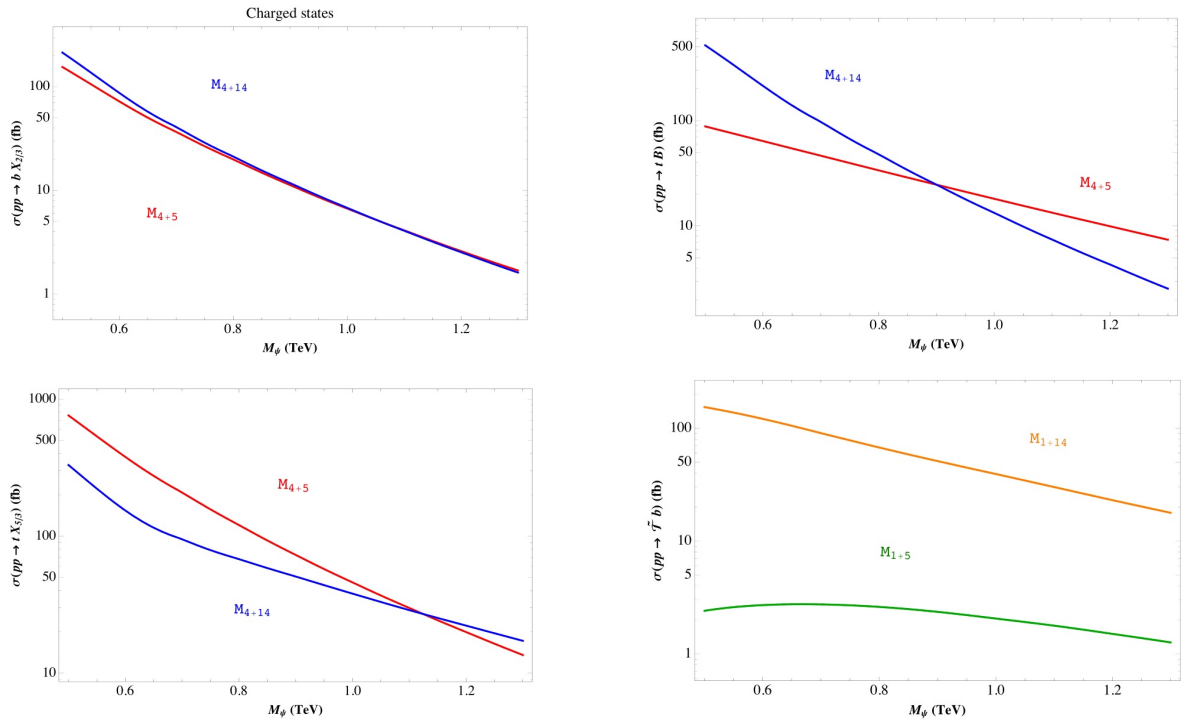

Figure 7.7: Single-partner production cross sections at 14 TeV for $\xi = 0.2$ and for the charged final states. Two different situations $\alpha_i = 0, 1$ (thick-dashed curves) are plotted to compare the impact on the production from the fermion-resonance Lagrangian 6.12. Taken from Ref. [95].

performed and for every event a corresponding candidate quark mass was reconstructed. Upper limits were set in [108] for the pair production cross sections as a function of the implied vector-like quark masses. By comparing these limits with the predicted theoretical cross section of the pair production, the production of 2/3 or $-4/3$ electrically charged vector-like quarks is excluded at 95% confidence level for masses below 1295 GeV (1275 GeV expected). More generally, the results set upper limits on the product of the production cross section and branching fraction to Wb for any new heavy quark decaying to this channel.

Such limits have been imposed in $\sigma \times \mathrm{Br}$ for all of our models and are translated into exclusion regions for the parameter spaces involved by ξ, M_η and M_Ψ. Computation of $\mathrm{Br}(T \to Wb)$ and $\mathrm{Br}(\tilde{T} \to Wb)$ is performed including a scalar resonance in the final states for the total width, with a posterior simulation via MadGraph 5 of the pair production cross section of TT and $\tilde{T}\tilde{T}$ at $\sqrt{s} = 13\,\mathrm{TeV}$ for the four-plet and singlet models respectively. Fig. 7.9 gathers the allowed parameter spaces (M_Ψ, ξ) for all the four-plet and singlet models, with a total decay width summing the standard modes Wb, Zt and ht up (1st-2nd plots), and augmented by ηt (3rd-4th graphs). Consequently, the branching ratio for any channel will be also M_η-dependent and will entail a parametric dependence on the extra fermion-resonance interactions regarded here in 6.12. Their impact is scanned along two different situations: the dashed border regions stand for the allowed parameter spaces assuming extra fermion-resonance couplings weighted by $\alpha_i = 1$, whilst the others

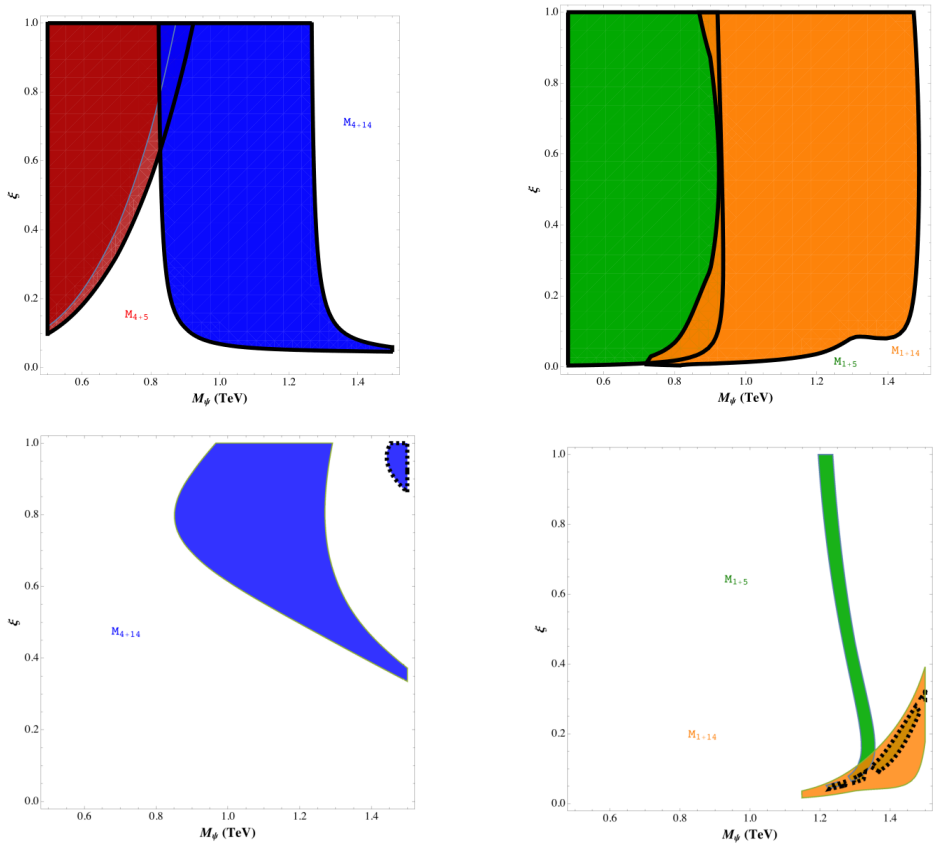

Figure 7.8: Parameter space (M_Ψ, ξ) obtained from recent bounds on top partners searches through top-like decays into Wb final states: prior to the inclusion of the scalar η into the final states (1st-2nd plots) and after its inclusion by setting $M_\eta = 3\,\text{TeV}$ (3rd-4th plots). Bound from [108] on top partner searches through top-like decays into Wb final states have been imposed at all model. Two situations have been explored $\alpha_i = 0, 1$ (thick-dashed border). Taken from Ref. [95].

zones denote no additional interactions, i.e. $\alpha_i = 0$. The scalar resonance mass is fixed at the benchmark value $M_\eta = 3\,\text{TeV}$ at the 3rd-4th graphs. As a conclusion, the recent upper limits on top-like partners production permit part of the parameter spaces from $\text{M}_{14,4}$ and from the singlet models if the scalar resonance η is disregarded, and whether the extra fermion-scalar interactions are considered or not. By including the scalar field into the final states a strongly bounded region, further constrained if the extra interactions in 6.12 are included, remains at $\text{M}_{14,4}$ and $\text{M}_{5,1}$ only. In this sense, those extra couplings are useful in discerning models and refining further their involved parameter space.

An additional insight into the parametric freedom of the assumed scenarios can be explored by fixing the partner mass scale and letting the scalar resonance one to vary. This entails of course the scalar resonance inclusion at the final states. Fig. 7.9 illustrates this by setting $M_\Psi = 1.25\,\text{TeV}$. The parameter spaces are notoriously split into a left and right-handed regions, with the intermediate

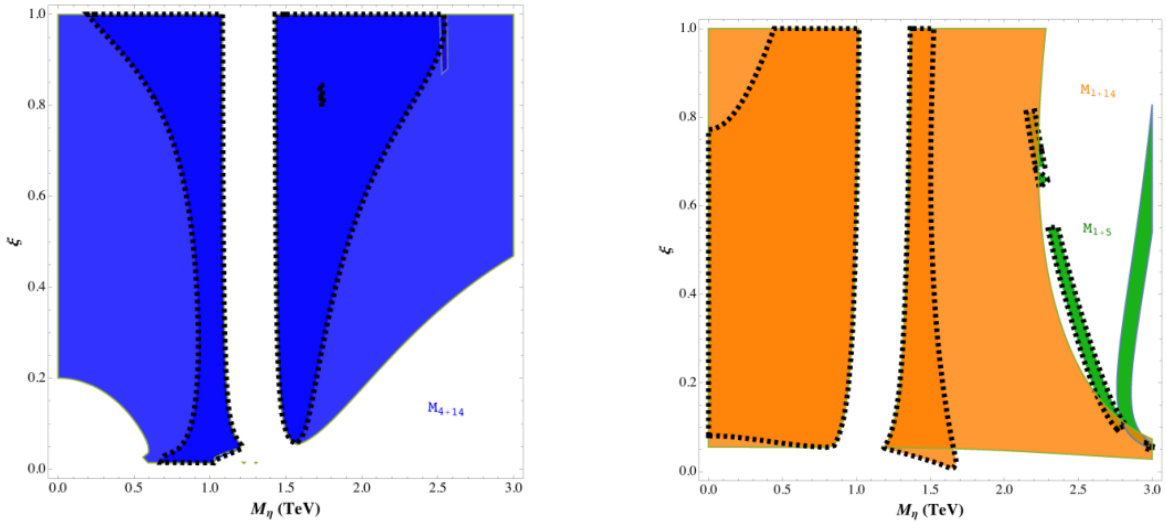

Figure 7.9: Parameter space (M_Ψ, ξ) by fixing $M_\Psi = 1250\,\text{GeV}$. Two situations have been explored, $\alpha_i = 0, 1$ (thick-dashed border). Taken from Ref. [95].

excluded ranges $M_\eta \sim 1.2 - 1.4\,\text{TeV}$ and $M_\eta \sim 0.9 - 1.2\,\text{TeV}$ at the **14**-embedding scenarios, and with $\text{M}_{5,1}$ favouring the higher scalar mass range $\sim 2.8 - 3\,\text{TeV}$. The inclusion of extra derivative couplings reduce a bit the higher and lower range masses at $\text{M}_{14,4}$, shifting the range masses to a lower one at $\text{M}_{5,1}$, while strongly constricting the right handed region to $M_\eta \sim 1.2 - 1.6\,\text{TeV}$ at $\text{M}_{14,1}$. Consistent ξ-values are still feasible.

Appendix A Transition Amplitures for $QQ \to VV \to QQh$

There are six channels of type $QQ \to ZZ \to QQh$, and another six of type $QQ \to WW \to QQh$. We begin with the channels that involve ZZ-fusion, with all the possibilities (at lowest order) depicted in Fig. (A.1). Because the difficulties (due very large terms) at calculating explicit expressions for the cross section for these processes, we will give just the transition amplitude for each case. Let us analyse the first case, depicted in Fig. (A.1a). Feynman rules determine a transition amplitude $\mathcal{M}_a(QQ \to ZZ \to QQh)$ given by

$$\begin{aligned}
-i\mathcal{M}_a(QQ' \to ZZ \to QQ'h)(2\pi)^4\delta^4(p_1+p_2-p_3-p_4-p_5) = \int \frac{d^4q_1}{(2\pi)^4}\frac{d^4q_2}{(2\pi)^4}(2\pi)^4\delta^4(p_1-p_3-q_1) \\
\times (2\pi)^4\delta^4(p_2-p_4-q_2)(2\pi)^4\delta^4(q_1+q_2-p_5)\bar{u}(p_3)\left[\frac{-ig}{2c_\theta}\gamma^\mu\left(v_Q-a_Q\gamma^5\right)\right]u(p_1) \\
\times \bar{u}(p_4)\left[\frac{-ig}{2c_\theta}\gamma^\nu\left(v_{Q'}-a_{Q'}\gamma^5\right)\right]u(p_2)\left[\frac{-i\left(g_{\mu\sigma}-\frac{q_{1\mu}q_{1\sigma}}{m_Z^2}\right)}{q_1^2-m_Z^2}\right] \\
\times \left[\frac{-i\left(g_{\nu\sigma'}-\frac{q_{2\nu}q_{2\sigma'}}{m_Z^2}\right)}{q_2^2-m_Z^2}\right]\left(-i\frac{2m_Z^2}{v}g^{\sigma\sigma'}\right) \qquad \text{(A.1)}
\end{aligned}$$

from where

$$\begin{aligned}
\mathcal{M}_a(QQ' \to ZZ \to QQ'h) = \frac{g^2m_Z^2}{2v\cos^2\theta}g^{\sigma\sigma'}\bar{u}(p_3)\gamma^\mu\left(v_Q-a_Q\gamma^5\right)u(p_1)\bar{u}(p_4)\gamma^\nu\left(v_{Q'}-a_{Q'}\gamma^5\right)u(p_2) \\
\times \frac{(g_{\mu\sigma}-(p_1-p_3)_\mu(p_1-p_3)_\sigma/m_Z^2)(g_{\nu\sigma'}-(p_2-p_4)_\nu(p_2-p_4)_{\sigma'}/m_Z^2)}{[(p_1-p_3)^2-m_Z^2][(p_2-p_4)^2-m_Z^2]} \qquad \text{(A.2)}
\end{aligned}$$

The remain transition amplitudes are

$$\begin{aligned}
\mathcal{M}_b(QQ \to ZZ \to QQh) = \frac{g^2m_Z^2}{2v\cos^2\theta}g^{\sigma\sigma'}\bar{u}(p_3)\gamma^\mu\left(v_Q-a_Q\gamma^5\right)u(p_2)\bar{u}(p_4)\gamma^\nu\left(v_Q-a_Q\gamma^5\right)u(p_1) \\
\times \frac{(g_{\mu\sigma}-(p_2-p_3)_\mu(p_2-p_3)_\sigma/m_Z^2)(g_{\nu\sigma'}-(p_1-p_4)_\nu(p_1-p_4)_{\sigma'}/m_Z^2)}{[(p_2-p_3)^2-m_Z^2][(p_1-p_4)^2-m_Z^2]} \qquad \text{(A.3)}
\end{aligned}$$

$$\begin{aligned}
\mathcal{M}_c(\bar{Q}\bar{Q}' \to ZZ \to \bar{Q}\bar{Q}'h) = \frac{g^2m_Z^2}{2v\cos^2\theta}g^{\sigma\sigma'}\bar{v}(p_1)\gamma^\mu\left(v_Q-a_Q\gamma^5\right)v(p_3)\bar{v}(p_2)\gamma^\nu\left(v_{Q'}-a_{Q'}\gamma^5\right)v(p_4) \\
\times \frac{(g_{\mu\sigma}-(p_1-p_3)_\mu(p_1-p_3)_\sigma/m_Z^2)(g_{\nu\sigma'}-(p_2-p_4)_\nu(p_2-p_4)_{\sigma'}/m_Z^2)}{[(p_1-p_3)^2-m_Z^2][(p_2-p_4)^2-m_Z^2]} \qquad \text{(A.4)}
\end{aligned}$$

$$\begin{aligned}
\mathcal{M}_d(\bar{Q}\bar{Q} \to ZZ \to \bar{Q}\bar{Q}h) = \frac{g^2m_Z^2}{2v\cos^2\theta}g^{\sigma\sigma'}\bar{v}(p_2)\gamma^\mu\left(v_Q-a_Q\gamma^5\right)v(p_3)\bar{v}(p_1)\gamma^\nu\left(v_Q-a_Q\gamma^5\right)v(p_4) \\
\times \frac{(g_{\mu\sigma}-(p_2-p_3)_\mu(p_2-p_3)_\sigma/m_Z^2)(g_{\nu\sigma'}-(p_1-p_4)_\nu(p_1-p_4)_{\sigma'}/m_Z^2)}{[(p_2-p_3)^2-m_Z^2][(p_1-p_4)^2-m_Z^2]} \qquad \text{(A.5)}
\end{aligned}$$

$$\mathcal{M}_e(Q\bar{Q}' \to ZZ \to Q\bar{Q}'h) = \frac{g^2 m_Z^2}{2v\cos^2\theta} g^{\sigma\sigma'} \bar{u}(p_3)\gamma^\mu \left(v_Q - a_Q\gamma^5\right) u(p_1)\bar{v}(p_2)\gamma^\nu \left(v_{Q'} - a_{Q'}\gamma^5\right) v(p_4) \times \frac{(g_{\mu\sigma} - (p_1-p_3)_\mu(p_1-p_3)_\sigma/m_Z^2)(g_{\nu\sigma'} - (p_2-p_4)_\nu(p_2-p_4)_{\sigma'}/m_Z^2)}{[(p_1-p_3)^2 - m_Z^2][(p_2-p_4)^2 - m_Z^2]} \tag{A.6}$$

$$\mathcal{M}_f(Q\bar{Q} \to ZZ \to Q\bar{Q}h) = \frac{g^2 m_Z^2}{2v\cos^2\theta} g^{\sigma\sigma'} \bar{v}(p_2)\gamma^\mu \left(v_Q - a_Q\gamma^5\right) u(p_1)\bar{u}(p_3)\gamma^\nu \left(v_{Q'} - a_{Q'}\gamma^5\right) v(p_4) \times \frac{(g_{\mu\sigma} - (p_1+p_2)_\mu(p_1+p_2)_\sigma/m_Z^2)(g_{\nu\sigma'} - (p_3+p_4)_\nu(p_3+p_4)_{\sigma'}/m_Z^2)}{[(p_1+p_2)^2 - m_Z^2][(p_3+p_4)^2 - m_Z^2]} \tag{A.7}$$

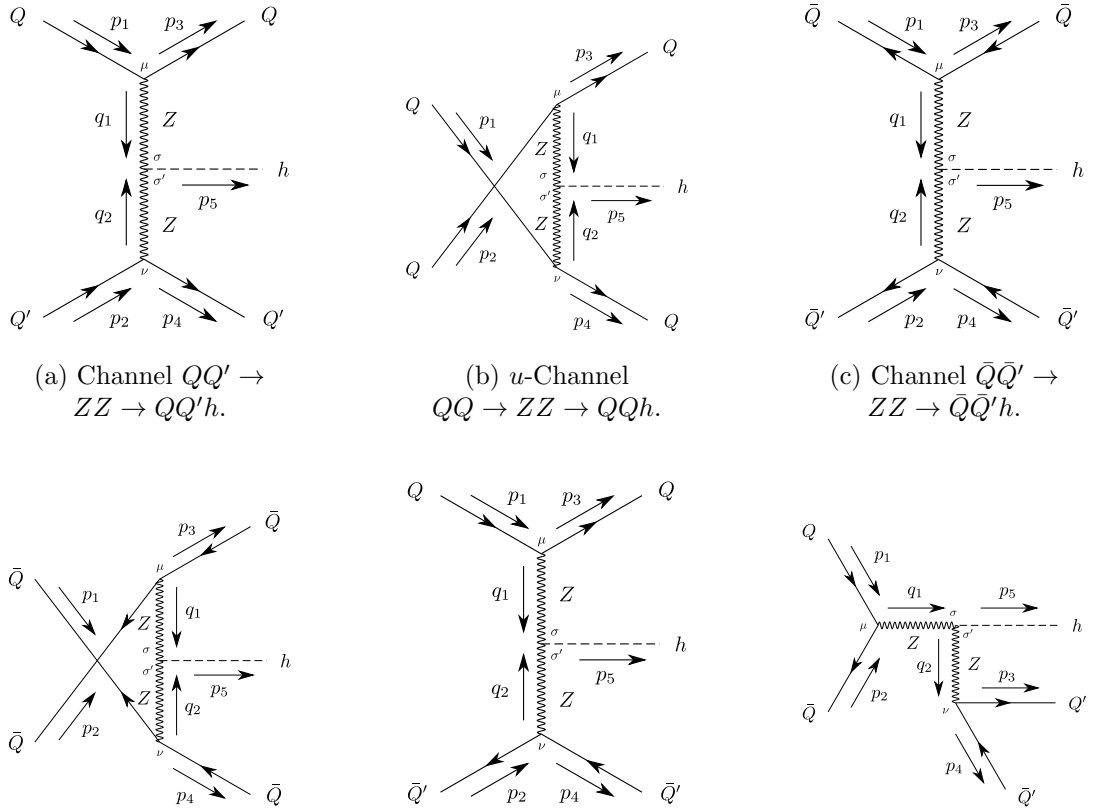

(a) Channel $QQ' \to ZZ \to QQ'h$.

(b) u-Channel $QQ \to ZZ \to QQh$.

(c) Channel $\bar{Q}\bar{Q}' \to ZZ \to \bar{Q}\bar{Q}'h$.

(d) u-Channel $\bar{Q}\bar{Q} \to ZZ \to \bar{Q}\bar{Q}h$.

(e) Channel $Q\bar{Q}' \to ZZ \to Q\bar{Q}'h$.

(f) s-Channel $Q\bar{Q} \to ZZ \to Q\bar{Q}h$.

Figure A.1: Feynman diagrams describing Higgs production process $QQ \to QQh$ of type $QQ \to ZZ \to QQh$ at lowest order.

On the other hand, all the possible channel (at lowest order) involving WW-fusion are depicted in Fig. (A.2). Their transition amplitudes are given by

$$\mathcal{M}_a(Q_u Q''_d \to WW \to Q'_d Q'''_u h) = \frac{g^2 m_W^2}{4v} V^*_{ud'} V_{u''d'''} g^{\sigma\sigma'} \bar{u}(p_3)\gamma^\mu \left(1-\gamma^5\right) u(p_1) \bar{u}(p_4)\gamma^\nu \left(1-\gamma^5\right) u(p_2) \times \frac{(g_{\mu\sigma} - (p_1-p_3)_\mu (p_1-p_3)_\sigma / m_W^2)(g_{\nu\sigma'} - (p_2-p_4)_\nu (p_2-p_4)_{\sigma'}/m_W^2)}{[(p_1-p_3)^2 - m_W^2][(p_2-p_4)^2 - m_W^2]} \quad \text{(A.8)}$$

$$\mathcal{M}_b(\bar{Q}_u \bar{Q}''_d \to WW \to \bar{Q}'_d \bar{Q}'''_u h) = \frac{g^2 m_W^2}{4v} V^*_{u'''d''} V_{ud'} g^{\sigma\sigma'} \bar{v}(p_1)\gamma^\mu \left(1-\gamma^5\right) v(p_3) \bar{v}(p_2)\gamma^\nu \left(1-\gamma^5\right) v(p_4) \times \frac{(g_{\mu\sigma} - (p_1-p_3)_\mu (p_1-p_3)_\sigma / m_W^2)(g_{\nu\sigma'} - (p_2-p_4)_\nu (p_2-p_4)_{\sigma'}/m_W^2)}{[(p_1-p_3)^2 - m_W^2][(p_2-p_4)^2 - m_W^2]} \quad \text{(A.9)}$$

$$\mathcal{M}_c(Q_u \bar{Q}''_u \to WW \to \bar{Q}'_d \bar{Q}'''_d h) = \frac{g^2 m_W^2}{4v} V^*_{ud'} V_{u''d'''} g^{\sigma\sigma'} \bar{u}(p_3)\gamma^\mu \left(1-\gamma^5\right) u(p_1) \bar{v}(p_2)\gamma^\nu \left(1-\gamma^5\right) v(p_4) \times \frac{(g_{\mu\sigma} - (p_1-p_3)_\mu (p_1-p_3)_\sigma / m_W^2)(g_{\nu\sigma'} - (p_2-p_4)_\nu (p_2-p_4)_{\sigma'}/m_W^2)}{[(p_1-p_3)^2 - m_W^2][(p_2-p_4)^2 - m_W^2]} \quad \text{(A.10)}$$

$$\mathcal{M}_d(Q_d \bar{Q}''_d \to WW \to Q'_u \bar{Q}'''_u h) = \frac{g^2 m_W^2}{4v} V^*_{d''u'''} V_{du'} g^{\sigma\sigma'} \bar{u}(p_3)\gamma^\mu \left(1-\gamma^5\right) u(p_1) \bar{v}(p_2)\gamma^\nu \left(1-\gamma^5\right) v(p_4) \times \frac{(g_{\mu\sigma} - (p_1-p_3)_\mu (p_1-p_3)_\sigma / m_W^2)(g_{\nu\sigma'} - (p_2-p_4)_\nu (p_2-p_4)_{\sigma'}/m_W^2)}{[(p_1-p_3)^2 - m_W^2][(p_2-p_4)^2 - m_W^2]} \quad \text{(A.11)}$$

$$\mathcal{M}_e(Q_u \bar{Q}'_d \to WW \to Q''_u \bar{Q}'''_d h) = \frac{g^2 m_W^2}{4v} V^*_{ud'} V^*_{u''d'''} g^{\sigma\sigma'} \bar{v}(p_2)\gamma^\mu \left(1-\gamma^5\right) u(p_1) \bar{u}(p_3)\gamma^\nu \left(1-\gamma^5\right) v(p_4) \times \frac{(g_{\mu\sigma} - (p_1+p_2)_\mu (p_1+p_2)_\sigma / m_W^2)(g_{\nu\sigma'} - (p_3+p_4)_\nu (p_3+p_4)_{\sigma'}/m_W^2)}{[(p_1+p_2)^2 - m_W^2][(p_3+p_4)^2 - m_W^2]} \quad \text{(A.12)}$$

$$\mathcal{M}_f(Q_d \bar{Q}'_u \to WW \to Q''_d \bar{Q}'''_u h) = \frac{g^2 m_W^2}{4v} V_{u'd} V_{u'''d''} g^{\sigma\sigma'} \bar{v}(p_2)\gamma^\mu \left(1-\gamma^5\right) u(p_1) \bar{u}(p_3)\gamma^\nu \left(1-\gamma^5\right) v(p_4) \times \frac{(g_{\mu\sigma} - (p_1+p_2)_\mu (p_1+p_2)_\sigma / m_W^2)(g_{\nu\sigma'} - (p_3+p_4)_\nu (p_3+p_4)_{\sigma'}/m_W^2)}{[(p_1+p_2)^2 - m_W^2][(p_3+p_4)^2 - m_W^2]} \quad \text{(A.13)}$$

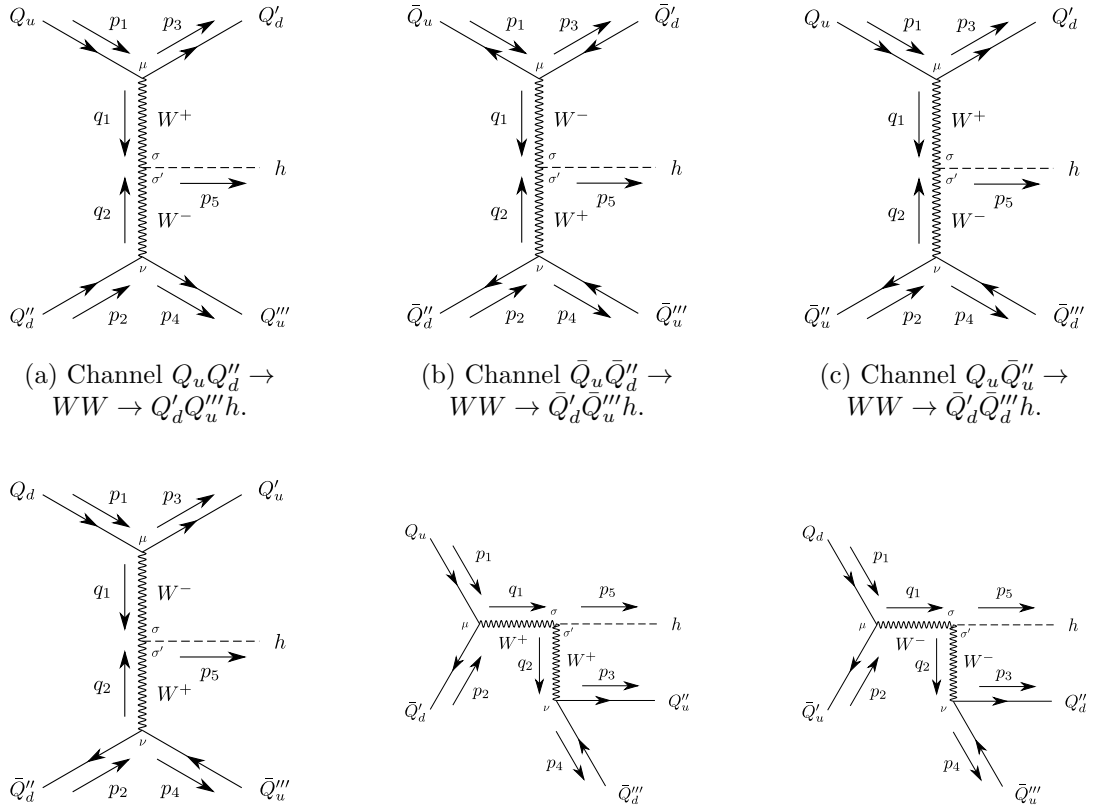

(a) Channel $Q_u Q''_d \to WW \to Q'_d Q'''_u h$.

(b) Channel $\bar{Q}_u \bar{Q}''_d \to WW \to \bar{Q}'_d \bar{Q}'''_u h$.

(c) Channel $Q_u \bar{Q}''_u \to WW \to \bar{Q}'_d \bar{Q}'''_d h$.

(d) Channel $Q_d \bar{Q}''_d \to WW \to Q'_u \bar{Q}'''_u h$.

(e) s-Channel $Q_u \bar{Q}'_d \to WW \to Q''_u \bar{Q}'''_d h$.

(f) s-Channel $Q_d \bar{Q}'_u \to WW \to Q''_d \bar{Q}'''_u h$.

Figure A.2: Feynman diagrams describing Higgs production process $QQ \to QQh$ of type $QQ \to WW \to QQh$ at lowest order.

Appendix B Group Representations and Generators

B.1 Low Dimensional Accidental Isomorphisms

Important low dimensional accidental isomorphisms:

$$\begin{aligned} \mathrm{Spin}(1) &\cong \mathbb{Z}_2 & \mathrm{Spin}(4) &\cong \mathrm{SU}(2) \times \mathrm{SU}(2) \\ \mathrm{Spin}(2) &\cong \mathrm{U}(1) & \mathrm{Spin}(5) &\cong \mathrm{Sp}(4) \\ \mathrm{Spin}(3) &\cong \mathrm{SU}(2) & \mathrm{Spin}(6) &\cong \mathrm{SU}(4) \end{aligned}$$

Table B.1: Matrix Lie groups.

Group	(Real) Dimension	Compact	Connected	Simply Connected	Components
$\mathrm{GL}(n;\mathbb{R})$	n^2	No	No	No	2
$\mathrm{GL}(n;\mathbb{C})$	$2n^2$	No	Yes	No	1
$\mathrm{SL}(n;\mathbb{R})$	n^2-1	No	Yes	No	1
$\mathrm{SL}(n;\mathbb{C})$	$2n^2-2$	No	Yes	No	1
$\mathrm{O}(n)$	$n(n-1)/2$	Yes	No	No	2
$\mathrm{SO}(n)$	$n(n-1)/2$	Yes	Yes	No	1
$\mathrm{U}(n)$	n^2	Yes	Yes	No	1
$\mathrm{SU}(n)$	n^2-1	Yes	Yes	Yes	1
$\mathrm{Sp}(2n)$	$2n^2+n$	No	Yes	No	1
$\mathrm{Sp}(2n;\mathbb{C})$	$4n^2+2n$	No	Yes	Yes	1

B.2 The Goldstone Matrix for $\mathbf{SO}(n)/\mathbf{SO}(n-1)$

From the spontaneous symmetry breaking $\mathrm{SO}(n) \to \mathrm{SO}(n-1)$ there will be $n-1$ Nambu-Goldstone bosons. The generators T_A of $\mathrm{SO}(n)$ can always be split as

$$\{T_A\}_{A=1}^{\frac{n(n-1)}{2}} = \{\hat{T}_{\hat{a}}\}_{\hat{a}=1}^{n-1} \cup \{T_a\}_{a=1}^{\frac{(n-1)(n-2)}{2}} \tag{B.1}$$

The non-broken generators T_a form an $\mathfrak{so}(n-1)$ algebra in the $\mathbf{n}$ irreducible representation of $\mathrm{SO}(n)$, and can be written as

$$T_a = \left(\begin{array}{c|c} \dfrac{t_a}{\vec{0}^{\,T}} & \dfrac{\vec{0}}{0} \end{array}\right) \quad \text{with} \quad \vec{0}^{\,T} = \underbrace{(0\,0\,\cdots\,0)}_{n-1} \tag{B.2}$$

where $\{t_a\}_{a=1}^{\frac{(n-1)(n-2)}{2}}$ must form an $\mathfrak{so}(n-1)$ algebra in the defining representation of $\mathrm{SO}(n-1)$. One way to write them is

$$(T_a)_{\mu\nu} = (T_{\alpha\beta})_{\mu\nu} = -\frac{i}{2}(\delta_{\alpha\mu}\delta_{\beta\mu} - \delta_{\beta\mu}\delta_{\alpha\mu}) \tag{B.3}$$

with $1 \le \alpha < \beta \le n-1$ and $\mu,\nu = 1,\ldots,n-1$. On the other hand, the $n-1$ broken generators $\hat{T}_{\hat{a}}$ can be written as

$$(\hat{T}_{\hat{a}})_{IJ} = -\frac{i}{\sqrt{2}}(\delta_I^{\hat{a}}\delta_J^n - \delta_J^{\hat{a}}\delta_I^n) \tag{B.4}$$

with $I,J = 1,\ldots,n$.

In this particular case of spontaneous symmetry breaking, the Goldstone matrix is given by

$$\Sigma[\phi] = \begin{pmatrix} 1_{n-1} - \dfrac{\vec{\phi}\,\vec{\phi}^{\,T}}{|\vec{\phi}|^2}\left(1-\cos\dfrac{|\vec{\phi}|}{f}\right) & \dfrac{\vec{\phi}}{|\vec{\phi}|}\sin\dfrac{|\vec{\phi}|}{f} \\ -\dfrac{\vec{\phi}^{\,T}}{|\vec{\phi}|}\sin\dfrac{|\vec{\phi}|}{f} & \cos\dfrac{|\vec{\phi}|}{f} \end{pmatrix} \tag{B.5}$$

with inverse

$$\Sigma[\phi]^{-1} = \begin{pmatrix} 1_{n-1} - \frac{\vec{\phi}\vec{\phi}^{\,T}}{|\vec{\phi}|^2}\left(1 - \cos\frac{|\vec{\phi}|}{f}\right) & -\frac{\vec{\phi}}{|\vec{\phi}|}\sin\frac{|\vec{\phi}|}{f} \\ \frac{\vec{\phi}^{\,T}}{|\vec{\phi}|}\sin\frac{|\vec{\phi}|}{f} & \cos\frac{|\vec{\phi}|}{f} \end{pmatrix} \tag{B.6}$$

B.3 $\mathbf{SU}(2) \times \mathbf{SU}(2)$

Every element of $U \in \mathrm{SU}(2) \times \mathrm{SU}(2)$ can be written as

$$U(\theta^i, \phi^j) = \exp(i\theta^i S_i) \otimes \exp(i\phi^j S_j) \tag{B.7}$$

where $i, j = 1, 2, 3$ and

$$S_i = \frac{\sigma_i}{2} \tag{B.8}$$

with σ_i the Pauli matrices. The representations $D^{(j_1,j_2)}$ of $\mathrm{SU}(2) \times \mathrm{SU}(2)$ are given by two parameters $j_1, j_2 \in \mathbb{Z}_0^+/2$. Explicitly

$$D^{(j_1,j_2)}[U(\theta^i, \phi^j)] = \exp\Big(i\theta^i d^{(j_1)}(S_i)\Big) \otimes \exp\Big(i\phi^j d^{(j_2)}(S_j)\Big) \tag{B.9}$$

where $d^{(j)}$ the corresponding irrep. of $\mathrm{SU}(2)$. Note that

$$\dim(D^{(j_1,j_2)}) = (2j_1 + 1)(2j_2 + 1) \tag{B.10}$$

Table B.2: The first few representations of $\mathrm{SU}(2) \times \mathrm{SU}(2)$ and their dimensions.

dim	(j_1, j_2)
1	$(0,0)$
2	$(\frac{1}{2},0), (0,\frac{1}{2})$
3	$(1,0), (0,1)$
4	$(\frac{3}{2},0), (0,\frac{3}{2}), (\frac{1}{2},\frac{1}{2})$
5	$(2,0), (0,2)$
6	$(\frac{5}{2},0), (0,\frac{5}{2}), (\frac{1}{2},1), (1,\frac{1}{2})$
7	$(3,0), (0,3)$

B.4 $\mathbf{SO}(4)$

Every element of $O \in \mathrm{SO}(4)$ can be written as

$$O(\theta^i, \phi^j) = \exp(i\theta^i S_i) \otimes \exp(i\phi^j S_j) \tag{B.11}$$

where $i, j = 1, 2, 3$ and

$$S_i = \frac{\sigma_i}{2} \tag{B.12}$$

with σ_i the Pauli matrices. The representations $D^{(j_1,j_2)}$ of SO(4) are given by two parameters $j_1, j_2 \in \mathbb{Z}_0^+/2$ such that $j_1 + j_2 \in \mathbb{Z}_0^+$, i.e. such that j_1 and j_2 are both simultaneously integers or half-integers. Explicitly

$$D^{(j_1,j_2)}[O(\theta^i, \phi^j)] = \exp\Big(i\theta^i d^{(j_1)}(S_i)\Big) \otimes \exp\Big(i\phi^j d^{(j_2)}(S_j)\Big) \tag{B.13}$$

where $d^{(j)}$ the corresponding representations of $\mathfrak{su}(2)$. Note that

$$\dim(D^{(j_1,j_2)}) = (2j_1 + 1)(2j_2 + 1) \tag{B.14}$$

Table B.3: The first few representations of SO(4) and their dimensions.

dim	(j_1, j_2)
1	$(0,0)$
2	-
3	$(1,0), (0,1)$
4	$(\frac{1}{2}, \frac{1}{2})$
5	$(2,0), (0,2)$
6	-
7	$(3,0), (0,3)$

B.5 SO(5)

The 10 generators T_A of $\mathfrak{so}(5)$ are split as

$$\{T_A\}_{A=1}^{10} = \{T_a\}_{a=1}^{6} \cup \{\hat{T}_{\hat{a}}\}_{\hat{a}=1}^{4} \tag{B.15}$$

with the T_a's forming an $\mathfrak{so}(4)$ algebra. Since $\mathrm{Spin}(4) \cong \mathrm{SU}(2)_L \times \mathrm{SU}(2)_R$ is the universal covering space of SO(4), these generators in turn can be conveniently split as

$$\{T_a\}_{a=1}^{6} = \left\{ T_{aL} = \begin{pmatrix} t_{aL} & 0 \\ 0 & 0 \end{pmatrix}, T_{aR} = \begin{pmatrix} t_{aR} & 0 \\ 0 & 0 \end{pmatrix} \right\}_{a=1}^{3} \tag{B.16}$$

where

$$(t_{aL})_{ij} = -\frac{i}{2}\left[\varepsilon_{abc}\delta_i^b\delta_j^c + (\delta_i^a\delta_j^4 - \delta_j^a\delta_i^4)\right] \tag{B.17}$$

$$(t_{aR})_{ij} = -\frac{i}{2}\left[\varepsilon_{abc}\delta_i^b\delta_j^c - (\delta_i^a\delta_j^4 - \delta_j^a\delta_i^4)\right] \tag{B.18}$$

with $i, j = 1, 2, 3, 4$ corresponding to generators of the subalgebras $\mathfrak{su}(2)_L$ and $\mathfrak{su}(2)_R$, respectively. Explicitly, they correspond to

$$t_{1L} = -\frac{i}{2}\begin{pmatrix} 0 & 0 & 0 & 1 \\ 0 & 0 & 1 & 0 \\ 0 & -1 & 0 & 0 \\ -1 & 0 & 0 & 0 \end{pmatrix} \quad t_{2L} = -\frac{i}{2}\begin{pmatrix} 0 & 0 & -1 & 0 \\ 0 & 0 & 0 & 1 \\ 1 & 0 & 0 & 0 \\ 0 & -1 & 0 & 0 \end{pmatrix} \quad t_{3L} = -\frac{i}{2}\begin{pmatrix} 0 & 1 & 0 & 0 \\ -1 & 0 & 0 & 0 \\ 0 & 0 & 0 & 1 \\ 0 & 0 & -1 & 0 \end{pmatrix}$$

$$t_{1R} = -\frac{i}{2}\begin{pmatrix} 0 & 0 & 0 & -1 \\ 0 & 0 & 1 & 0 \\ 0 & -1 & 0 & 0 \\ 1 & 0 & 0 & 0 \end{pmatrix} \quad t_{2R} = -\frac{i}{2}\begin{pmatrix} 0 & 0 & -1 & 0 \\ 0 & 0 & 0 & -1 \\ 1 & 0 & 0 & 0 \\ 0 & 1 & 0 & 0 \end{pmatrix} \quad t_{3R} = -\frac{i}{2}\begin{pmatrix} 0 & 1 & 0 & 0 \\ -1 & 0 & 0 & 0 \\ 0 & 0 & 0 & -1 \\ 0 & 0 & 1 & 0 \end{pmatrix}$$

On the other hand, the remaining four broken generators are given by

$$(\hat{T}_{\hat{a}})_{IJ} = -\frac{i}{\sqrt{2}}(\delta^{\hat{a}}_I \delta^5_J - \delta^{\hat{a}}_J \delta^5_I) \tag{B.19}$$

with $\hat{a} = 1, 2, 3, 4$ and $I, J = 1, 2, 3, 4, 5$. Explicitly, they correspond to

$$\hat{T}_1 = \frac{1}{\sqrt{2}}\begin{pmatrix} 0 & 0 & 0 & 0 & -i \\ 0 & 0 & 0 & 0 & 0 \\ 0 & 0 & 0 & 0 & 0 \\ 0 & 0 & 0 & 0 & 0 \\ i & 0 & 0 & 0 & 0 \end{pmatrix} \qquad \hat{T}_2 = \frac{1}{\sqrt{2}}\begin{pmatrix} 0 & 0 & 0 & 0 & 0 \\ 0 & 0 & 0 & 0 & -i \\ 0 & 0 & 0 & 0 & 0 \\ 0 & 0 & 0 & 0 & 0 \\ 0 & i & 0 & 0 & 0 \end{pmatrix}$$

$$\hat{T}_3 = \frac{1}{\sqrt{2}}\begin{pmatrix} 0 & 0 & 0 & 0 & 0 \\ 0 & 0 & 0 & 0 & 0 \\ 0 & 0 & 0 & 0 & -i \\ 0 & 0 & 0 & 0 & 0 \\ 0 & 0 & i & 0 & 0 \end{pmatrix} \qquad \hat{T}_4 = \frac{1}{\sqrt{2}}\begin{pmatrix} 0 & 0 & 0 & 0 & 0 \\ 0 & 0 & 0 & 0 & 0 \\ 0 & 0 & 0 & 0 & 0 \\ 0 & 0 & 0 & 0 & -i \\ 0 & 0 & 0 & i & 0 \end{pmatrix}$$

References

[1] P. Deligne, P. Etingof, D. Freed, L. Jeffrey, D. Kazhdan, J. Morgan, D. Morrison, and E. Witten, *Quantum fields and strings: A course for mathematicians Vol. 1.* (American Mathematical Society, 1999)

[2] E. Witten, *Symmetry and Emergence.* [arXiv:1710.01791v3 [hep-th]]

[3] D. J. Gross and F. Wilczek, *Ultraviolet Behavior of Non-Abelian Gauge Theories.* Phys. Rev. Lett. 30, 1343 (1973)

[4] H. D. Politzer, *Reliable Perturbative Results for Strong Interactions?.* Phys. Rev. Lett. 30, 1346 (1973)

[5] Particle Data Group, *Rewiew of Particle Physics, Volume 40 Number 10 October 2016.* http://pdg.lbl.gov/

[6] H. Suganuma, M. Fukushima and H. Toki, *Quantum Chromodynamics and Color Confinement; Proceedings of the International Symposium Osaka, Japan, 7 - 10 March 2000.* cds.cern.ch/record/406724

[7] Krishna Rajagopal, *Mapping the QCD Phase Diagram.* [hep-ph/9908360]

[8] Yasuyuki Akiba et al., *The Hot QCD White Paper: Exploring the Phases of QCD at RHIC and the LHC.* [arXiv:1502.02730v1 [nucl-ex]]

[9] Wit Busza, Krishna Rajagopal, and Wilke van der Schee, *Heavy Ion Collisions: The Big Picture and the Big Questions.* [arXiv:1802.04801v2 [hep-ph]]

[10] J. Cleymans, H. eschler, K. Redlich, S. Wheaton, *Comparison of Chemical Freeze-Out Criteria in Heavy-Ion Collisions.* [hep-ph/0511094]

[11] A. Andronic, P. Braun-Munzinger, K. Redlich, J. Stachel, *Decoding the phase structure of QCD via particle production at high energy.* [arXiv:1710.09425v1 [nucl-th]]

[12] M. Alford, K. Rajagopal, F. Wilczek, *Color-Flavor Locking and Chiral Symmetry Breaking in High Density QCD.* [hep-ph/9804403]

[13] Robert D. Pisarski, *Phenomenology of the chiral phase transition.* Nucl. Phys. B 110, 155 (1982)

[14] J. Cleymans, K. Redlich, H. Satz et al., *On the phenomenology of deconfinement and chiral symmetry restoration.* Z. Phys. C - Particles and Fields (1986) 33: 151

[15] H. Schulz, G. Röpke, *A note on the massive quark matter phase.* Z. Phys. C - Particles and Fields (1987) 35: 379

[16] Bertrand C. Barrois, *Superconducting quark matter.* Nucl. Phys. B 129, 390 (1977)

[17] D. Bailin, A. Love, *Superfluidity and superconductivity in relativistic fermion systems.* Phys. Rept. 107, 325 (1984)

[18] M. Alford, K. Rajagopal, F. Wilczek, *QCD at Finite Baryon Density: Nucleon Droplets and Color Superconductivity.* [hep-ph/9711395]

[19] Frithjof Karsch, *Lattice Results on QCD Thermodynamics.* [hep-ph/0103314]

[20] Y. Aoki, G. Endrodi, Z. Fodor, S. D. Katz, and K. K. Szabo, *The order of the quantum chromodynamics transition predicted by the standard model of particle physics.* [hep-lat/0611014]

[21] Szabocls Borsanyi et al., *Full result for the QCD equation of state with 2+1 flavors.* [arXiv:1309.5258v2 [hep-lat]]

[22] Xiaofeng Luo and Nu Xu, *Search for the QCD Critical Point with Fluctuations of Conserved Quantities in Relativistic Heavy-Ion Collisions at RHIC: An Overview.* [arXiv:1701.02105v3 [nucl-ex]]

[23] Szabolcs Borsanyi et al., *Is there still any Tc mystery in lattice QCD? Results with physical masses in the continuum limit III.* [arXiv:1005.3508v1 [hep-lat]]

[24] A. Bazavov et al., *Chiral and deconfinement aspects of the QCD transition.* Phys. Rev. D 85, 054503 (2012)

[25] Heng-Tong Ding, *Recent lattice QCD results and phase diagram of strongly interacting matter.* Nucl. Phys. A 931, 52 (2014)

[26] A. Manohar and H. Georgi, *Chiral Quarks and The Non-Relativistic Quark Model.* Nucl. Phys. B 234, 189 (1984)

[27] A. Bazavov et al., *Equation of state and QCD transition at finite temperature.* Phys. Rev. D 80, 014504 (2009)

[28] Philippe de Forcrand, *Simulating QCD at finite density.* [arXiv:1005.0539v2 [hep-lat]]

[29] Z. Fodor and S. D. Katz, *Lattice determination of the critical point of QCD at finite T and mu.* [hep-lat/0106002]

[30] Anyi Li et al., *Study of QCD critical point using canonical ensemble method.* Nucl. Phys. A 830, 633 (2009)

[31] Philippede Forcrand and Slavo Kratochvila, *Finite density QCD with a canonical approach.* Nucl. Phys. B 153, 62 (2006)

[32] M. A. Stephanov, *QCD phase diagram and the critical point.* [hep-ph/0402115]

[33] Si-xue Qin, et al., *Phase Diagram and Critical End Point for Strongly Interacting Quarks.* Phys. Rev. Lett. 106, 172301 (2011)

[34] Christian S. Fischer and Jan Luecker, *Propagators and phase structure of Nf=2 and Nf=2+1 QCD.* Phys. Lett B 718, 1036 (2013)

[35] P. W. Higgs, *Broken Symmetries and the Masses of Gauge Bosons*. Phys. Rev. Lett. 13, 508 (1964)

[36] G. S. Guralnik, C. R. Hagen, and T. W. B. Kibble, *Global Conservation Laws and Massless Particles*. Phys. Rev. Lett. 13, 585 (1964)

[37] F. Englert and R. Brout, *Broken Symmetry and the Mass of Gauge Vector Mesons*. Phys. Rev. Lett. 13, 321 (1964)

[38] G.'t Hooft and M. Veltman, *Regularization and renormalization of gauge fields*. Nucl. Phys. B 44, 189 (1972)

[39] The LEP Collaborations, *A Combination of Preliminary Electroweak Measurements and Constraints on the Standard Model*. [hep-ex/0312023]; The ALEPH Collaboration, *Precision Electroweak Measurements on the Z Resonance*. [hep-ex/0509008]

[40] Zhenyu Han, *Effective Theories and Electroweak Precision Constraints*. [arXiv:0807.0490v1 [hep-ph]]

[41] C. P. Burgess, *Introduction to Effective Field Theory*. [hep-th/0701053]

[42] Ira Z. Rothstein, *TASI Lectures on Effective Field Theories*. [hep-ph/0308266]

[43] Emmanuelle Perez and Eram Rizvi, *The Quark and Gluon Structure of the Proton*. [arXiv:1208.1178v2 [hep-ex]]

[44] Thomas G. Rizzo, *Gluon final states in Higgs-boson decay*. Phys. Rev. D 22, 178 (1980)

[45] Abdelhak Djouadi, *The Anatomy of Electro Weak Symmetry Breaking Tome I: The Higgs boson in the Standard Model*. [hep-ph/0503172v2]

[46] LHC Higgs Cross Section Working Group, *Handbook of LHC Higgs Cross Sections: 1. Inclusive Observables*. [arXiv:1101.0593v3 [hep-ph]]

[47] Fred Jegerlehner, *The hierarchy problem and the cosmological constant problem in the Standard Model*. arXiv:1503.00809v1 [hep-ph]

[48] M. S. Al-sarhi, I. Jack, and D. R. T. Jones, *Quadratic divergences in gauge theories*. Phys. C Particles and Fields 55, 283 (1992)

[49] D. R. Timothy Jones, *Comment on "Bare Higgs mass at Planck scale"*. Phys. Rev. D 88, 098301 (2013)

[50] Yuta Hamada, Hikaru Kawai, and Kin-ya Oda, *Bare Higgs mass at Planck scale*. Phys. Rev. D 87, 053009 (2013)

[51] Sheldon L. Glashow, *Partial-symmetries of weak interactions*. Nucl. Phys. 22, 579 (1961)

[52] ATLAS Collaboration, *Observation of a new particle in the search for the Standard Model Higgs boson with the ATLAS detector at the LHC*. Phys. Lett. B 716, 1 (2012)

[53] CMS Collaboration, *Observation of a new boson at a mass of 125 GeV with the CMS experiment at the LHC*. Phys. Lett. B 716, 30 (2012)

[54] ATLAS Collaboration, CMS Collaboration, *Combined Measurement of the Higgs Boson Mass in pp Collisions at sqrt[s]=7 and 8 TeV with the ATLAS and CMS Experiments*. Phys. Rev. Lett. 114, 191803 (2015)

[55] J. E. Anderson. *A Conceptual Framework for Evaluating and Quantifying Naturalness*, Conservation Biology, Vol. 5, No. 3, p. 347 (1991)

[56] R. Courant and H. Robbins, *What is Mathematics?*. Oxford University Press, Oxford (1941)

[57] Kenneth G. Wilson, *Renormalization Group and Strong Interactions*. Phys. Rev. D 3, 1818 (1971)

[58] Steven Weinberg, *Implications of dynamical symmetry breaking*. Phys. Rev. D 13, 974 (1976); *Implications of dynamical symmetry breaking: An addendum*. Phys. Rev. D 19, 1277 (1979)

[59] Leonard Susskind, *Dynamics of spontaneous symmetry breaking in the Weinberg-Salam theory*. Phys. Rev. D 20, 2619 (1979)

[60] Eldad Gildener, *Gauge-symmetry hierarchies*. Phys. Rev. D 14, 1667 (1976)

[61] Gerard 't Hooft, *Chiral Symmetry, and Spontaneous Chiral Symmetry Breaking*. NATO Sci.Ser.B 59 (1980)

[62] Edited by G. 't Hooft et al. *Recent Developments in Gauge Theories*, N.Y., Plenum Press, 1980. 438p.

[63] R. Barbieri and G. F. Giudice, *Upper bounds on supersymmetric particle masses*. Nucl. Phys. B 306, 63 (1988)

[64] J. A. Casas, J. R. Espinosa and I. Hidalgo, *Implications for New Physics from Fine-Tuning Arguments: I. Application to SUSY and Seesaw Cases*, [hep-ph/0410298v1]

[65] J. A. Casas, J. R. Espinosa and I. Hidalgo, *Implications for New Physics from Fine-Tuning Arguments: II. Little Higgs Models*. [hep-ph/0502066v1]

[66] Michael Dine, *Naturalness Under Stress*. [arXiv:1501.01035v2 [hep-ph]]

[67] Gian Francesco Giudice, *Naturally Speaking: The Naturalness Criterion and Physics at the LHC*. [arXiv:0801.2562v2 [hep-ph]]

[68] Riccardo Barbieri and Alessandro Strumia, *The "LEP paradox"*. [hep-ph/0007265v2]

[69] L. Giusti, A. Romanino and A. Strumia, *Natural ranges of supersymmetric signals*. [hep-ph/9811386]

[70] Andrew Fowlie, *The little-hierarchy problem is a little problem: understanding the difference between the big- and little-hierarchy problems with Bayesian probability.* [arXiv:1506.03786v2 [hep-ph]]

[71] Riccardo Barbieri, Alex Pomarol, Riccardo Rattazzi and Alessandro Strumia, *Electroweak symmetry breaking after LEP1 and LEP2.* [hep-ph/0405040v2]

[72] Philip Bechtle, Tilman Plehn, Christian Sander, *The Status of Supersymmetry after the LHC Run 1.* [arXiv:1506.03091v1 [hep-ex]]

[73] Alessandro Strumia, *The fine-tuning price of the early LHC.* [https://arxiv.org/abs/1101.2195]

[74] H. Miyazawa, *Baryon Number Changing Currents.* Prog. Theor. Phys. 36 (6), 1266 (1966); H. Miyazawa, *Spinor Currents and Symmetries of Baryons and Mesons.* Phys. Rev. 170, 1586 (1968)

[75] J. L. Gervais and B. Sakita, *Field theory interpretation of supergauges in dual models.* Nucl. Phys. B 34, 632 (1971)

[76] Yu. A. Golfand and E. P. Likhtman, JETP Lett. 13, 323 (1971) [Reprinted in Supersymmetry, Ed. S. Ferrara, (North-Holland/World Scientific, Amsterdam - Singapore, 1987), Vol. 1, page 7].

[77] D. V. Volkov and V. P. Akulov, Pisma Zh.Eksp.Teor.Fiz. 16 (1972) 621; Phys. Lett. B46 (1973) 109; D. V. Volkov, V. P. Akulov, V.P. Akulov, D.V. Volkov, Teor.Mat.Fiz. 18 (1974) 39

[78] P. Ramond, *Dual Theory for Free Fermions.* Phys. Rev. D 3, 2415 (1971)

[79] A. Neveu and J. H. Schwarz, *Tachyon-free dual model with a positive-intercept trajectory.* Phys. Rev. D 34, 517 (1971)

[80] J. Wess and B. Zumino, *Supergauge transformations in four dimensions.* Nucl. Phys. B 70, 39 (1974)

[81] Kenneth Lane, *An introduction to technicolor.* [hep-ph/9401324v2]

[82] Francesco Sannino, *Technicolor and Beyond: Unification in Theory Space.* [arXiv:1010.3461v1 [hep-ph]]

[83] John H. Schwarz, *The Early History of String Theory and Supersymmetry.* [arXiv:1201.0981v1 [physics.hist-ph]]

[84] A. D. Linde, *Chaotic inflation.* Phys. Lett. B 129, 177 (1983)

[85] V. Agrawal, S. M. Barr, John F. Donoghue, D. Seckel, *The anthropic principle and the mass scale of the Standard Model.* [hep-ph/9707380v2]

[86] Michael J. Dugan, Howard Georgi and David B. Kaplan, *Anatomy of a composite Higgs model.* Nucl. Phys. B 254, 299 (1985);

[87] Christophe Grojean, Oleksii Matsedonskyi, Giuliano Panico, *Light top partners and precision physics*. [arXiv:1306.4655v2 [hep-ph]]

[88] David B. Kaplan, Howard Georgi and Savas Dimopoulos, *Composite Higgs scalars*. Phys. Lett. B 136, 187 (1984);

[89] Giuliano Panico, Andrea Wulzer, *The Composite Nambu–Goldstone Higgs*. [arXiv:1506.01961v2 [hep-ph]]

[90] S. Coleman, J. Wess, and Bruno Zumino, *Structure of Phenomenological Lagrangians. I*. Phys. Rev. 177, 2239 (1969)

[91] Curtis G. Callan, Jr., Sidney Coleman, J. Wess, and Bruno Zumino, *Structure of Phenomenological Lagrangians. II*. Phys. Rev. 177, 2247 (1969)

[92] Kaustubh Agashe, Roberto Contino, Alex Pomarol, *The minimal composite Higgs model*. Nucl. Phys. B 719, 165 (2005)

[93] Giacomo Cacciapaglia and Francesco Sannino, *Fundamental composite (Goldstone) Higgs dynamics*. J. High Energ. Phys. (2014) 2014: 111

[94] J. A. Evans, J. Galloway, M. A. Luty et al., *Minimal conformal technicolor and precision electroweak tests*. J. High Energ. Phys. (2010) 2010: 86

[95] Juan Yepes, Alfonso Zerwekh, *Top partner-resonance interplay in a composite Higgs framework*. [arXiv:1711.10523v1 [hep-ph]]

[96] David Marzocca, Marco Serone and Jing Shu, *General Composite Higgs Models*. [arXiv:1205.0770v3 [hep-ph]]

[97] Alex Pomarol and Francesco Riva, *The Composite Higgs and Light Resonance Connection*. [arXiv:1205.6434v2 [hep-ph]]

[98] Michele Redi and Andrea Tesi, *Implications of a Light Higgs in Composite Models*. [arXiv:1205.0232v2 [hep-ph]]

[99] Giuliano Panico, Michele Redic, Andrea Tesi and Andrea Wulzer, *On the Tuning and the Mass of the Composite Higgs*. [arXiv:1210.7114v2 [hep-ph]]

[100] Roberto Contino, *Tasi 2009 lectures: The Higgs as a Composite Nambu-Goldstone Boson*. arXiv:1005.4269v1 [hep-ph]

[101] David B. Kaplan, *Flavor at ssc energies: A new mechanism for dynamically generated fermion masses*. Nucl. Phys. B 365, 259 (1991)

[102] Andrea De Simone, Oleksii Matsedonskyi, Riccardo Rattazzi and Andrea Wulzer, *A First Top Partner Hunter's Guide*. [arXiv:1211.5663v2 [hep-ph]]

[103] Abdelhak Djouadi, Alexander Lenz, *Sealing the fate of a fourth generation of fermions*. Phys. Lett. B 715, 310 (2012)

[104] Otto Eberhardt et al., *Impact of a Higgs Boson at a Mass of 126 GeV on the Standard Model with Three and Four Fermion Generations*. Phys. Rev. Lett. 109, 241802 (2012)

[105] J. A. Aguilar-Saavedra et al., *Handbook of vectorlike quarks: Mixing and single production*. Phys. Rev. D 88, 094010 (2013)

[106] Oleksii Matsedonskyi, Giuliano Panico, Andrea Wulzer, *Light Top Partners for a Light Composite Higgs*. [arXiv:1204.6333v2 [hep-ph]]

[107] The ATLAS Collaboration, *Search for pair production of vector-like top quarks in events with one lepton jets and missing transverse momentum in sqrt(s)=13 TeV pp collisions with the ATLAS detector*. [arXiv:1705.10751v2 [hep-ex]]

[108] CMS Collaboration, *Search for pair production of vector-like quarks in the bWbW channel from proton-proton collisions at sqrt(s)=13 TeV*. [arXiv:1710.01539v2 [hep-ex]]

[109] Tarek Ibrahim and Pran Nath, *MSSM extension with a mirror fourth generation, neutrino magnetic moments, and CERN LHC signatures*. Phys. Rev. D 78, 075013 (2008)

[110] Chun Liu, *Supersymmetry and Vector-like Extra Generation*. arXiv:0907.3011v1 [hep-ph]

[111] Stephen P. Martin, *Extra vectorlike matter and the lightest Higgs scalar boson mass in low-energy supersymmetry*. Phys. Rev. D 81, 035004 (2010)

[112] F. del Aguila, M. Perez-Victoria, J. Santiago, *Observable contributions of new exotic quarks to quark mixing*. hep-ph/0007316

[113] J. A. Aguilar-Saavedra, *Identifying top partners at LHC*. [arXiv:0907.3155v2 [hep-ph]]

[114] G. Cacciapaglia, A. Deandrea, D. Harada et al., *Bounds and Decays of New Heavy Vector-like Top Partners*. J. High Energ. Phys. 11, 159 (2010)

[115] Yasuhiro Okada, Luca Panizzi, *LHC signatures of vector-like quarks*. [arXiv:1207.5607v3 [hep-ph]]

[116] F. Garberson, T. Golling, *Generalization of exotic quark searches*. Phys. Rev. D 87, 072007 (2013)

[117] Mathieu Buchkremer, et al., *Model-independent framework for searches of top partners*. Nucl. Phys. B 876, 376 (2013)

[118] Da Liu, Ian Low, and Carlos E. M. Wagner, *Modification of Higgs Couplings in Minimal Composite Models*. Phys. Rev. D 96, 035013 (2017)

[119] Oleksii Matsedonskyi, Francesco Riva, and Thibaud Vantalon, *Composite Charge 8/3 Resonances at the LHC*. T. J. High Energ. Phys. (2014) 2014: 59

[120] G. F. Giudice, C. Grojean, A. Pomarol, R. Rattazzi, *The Strongly-Interacting Light Higgs*. [hep-ph/0703164]

[121] G. Ecker, J. Gasser, H. Leutwyler, A. Pich, E. De Rafael, *Chiral lagrangians for massive spin-1 fields*. Phys. Lett. B 223, 425 (1989)

[122] Roberto Contino, David Marzocca, Duccio Pappadopulo, and Riccardo Rattazzi, *On the effect of resonances in composite Higgs phenomenology*. J. High Energ. Phys. (2011) 2011: 81

[123] Sebastián Norero, Juan Yepes, and Alfonso Zerwekh, *Scalar resonance in a top partner model*. arXiv:1807.02211v1 [hep-ph]

[124] R. Contino, C. Grojean, D. Pappadopulo et al., *Strong Higgs Interactions at a Linear Collider*. J. High Energ. Phys. (2014) 2014: 6

[125] D. Pappadopulo, A. Thamm, R. Torre et al., *Heavy vector triplets: bridging theory and data*. J. High Energ. Phys. (2014) 2014: 60